# Phosphorylation of Heterogeneous Ribonucleoprotein A1 In Human Diploid Fibroblasts: Implications for p38 MAP Kinase

**by**

**Ileana Rios**

**A dissertation submitted to the Graduate Center Faculty in Biology in partial fulfillment of the requirements for the degree of Doctor of Philosophy,**

**The City University of New York**

**2006**

UMI Number: 3287106



ProQuest Information and Learning Company
300 North Zeeb Road
P.O. Box 1346
Ann Arbor, MI 48106-1346

This manuscript has been read and accepted for
The Graduate Faculty In Biology in satisfaction of the
dissertation requirements for the degree of Doctor of Philosophy.

| | |
|---|---|
| 12/21/05 | Dr. Karen Hubbard |
| Date | Chair of Examining Committee |
| 12/21/05 | Dr. Richard Chappell |
| Date | Executive Officer |

Dr. Linda Spatz
_____

Dr. Serafin Pinol-Roma
_____

Dr. Zahra Zakeri
_____

Dr. Vincent Cristofalo
_____

**Supervisory Committtee**

**THE CITY UNIVERSITY OF NEW YORK**

# ABSTRACT

Phosphorylation of Heterogeneous Ribonucleoprotein A1 in Human Diploid Fibroblasts: Implications for p38 MAP kinase

By

Ileana Rios

Advisor: Dr. Karen Hubbard

Heterogeneous nuclear ribonucleoproteins (hnRNP's) are several classes of RNA binding proteins which are important in the biogenesis of mature RNA (mRNA). We have previously found that hnRNP protein A1 has diminished protein levels in senescent human diploid fibroblasts (HDF). This RNA binding protein modulates splice site usage, general splicing factors, polyadenylation, and cleavage efficiency. hnRNP A1 has also been implicated in mRNA stability and transport from the nucleus. Thus, the alteration in activity of the hnRNP A1 protein may affect the level of expression of mature mRNA's and contribute to the senescent phenotype.

Protein levels of hnRNP A1 decrease in senescent HDF and this decrease parallels the observed alteration of nucleic acid binding properties. We have previously shown that in young HDF's hnRNP A1 accumulates in the nucleus while in senescent HDF hnRNP A1 disperses to the cytoplasm in a punctate pattern, the mechanism underlying this localization pattern is unknown.

In this study we have examined the phosphorylation status of hnRNP A1 in young and senescent fibroblasts and have found that in senescent fibroblasts the phosphorylation of hnRNP A1 increases relative to its total albeit diminished protein levels.

Recent studies have implicated p38 MAP in the modulation of oncogenic *ras*-induced premature senescence. Other studies have shown that post-translational modification by phosphorylation is necessary and sufficient for hnRNP A1 cytoplasmic accumulation. The p38 MAP kinase pathway has been shown to induce hnRNP A1 cytoplasmic accumulation during osmotic shock. Thus, this pathway was examined as a putative modulator of hnRNP A1 protein levels.

Our findings suggest that both p38 MAP kinase levels and activity are elevated in senescent fibroblasts consistent with that reported in other fibroblast systems. We have shown that hnRNP A1 co-immunoprecipitates with phosphorylated p38 MAP kinase which suggests an *in vivo* interaction. We have also demonstrated that inhibition of p38 MAP kinase activity modulates total protein levels of hnRNP A1. Since phosphorylation is known to have an important role in the regulation of protein binding to nucleic acids, the phosphorylation status of hnRNP A1 in addition to its differential nucleo/cytoplasmic protein levels may have a critical effect in its RNA binding activity and localization with ultimate consequences for gene expression during senescence.

# ACKNOWLEDGEMENTS

I owe a debt of gratitude to my entire family for their unwavering support of my graduate studies. To my son, Danilo whose preternatural patience and wisdom about my academic committments astounded me at times, and without whom, life would be a meaningless void, I am because you are. To my very special friends who have served as exemplary role models, Geraldine Moriba-Meadows, Vera Cheek, and Nanette Bracero, I thank you .

I am grateful to my mentor, Professor Karen Hubbard for giving me the opportunity to work with her and for guiding me throughout the years. I thank the members of my thesis committee, Dr. Linda Spatz, Dr. Serafin Pinol-Roma, Dr. Vincent Cristofalo, and Dr. Zahra Zakeri for their invaluable advice and critical analysis of my work. I want to acknowledge Joan Reid at the Graduate Center for all her support and understanding during my studies.

I also want to express my gratitude to members of the MCD department for their camaraderie and support: Dr. Jerry Guyden, Dr. Sally Hoskins, Dr. Shubha Govind, Dr. Mark Pezzano, Dr. Mako Osada, Kena Ou, and Mitchell Thorne.

To the following colleagues I owe many thanks and many late night laughs: Dr. Jorge Morales, Martin Indarte, Rosemary Plaza, Brendan Sayers, Rita Lewis, and Claudette Davis.

The following program provided financial support for my Ph.D studies:

The RISE Program

Program director: Professor Michael Weiner

# TABLE OF CONTENTS

## LIST OF TABLES

## LIST OF FIGURES

# Chapter 1.

# Introduction: Overview of the literature

## 1.1 Replicative Senescence

Normal human diploid fibroblasts in culture undergo a finite number of cell divisions before undergoing permanent growth arrest known as replicative senescence. This *in vitro* finite replicative lifespan termed the Hayflick limit (1) is not only characteristic of human fibroblasts but for other somatic cell types including lymphocytes, keratinocytes, and endothelial cells (2). During each round of DNA replication the telomeric ends of linear chromosomes undergo progressive shortening in the absence of telomerase and it is thought that telomere erosion is one mechanism that is responsible for replicative senescence (3,4.) The defining feature of senescent fibroblasts is the failure to undergo DNA replication in the presence of growth factors or serum stimulation (1). In the 1960's Hayflick demonstrated that cultured human fibroblasts had a limited growth capacity (1).

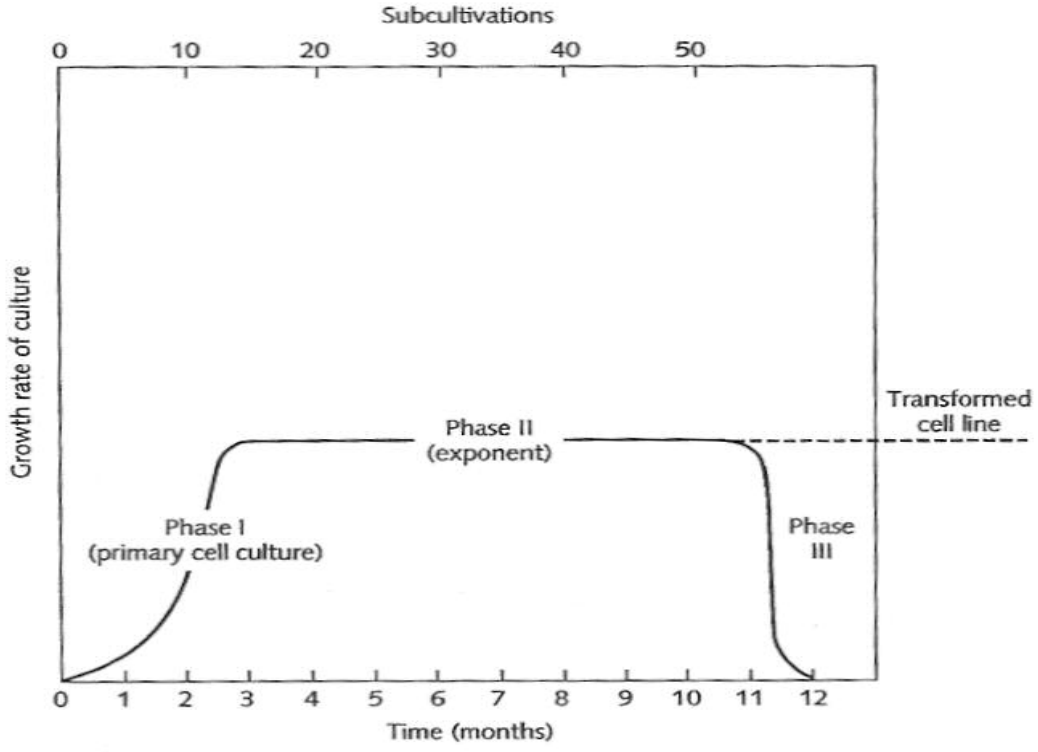

**Figure.1.** Depiction of the different phases of *in vitro* replicative senescence (6).

Phase I – the primary culture, the cells grow slowly initially, but the growth rate increases. This phase ends when the cells reach 100% confluence.

Phase II- this phase is characterized by a rapid rate of proliferation during which there are high numbers of cells in the culture. Cell division can be measured by determining the time it takes for the cell population to double in number.

Phase III- cells in this phase are marked by a progressive slowing of the growth rate, a reduced capability of the cells to respond to growth factors and a decrease in the number of cells that synthesize DNA. The amount of time that is required for the population to double increases. Cells eventually stop growing and arrest in the late G1 phase of the cell cycle. Phase III is characteristic of the senescent phenotype and although the cells may remain metabolically active for extended periods, the end result is death of the culture. (6).

The Hayflick limit is also referred to as mortality 1 stage (M1) and expression of viral oncogenes such as SV40 large T antigen and HPV E6 and E7 oncoproteins can significantly extend *in vitro* life span (7,8). These cultures eventually stop dividing and undergo a crisis stage marked by extensive cell death referred to as mortality 2 (M2). A very small number of cells can emerge from crisis (M2) and become immortalized (7,8).

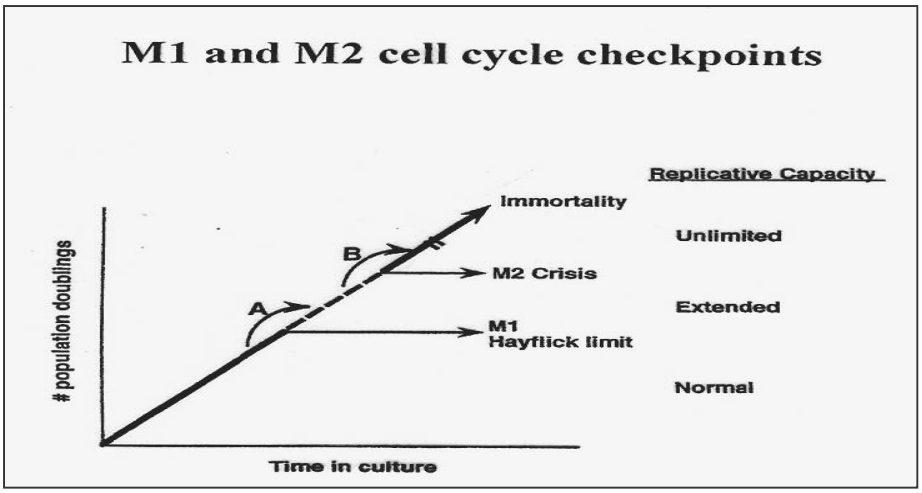


**Figure 2.** M1 and M2 cell cycle check points (10).

Depending on the cell type, the Hayflick limit ranges from 50-100 population doublings (PD). Replicative senescence has been described as resulting from telomere shortening (11). Senescent cells complete a finite number of cell divisions in culture after which they become irreversibly growth arrested in the G-1 phase of the cell cycle (12). At this point they have a BrdU labeling index of less than 5% which indicates that less than five percent of the cells are undergoing DNA synthesis. Furthermore, senescence is characterized by the absence of one population doubling in a 2-4 week period at terminal passage (13). Senescent cells comprise a post-mitotic population that is unresponsive to mitogenic stimulation and unable to enter the synthesis phase (S-phase) of the cell cycle (14). These cells arrest with a G-1 DNA content and do not resemble early passage cells that are growth-arrested in a reversible, non-proliferative state which is termed $G_0$ or quiescence.( 8)

However, senescent cells do not enter the cell cycle following mitogenic stimulation. A significant feature of senescent cells is that they remain metabolically

active for periods ranging from months to years (15). In addition they acquire characteristic phenotypic changes which include enlargement and flattening of the cells, increased lysosome biogenesis, vacuolated cytoplasm, and an increase in cytoplasmic filaments (reviewed in 16). Similarly they accumulate oxidized proteins and studies have demonstrated that human fetal foreskin fibroblasts (BJ fibroblasts) undergo a marked decline in all proteosome activities and accumulate oxidatively modified forms of cross-linked proteins (17). Senescent cells also share several features with terminally differentiated cells in that they are irreversibly and stably growth arrested, however replicative senescence is a consequence of a finite number of cell divisions accompanied with distinct morphological and genetic changes.

There are close to a hundred genes that have been reported to be differentially expressed in senescent fibroblasts (18). Genetic changes include decreased immediate early *c-fos* expression in response to mitogenic stimulation in senescent HDF (19). Senescent cells also express β-galatactosidase which is not expressed by quiescent, terminally differentiated, or immortal cells (21,22,23,24). Along with increased collagenase expression, the extracellular matrix protein, fibronectin is also overexpressed in senescent cells (25).

Other senescence–associated changes include but are not limited to the alteration of expression/regulation of numerous transcription factors such as AP-1, FosB, JunB, E2F-1, E2F-2, E2F-5 which are underexpressed (18,26). In addition to altered expression of cell cycle proteins, replicative senescence is also accompanied by an upregulation of p53, $p21^{Sdi,Cip1,Waf1}$, and p16 protein which collectively function to induce a permanent cell cycle growth arrest (29).

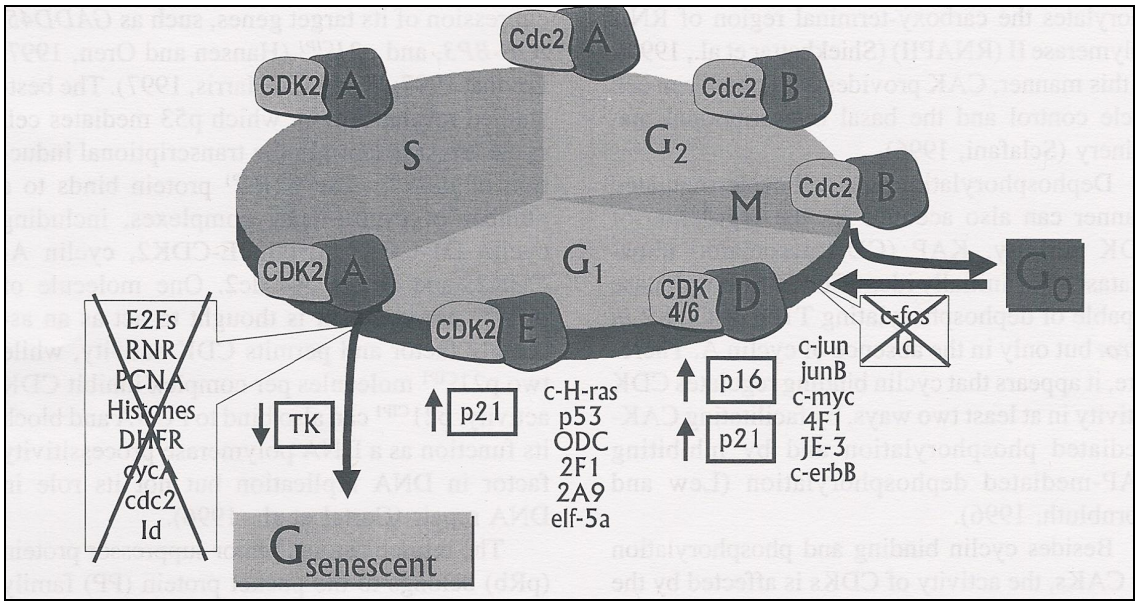


**Figure 3.** The orderly progression of cells through the G1 phase, DNA synthesis ( S-phase), G2 and mitosis (M phase) is regulated by CDKs bound to their cyclin partners (18).

During the G1 phase of the cell cycle phosphorylation of the retinoblastoma protein, pRb is carried out by both Cyclin D-Cdk4/6 and Cyclin E- CDK2 complexes and this phosphorylation event releases the E2F transcription factors which are required for the expression of genes that are in turn required for the initiation of the S-phase (30). Many of the cell cycle regulatory proteins such as the cyclin-dependant protein kinases (CDK-1, CDK-2, CDK-4) and cyclins (Cyclins A, B, D3, H) are underexpressed in senescent fibroblasts (reviewed in 18). CDK4 and CDK6 are required by the mitotic machinery to traverse the G-1 phase of the cell cycle and in senescent cells the activity of these kinases is decreased. This is partly due to the expression of high levels of the cyclin dependant kinase inhibitors (CDKI) $p21^{Sdi,Cip1,Waf1}$ and $p16^{INK4}$ : in late passage cells $p21^{Sdi,Cip1,Waf1}$ associates with both CDK2-Cyclin E complexes and CDK4/6-Cyclin D complexes. $p16^{INK4A}$ exclusively associates with CDK4/6-CyclinD complexes

(24,29). Conversely, absence of $p16^{INK4A}$ relieves its inhibitory effect in CDK4/cyclinD complexes and allows for Rb phosphorylation with subsequent E2F-1 accumulation. The activity of the retinoblastoma protein, pRB is modulated by phosphorylation and one of its functions is to interact with and bind to a class of transcription factors known as the E2F family. In the hypophosphorylated form pRB is active and binds E2F $^{1-3}$ and prevents the induction of genes that require E2F for expression (30).

A second growth suppressor protein expressed from the INK4a locus, $p14^{ARF}$ upregulates p53 protein levels by targeting the ubiquitin ligase MDM2 for degradation. MDM2 negatively regulates p53 protein levels (31,32). Both p53 and Rb are believed to play important roles in the establishment and maintenence of the senescent phenotype. These two tumor-suppressor genes undergo senescence- related changes. p53 functions as a transcription factor and has a role in cell cycle arrest, and is normally found in low levels in growing cells. In response to DNA damage or hypoxia the transcriptional activity and protein levels of p53 increase which results in an increase in the expression of its target genes, p21, GADD45, and IGF-BP3 (22,33,34). $p21^{Sdi,Cip1,Waf1}$ acts as a CDK inhibitor and contributes to cell cycle arrest.

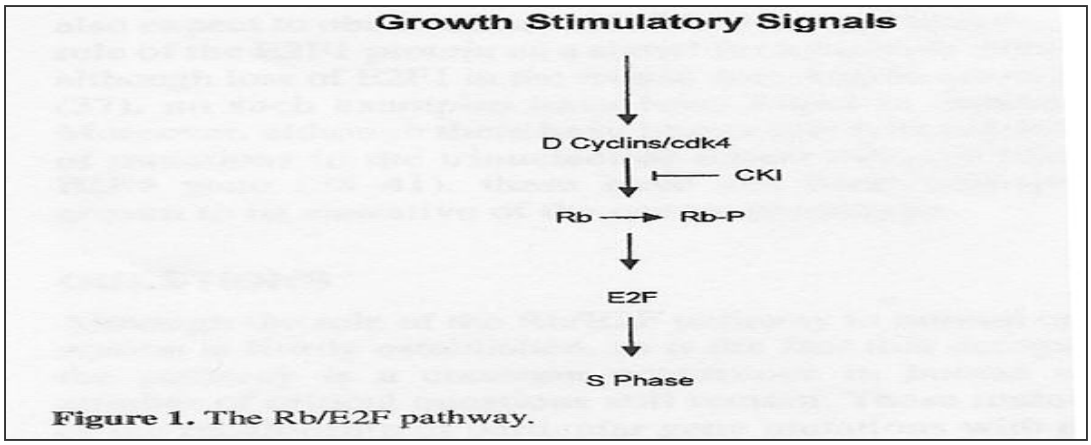


**Figure. 4.** The Rb/E2F pathway and cancer (30.)

In addition to the underexpressed cell cycle regulatory proteins, senescent cells underexpress genes which are known to be involved in DNA/protein synthesis, repair, and structure such as the replication dependant histones, H1, H2a, H2b, H3, H4, PCNA , and Polα (19,36,37,38,39).

Recent studies have demonstrated a reversal of cellular senescence in senescent HDF using lentiviruses to stably express genes in non-dividing cells (40,41). This reversal was dependant upon protein levels of the tumor suppressor p16 which regulates pRB. When p53 was inactivated, senescent fibroblasts with low levels of p16 underwent proliferation while those expressing high levels of p16 failed to do. These studies concluded that a telomere-dependant growth arrest maintained by p53 was reversible by p53 inactivation however cells with high levels of p16 were unable to proliferate in the presence of inactivated pRb (40).

What is the relevance of replicative senescence to organismal aging? Early studies which inversely correlated donor age with *in vitro* life span have been re-evaluated with the conclusion that definitve evidence for this relationship is lacking. Furthermore studies have demonstrated that there is no significant age correlation with *in*

*vitro* life span studies in HDF (42,43). However, the HDF as a cellular model for aging has been widely utilized to study both genetic and regulatory mechanisms under controlled environmental conditions.

## 1.2 Heterogeneous Nuclear Ribonucleoproteins

hnRNP's, heterogeneous nuclear ribonucleoproteins are RNA-binding proteins which are predominantly found in the nucleus and form complexes with RNA polymerase II transcripts.(44). They bind to specific sequences on pre-mRNA which are important for pre-mRNA processing such as the 5'and 3' splice sites and the polypyrimidine stretch, (45,46,47,48). Collectively, hnRNP's are proteins which bind heterogeneous RNA (hnRNA) and are not stable components of other ribonucleoprotein complexes such as the small nuclear RNP's (snRNP's) (23). To date about 24 major hnRNP's designated hnRNP A to U have been identified by immunoprecipitation as components of hnRNP's *in vivo* (49,50,51). These proteins associate with nascent mRNA (pre-mRNA) in the nucleus and facilitate mRNA processing in association with hnRNP's and other RNA-binding proteins (52). hnRNP's in general have multiple functions which include regulation of alternative splicing, rRNA transcription, mRNA transport, polyadenylation, mRNA stability and turnover, and telomere biogenesis (18). These proteins are expressed in a cell-type specific manner *in vivo* and studies have shown that hnRNP's predominate in the nucleus however, hnRNP proteins such as A1, D, F/H also localize to the cytoplasm of several tissues (44).

hnRNPs have a modular structure consisting of one or more RNA binding modules and an auxillary domain (52). Currently three types of RNA binding domains have been identified: 1) the RBD/RRM/RNP-CS motif which is a RNA-binding domain/RNA-recognition motif/RNP consensus motif; 2) the RGG box, and 3) the K-homology (KH) motif (52).

hnRNP A1 is a protein which in addition to hnRNP A2, B1/B2, C1/C2 comprise a basic core group of modular RNA binding proteins that are immunologically related to easc other (55,62,63). hnRNP A1 protein is among the best characterized of the 24 hnRNP proteins identified thus far. This basic protein migrates in the 34 kDa range (55, 56). Structurally hnRNP A1 protein consists of two copies of the RNA-recognition motif (RRM) at the N-terminal and a glycine-rich (RGG box-containing) auxiliary domain at the C-terminal. (49). RNP 1 and RNP 2 are conserved submotifs of RRM 1 and RRM2. RNP 1 consists of an octapeptide which is the most conserved segment of the RNP motif while the RNP 2 hexapeptide is not as conserved (52,56).

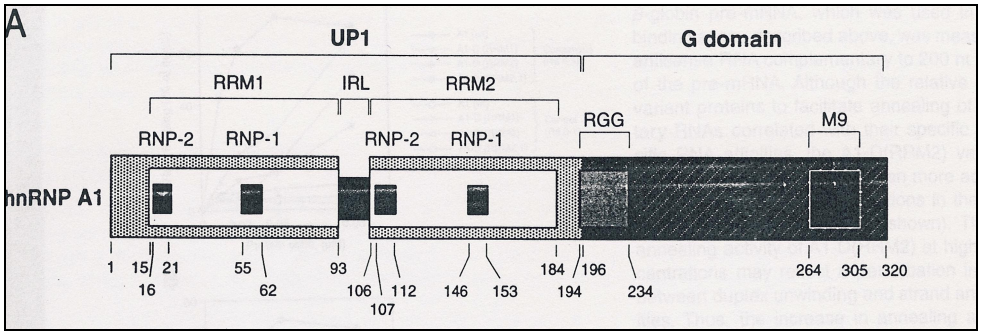


**Figure 5.** Schematic domain structure of human hnRNP A1 (52).

The binding features of this motif have been determined in part by peptide binding studies and by photochemical crosslinking of phenyalanine residues with RNP 1 and RNP 2 motifs (59,69). The carboxy terminal RGG box has closely spaced Arg-Gly Gly repeats and this domain has been postulated to mediate protein -protein interactions and indeed the glycine-rich carboxy domain of hnRNP A1 has been shown to selectively interact with other RNA-binding domains (61). The UP1 component is the proteolytic product of hnRNP A1 that lacks the C-terminal domain.

In addition the C-terminal domain contains a short sequence called M9 which is required for the shuttling properties of A1 (64). This sequence (amino acids 268-305) is involved in the bidirectional transport of hnRNP A1 (65,66,67). The M-9 motif interacts directly with two transport receptors, Trn 1 and Trn2b and mediates hnRNP A1 import (68,69,70). More recent studies have identified a short peptide sequence, the F-peptide (301-319aa) adjacent to the M-9 sequence which has been shown to mediate bidirectional transport of hnRNP A1 (71).

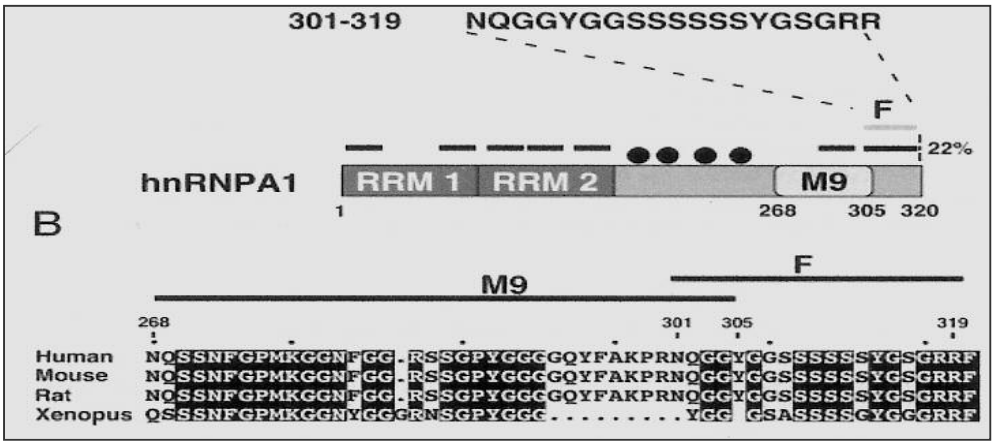


**Figure 6.** hnRNP peptides identified by MALDI-TOF (71).

The role of these motifs in the modulation of alternative splicing of pre-mRNA has been examined. hnRNP A1 has been demonstrated to antagonize the activity of SF2/ASF in 5' splice site selection; increasing the ratio of hnRNP A1 to SF2/ASF promotes the distal 5' distal splice site selection while higher concentrations of SF2/ASF promotes proximal 5' splice site selection (72). Subsequent analysis with variant recombinant proteins with either duplicated or deleted RRM's demonstrates that both RRM's are required for alternative splicing; however results suggested that RRM2 is significantly more involved in distal 5' splice site selection, see figure 5, (52). The C-

terminal glycine rich domain is necessary for alternative splicing activity and for stable RNA-binding and is also involved in strand annealing and in protein-protein interactions (56, 73).

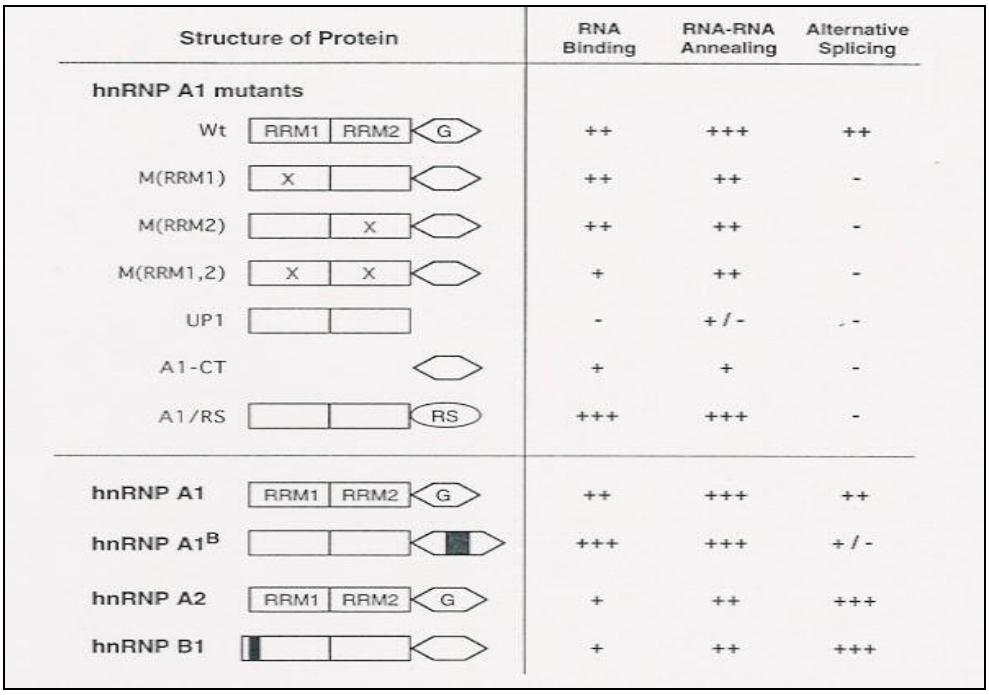


**Figure 7.** Summary of the activities of hnRNP A1 mutants and other hnRNP A/B proteins (56).

## Properties of hnRNP A1

hnRNP A1 protein has been extensively studied and the following illustrate its more relevant functions:

a) hnRNP A1 protein has been shown to be involved in the annealing of complementary RNA molecules *in vitro*, the net effect of which may be to enhance base-pairing interactions (74,75). Similarly, it may also serve to modify the conformation of pre-mRNA and therby facilitate splicing (76,77).

b) A1 protein is involved in telomere biogenesis and it has been shown that the ectopic expression of this protein promotes telomere elongation in mammalian cells in addition, both UP1 (the catalytic subunit of A1 residues 1-195) and A1 specifically bind single-stranded telomeric repeats *in vitro* as shown with gel shift assays (78). Recent studies have also demonstrated that hnRNP A1 protects telomeric sequences from nuclease activities *in vitro* (78).

c) hnRNP A1 shuttles between the nucleus and cytoplasm in both a transcription-dependant and independent manner (79). Furthermore UV crosslinking of RNA-protein complexes demonstrated that cytoplasmic A1 protein is bound to poly$A^+$ RNA (mRNA). These findings strongly suggest that A1 is involved in RNA export (79).

d) hnRNP A1 protein is also involved in modulating mRNA stability and turnover (85). AU-rich elements (ARE's) are repeated pentamer (AUUUA) sequences found in the 3'-untranslated region (UTR) of many unstable mRNA's (80). These conserved sequences promote the removal of the poly-A tail and destabilizes mRNA. AU-rich elements have been shown to act as binding sites for cytoplasmic and nuclear proteins (81,82,83,84) and accordingly function as important *cis*-acting sequences in posttranscriptional gene

expression (85). Cytoplasmic hnRNP A1 binds with high affinity to these reiterated sequences and in doing so confers mRNA stability *in vivo*; RNA polymerase II inhibition (with concomitant A1 cytoplasmic accumulation ) has been shown to decrease ARE-dependant mRNA turnover of c-fos mRNA (86). The regulation of mRNA turnover is intricately involved in the fate of cytoplasmic mRNA and factors which confer mRNA stability will ultimately affect gene expression.

e) hnRNP A1 protein has been previously shown to modulate the effects of the serine-arginine (SR) splicing factor 2, SF2/ASF and promote distal 5' splice site selection (56). This involvement in the regulation of alternative splicing is achieved through the antagonistic effects of hnRNP A1 protein. An increase in the concentration of SF2/ASF will promote selection of a proximal 5' splice site which is counteracted in a concentration-dependant manner by hnRNP A1 (56). Additionally crosslinking studies show that SF2/ASF and hnRNP A1 exhibit competitive binding to pre-mRNA (87).

f) More recently it was shown by Zhu et al., 2002 that hnRNP A1 expression levels affected the level of cell cycle mRNA isoforms. Overexpression of hnRNP A1 in HDF modulated the two mRNA isoforms of the INK4A locus, $p14^{ARF}$ and $p16^{INK4a.}$ Both proteins are known growth suppressors and when the ratio of hnRNP A1 to ASF/SF2 was increased it preferentially resulted in the generation of $p14^{ARF}$ isoform, consistent with the selection of the more distal 5' splice site, figure 8 (88).

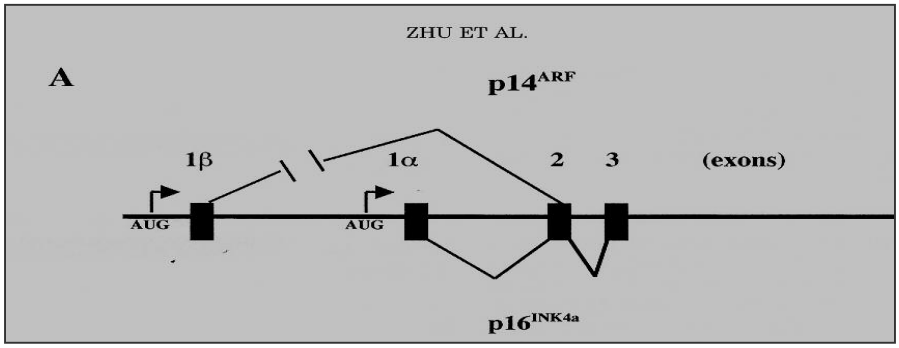


**Figure 8.**Schematic illustration of the INK4A locus (88).

g) Concentrations of SR proteins and hnRNP A1 proteins vary in different cell types and and this differential expression may affect alternative splicing of many pre-mRNA's, Rooke et al., 2003 found that hnRNP A1 is involved in the regulation of C-src exon 1 and may act as a splicing repressor of c-src (89).

## Posttranslational modifications of hnRNP A1

Phosphorylation is involved in the regulation of protein binding to nucleic acids, and reversible phosphorylation has a significant role in the regulation of key cellular processes such as cell cycle, growth, differentiation, and apoptosis (123,126,160). In addition phosphorylation can alter protein-protein interactions, induce conformational changes in protein structure, and target proteins for degradation. hnRNP's undergo several types of post-translational modifications: phosphorylation of serine residues, methylation of arginine residues, sumoylation and, ubiquitination. (90,91,92,93,94). hnRNP's A,B,C,G,K,and U are all phosphorylated *in vivo* (95,55,96). The *in vitro* strand-annealing activity of hnRNP A1 protein is diminished when it is phosphorylated by protein kinase C ζ, (PKCζ). Subsequent dephosphorylation by protein phosphatase 2A (PP2A) restored the strand annealing activity of hnRNP A1 (97). Strand annealing activity can mediate the RNA-RNA interactions which occur in the spliceosome and are crucial to the splicing process (98). Overexpression of PKCζ or PKA can induce cytoplasmic accumulation of hnRNP A1 (71,94,96). Moreover the accumulation of cytoplasmic hnRNP A1 is regulated by phosphorylation (71). It has been demonstrated that in response to osmotic shock hnRNP A1 localized to the cytoplasm in a p38 MAP kinase mediated manner (93). This cytoplasmic localization of hnRNP A1 affected the selection of distal 5' splice site usage by lowering the concentration of hnRNP A1 to splicing factor SF2/ASF in the nucleus and thereby promoting *proximal* 5' splice site selection. Thus the cellular distribution of hnRNP A1 protein due to post-translational modification appears to have relevant downstream effects on its' RNA binding properties and on subsequent RNA processing.

## 1.3 p38 MAP kinase

MAP kinases encompass signal transduction pathways that regulate cellular proliferation, differentiation and survival. There are three major classes of kinase pathways which include p38 MAP kinase and c-Jun N-terminal kinases (JNK) which are strongly activated by environmental genotoxic stress stimuli as well as the extracellular signal-regulated kinases (ERK1 and ERK2) which are both activated in response to mitogenic stimulation (99).

Each family of MAP kinase is composed of a module of three kinases: a MAP kinase kinase kinase (MKKK) which phosphorylates and activates a MAP kinase kinase (MKK), which then phosphorylates and activates a MAP kinase, MAPK (100). The upstream MAPKKK's are serine/threonine kinases and are activated after phosphorylation or by interacting with a small GTP- binding protein of the RAS or Rho family in response to extracelluar stimuli (101). p38 MAP kinase has four different isoforms (α,β,γ,δ) which are 57-73% identical in their amino acid sequences but have different expression patterns and sensitivities to the pyridinyl imadazole inhibitors, SB203580 and SB202190 (102,103,104,105,106). These two inhibitors interact with and inhibit p38 MAP kinase isoforms α and β (107). Other differences include differential activation by MKK 3,4, and 6 (106, 108); and substrate specificities ( 106,107,108).

p38 MAP kinase is activated by MKK3/6 which results in the dual phosphorylation of the threonine and tyrosine residues of the -Thr-Gly Tyr- -sequence located in the activation loop (T-loop) (109). Activated MAP kinases can be deactivated by dephosphorylation at the activating residues, tyrosine or threonine residues or both, by the action of dual specificity phosphatases (DSP) which are also called MAP kinase

phosphatases (MKP) (110). MAPK's are present in the nucleus where they phosphorylate numerous transcription factors (111,112,113). However, once activated, MAPK can activate transcription factors and downstream kinases in various cellular compartments (100). Other studies have demonstrated that that p38 MAP kinase is present in both nuclear and cytoplasmic compartments and activation by UV radiation does not induce a substantial redistribution of p38 MAP kinase from the cytoplasm to the nucleus (114).

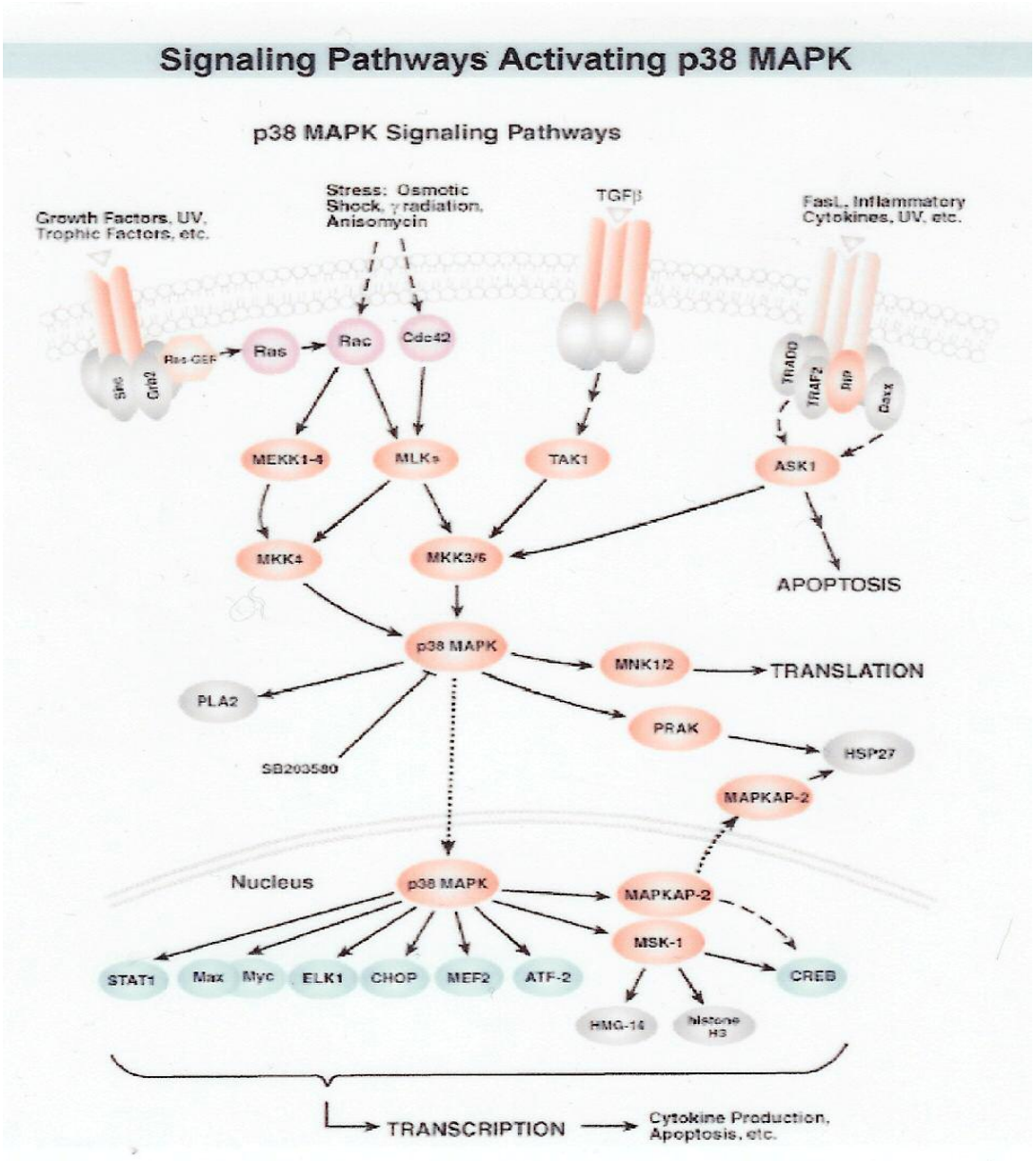


**Figure 9**. Overview of the p38 MAP kinase signaling pathway (Cell Signaling™).

## 1.4 Significance of phosphorylation of hnRNP A1 during replicative senescence

Heterogeneous nuclear ribonucleoproteins are RNA binding proteins which form complexes with RNA polymerase II transcripts. hnRNP A1 is well characterized and has been found to modulate splice-site usage and general splicing factors. In addition hnRNP A1 binds with high affinity to A-U rich sequences at the 3' untranslated region of many unstable mRNA's which confer stability *in vitro* (85). This protein shuttles between the nucleus and cytoplasm and has a role in RNA export (79).

hnRNP A1 is phosphorylated *in vivo*, however it is only weakly phosphorylated under steady state conditions. Three major studies published in the 1990's examined the effects of phosphorylation of hnRNP A1 on its RNA-binding activities. These studies collectively identified serine residues as major sites for phosphorylation by PKA and PKCζ. The phosphorylation of hnRNP A1 on specific serine residues was shown to diminish its strand annealing properties and regulate the RNA binding properties of cytoplasmic hnRNP A1 (85,96,97).

Recent studies have shown that hnRNP A1 cytoplasmic accumulation in response to osmotic shock is modulated by phosphorylation of a short peptide sequence adjacent to the M-9 motif (71). Furthermore cytoplasmic accumulation of hnRNP A1 was shown to affect its alternative splicing regulation (93). Thus phosphorylation of hnRNP A1 can therefore potentially modulate both its nuclear and cytoplasmic RNA processing activities.

Protein levels of hnRNP A1 have been shown to to decrease in senescent HDF with a concomitant decrease in its *in vitro* RNA binding activity (116). Our preliminary

studies suggest that the levels of phosphorylated hnRNP A1 increases relative to its total protein level in senescent HDF. We have also observed a distinct cytoplasmic localization of hnRNP A1 in senescent HDF compared to young HDF. Collectively these findings suggest that post-translational modification by phosphorylation of hnRNP A1 may have a regulatory role during senescence.

The experimental goals outlined in this study are to examine phosphorylation of heterogeneous nuclear ribonucleoprotein A1 (hnRNP A1) as a function of *in vitro* age in IMR-90 HDF. Furthermore, evidence for involvement of the stress-activated kinase, p38 MAP kinase as a putative modulator of hnRNP A1 protein levels will be examined. Our hypothesis is that phosphorylation of hnRNP A1 in senescent fibroblasts results in its differential subcellular localization which may in turn affect gene expression during replicative senescence and contribute to the senescent phenotype.

# Chapter 2.

# Materials and Methods

## 2.1 Cell strains and culture conditions

Experiments were carried out with young, $G_0$-arrest, and senescent IMR-90 fibroblasts. This cell strain was derived from fetal lung fibroblasts and cells were cultured at 37$^{o}$C in DMEM-HAM media supplemented with 10% fetal bovine serum (FBS) and 1% penicilllin/streptomycin (Mediatech, Gibco-Life technologies). Cells were kept in a 37$^{o}$C, 5% $CO_2$ incubator. Media was changed twice weekly and cells were serially passaged at a ratio of 1:4 for IMR-90 cell until terminal passage was reached (13). IMR-90 fibroblasts undergo up to 70 population doublings before reaching a senescent state. Population doublings were calculated as follows: it was determined that each 1:4 split represents two population doublings for previous experiments in which cell numbers were determined at each passage (13). Growth arrest cells were prepared by replacing 10% FBS supplemented media with 0% FBS supplemented media for 72 hours. Experiments were also carried out in the human diploid fetal bone marrow fibroblast cell strain HS-74 obtained from H. Smith (117). Life span determinations have been previously described (118).

## 2.2 Cell lysis and protein quantitation

Each culture dish was rinsed 3 times with ice cold 1X phosphate buffered saline (PBS) and placed on ice. <u>For detection of phosphorylated hnRNP proteins:</u> 0.5 ml of cold 1% Empigen BB buffer in 1X PBS containing 1mM EDTA, 0.1mM dithiothreitol, 10mM sodium fluoride and 100ul of Sigma phosphatase inhibitor cocktail I was added to each 100mm culture dish. Plates were scraped and lysate was collected in a 1.5 ml microfuge tube and sonicated for 5 seconds 3 times. The lysate was cleared at 14,000g for 10 minutes. Supernatant was transferred to a fresh microfuge tube, and immediately added

to immunoprecipitation reaction. For co-immunoprecipitation assays: cells were prepared under non-denaturing lysis conditions in 1ml of 1X cell lysis buffer from Cell Signaling containing 20mM Tris (pH 7.5), 150mM sodium chloride, 1mM EDTA, 1mM EGTA, 1% Triton X-100, 2.5mM sodium pyrophosphate, 1mM sodium vanadate, 1ug/ml leupeptin, and 1mM PMSF. Plates were incubated on ice for 5 minutes, scraped, transferred to microfuge tube, sonicated for 5 seconds 3 times. Lysates were cleared at 14,000g for 10 minutes, transferred to fresh microfuge tube and stored at -80$^{o}$C. All other lysates were prepared in 1X SDS-lysis buffer containing 62.5mM Tris-HCl (pH 6.8 at 25$^{o}$C, 2% SDS, 10% glycerol, 50mM DTT, 0.01% w/v bromophenol blue, sonicated for 5 seconds 3X, and stored at -80$^{o}$C. Protein concentration was quantified in triplicate by Bradford-Lowry protein assay (Bio-Rad™) using bovine serum albumin as a standard for protein concentration.

**2.3 Immunoprecipitation**

Whole cell lysates were immunoprecipitated for hnRNP A1 and C proteins using 4B10 and 4F4 monoclonal antibodies, respectively, generously provided by Dr. Serafin Pinol-Roma (50, 119). 200ul of 4B10 or 3ul 4F4 antibody were pre-incubated with 20 ul of Protein A-sepharose beads for 1 hour at 4$^{o}$C followed by incubation with lysate for 1 hour at 4$^{o}$C. Immunoprecipitates were microcentrifuged, washed 3 times with lysis buffer, resuspended in 2x sample buffer and immediately subjected to 12% SDS-PAGE. All other immunoprecipitations were performed according to manufacturer's protocol.

**2.4 Immunoblot analysis**

Cell extracts and immunoprecipitates were identified immunologically using standard immunoblot protocols (152). These were suspended in protein sample loading buffer (120), separated by 12%% SDS-PAGE and run at 120V 50mA for 4 hours. Proteins were transferred to a PVDF membrane electrophoretically in 25mM Tris base, 190mM glycine, and 20% ethanol. Nonspecific binding was blocked by incubating the blot for 1 hr in blocking buffer: 5% nonfat dry milk in 1x TBS-Tween-20. Membranes were incubated in a 1:15 dilution of 4B10 in 3% bovine serum albumin (BSA), 0 .1% Tween-20 in 1X PBS overnight at $4^{o}$C. Blots were washed 3 times for 5 minutes each in wash buffer (1X PBS- 0.1% Tween-20.) Blots were then incubated in a 1:2000 dilution of $2^{o}$ anti-mouse-HRP conjugated antibody for 1 hour at room temperature. Blots were washed 3 times for 10 minutes each in wash buffer, followed with detection of protein bands using enhanced chemiluminescence (ECL-Plus™) from Amersham.

**2.5 Metabolic labeling studies**

HS-74 HDF were metabolically labeled overnight with 0.5mCi/ml $^{32}$P-ortho-phosphate and cell lysates were prepared in RIPA buffer (1% NP-40, 1% sodium deoxycholate, 0.1% SDS, 0.15M NaCl) containing 10ug/ml of leupeptin and pepstatin, 1mM phenylmethylsulfonyl fluoride, 0.25mM orthovanadate, 20mM B-glyerophosphate and 10mM sodium fluoride. Endogeneous hnRNP A1 was immunoprecipitated with 4B10 monoclonal antibody and its phosphorylation was determined by autoradiography following 12% SDS-PAGE.

## 2.6 SYPRO™ Molecular Probes total protein stain of hnRNP A1

Cell lysates were immunoprecipitated with 4B10 and subjected to 15% SDS-PAGE. Gels were fixed in 50% methanol and 10% acetic acid, washed 3x with dH2O, stained in 100 ml SYPRO total protein stain followed by destaining in 15% 1,2-propanediol and 50mM sodium acetate, pH 4.0. Protein bands were visualized with a UV transilluminator and images were obtained with a Kodax 667 black and white film.

## 2.7 Immunodetection of phosphorylated hnRNP A1

Cells were prepared under conditions that disrupt the hnRNP core complex: these were lysed in 0.5ml 1% Empigen BB detergent with added phosphatase inhibitors, and sonicated for 5 seconds, 3 times each. Samples were cleared at 14,000g for 10 minutes at 4$^{o}$C and incubated with 4B10- Protein-A-sepharose beads at 4$^{o}$C for 1 hour. The immune complex was collected and extensively washed with lysis buffer. Beads were drained of excess buffer with a loading tip and resuspended in 2X sample loading buffer containing dithiothreitol. Immunoprecipitation reactions were subjected to 12.5% SDS-PAGE, transferred to PVDF membrane, and blocked for 1 hour in 3% BSA in 1X PBS-0.5% Tween-20. Membranes were washed in wash buffer (0.5%T-20 1XPBS) 3 times for 10 minutes followed by incubation in 1ug/ml anti-phosphoserine antibody (Zymed™) for 1 hour at room temperature. The membranes were washed 3 times for 10 minutes and incubated in a 1:2000 dilution of 2$^{o}$ HRP-anti- rabbit antibody. Membranes were washed 3 times 10 minutes and bands visualized using enhanced chemiluminescence (ECL PLUS™).

## 2.8 Immunofluorescence microscopy

Cells were cultured overnight in chamber slides and fixed with 4% paraformaldehyde for 20 minutes at room temperature and washed in PBS 3 times followed by incubation in 2% Triton-X 100 for 10 minutes at room temperature. Wells were washed 3 times for 5 minutes each with 1X PBS, followed by incubation in a 1:15 dilution of 4B10 and 1:1000 7G2 (hnRNP A1 and nucleolin respectively), in a 3% BSA, 1X PBS solution. (Antibodies kindly donated by Dr. Pinol-Roma). The wells were washed 3 times with 1X PBS and incubated at room temperature with a 1:500 dilution of anti-mouse fluorescence-linked whole antibody from sheep (Amersham Life Sciences™) in 3% BSA, 1X PBS. Wells were washed 3 times in 1X PBS for 10 minutes at room temperature, drained of excess PBS, and coverslipped. Fluorescence was detected by Axioplan fluorescence microcope at a magnification of 400x. Images were documented with AxioVision™ software.

## 2.9 *In vitro* dephosphorylation of hnRNP A1 by PP2A

Cells were cultured under the appropriate conditions and prepared in Empigen lysis buffer with and without phosphatase inhibitor cocktail I (Sigma™). These lysates were assayed and immediately subjected to the following experimental conditions: a) 400ug of lysate (prepared with and without Phosphatase inhibitors) was dephosphorylated *in vitro* by adding 0.4U* of Protein Phosphatase 2A (PP2A Ser/Thr) from US Biologicals and incubating the reaction at 30$^{o}$C for 2 minutes (121,122,123,124,125,126). The reactions were placed on ice followed with immunoprecipitation with preincubated 4B10-Protein A Sepharose beads for 1 hour at 4$^{o}$C. The immune complex was collected and washed 3

times with lysis buffer, resuspended in 3X sample buffer, boiled for 5 minutes, vortexed, microcentrifuged for 1minute, and separated by 12% SDS-PAGE. The membranes were immunoblotted with a 1ug/ml dilution of Zymed™ anti phosphoserine polyclonal antibody, a 1:500 secondary anti-rabbit antibody followed with detection using ECL™Plus. Protein Phosphatase 2A is inhibited with 10nm okadaic acid (US Bio™). For the second experimental condition, cells were incubated wth 10nm okadaic acid for 2 hours at 37°C. Cell lysates were prepared with 1% Empigen BB lysis buffer in the absence of phosphatase inhibitors. These samples were prepared as discussed above. *Unit definition: one unit releases 1nmole of phosphate per min from 15uM ($^{32}$P) labeled Phosphorylase A at 30°C.

**2.10 p38 MAP kinase Assay (Cell Signaling™)**

Cells were cultured under appropriate conditions and lysed in 1X cell lysis buffer containing 20mM Tris (pH 7.5), 150mM sodium chloride, 1mM EDTA, 1mM EGTA, 1% Triton X-100, 2.5 mM sodium pyrophosphate, 1mM sodium vanadate, 1ug/ml leupeptin, and 1mM PMSF (Cell Signaling™). Plates were incubated on ice for 5minutes, scraped, transferred to microfuge tube and sonicated 3 times for 5 seconds each on ice. Lysates were cleared at 14,000g for 10 minutes at 4°C, transferred to a fresh microfuge tube, and aliquoted. Protein concentration was determined using Bio-Rad reagents. 200ug of total protein lysate was incubated with 20ul of resuspended Immobilized Phospho-p38 MAP (P-p38) kinase (Thr180/Tyr182) antibody (Cell Signaling). The IP reactions were incubated with gentle rocking overnight at 4°C and microcentrifuged. The immune complex was washed 2 times with 500ul 1X lysis

buffer, 2 times with 500ul 1X kinase buffer and resuspended in 50ul 1X kinase buffer supplemented with 200uM ATP and 2ug ATF-2 fusion protein. The reactions were incubated for 30 minutes at 30$^{o}$C and terminated with 25ul 3X SDS sample buffer. Reactions were boiled for 5 minutes, vortexed, micro-centrifuged for 2 minutes, and loaded onto 12% gel followed by SDS-PAGE. Gels were electrophoretically transferred to PVDF membrane, followed with immunoblotting with primary antibody to Phos-ATF-2 (Thr 71). The protein bands were visualized using ECL-Plus™.

**2.11 *Co*-immunoprecipitation analysis**

Cells were cultured under appropriate conditions and lysed in 1X cell lysis buffer from Cell Signaling containing 20mM Tris (pH 7.5), 150mM sodium chloride, 1mM EDTA, 1mM EGTA, 1% Triton X-100, 2.5 mM sodium pyrophosphate, 1mM sodium vanadate, 1ug/ml leupeptin, and 1mM PMSF, incubated on ice for 5 minutes, scraped, transferred to a microfuge tube and sonicated 4 times for 5 seconds each on ice. Lysates were cleared at 14,000g for 10 minutes at 4$^{o}$C and transferred to fresh microfuge tube, and aliquoted. Protein concentrations were determined and normalized for all samples. Depending upon the experiment different amounts of protein were incubated with 20ul of resuspended Immobilized Phospho-p38 MAP kinase (Thr180/Tyr182) beads (Cell Signaling™). These IP reactions were incubated with gentle rocking overnight at 4$^{o}$C, the immune complex was microcentrifuged washed 4X with 500ul 1X lysis buffer, resuspended in 3X SDS sample buffer, boiled for 5 minutes, vortexed, microcentrifuged for 1 minute, followed by 12% SDS-PAGE. This was followed with immunoblotting with antibodies to the following proteins hnRNP A1, hnRNP C, GAPDH, BAX, and

endonuclease G. Lysates were also immunoprecipitated with 4B10 (as described earlier) and immunoblotted with antibodies to p38 MAP kinase and P-p38 MAP kinase.

### 2.12 Inhibition of *in vivo* p38 MAP kinase activity

In order to observe the effects of *in vivo* p38 MAP kinase inhibition on total hnRNP A1 levels in IMR-90 fibroblasts, log phase and senescent cells were treated with 2.5uM SB203580 or dimethyl sulfoxide (DMSO) equivalent for 1 hour at 37$^{o}$C. Lysates were collected in the appropriate lysis buffer for whole cell and co-immunoprecipitation analysis.

The levels of hnRNP A1 in SB203580 or DMSO treated IMR-90 cells were assayed by immunoblotting of normalized whole cell lysates prepared from log phase, G-$_0$ arrest, and senescent cells treated with 2.5uM SB203580 for 1 hour. Cells prepared under the same experimental conditions were immunoprecipitated with Immobilized Phospho-p38 MAP kinase (Thr180/Tyr182) beads, subjected to 12% SDS-PAGE and immunoblotted with 4B10 antibodies.

### 2.13 Transient transfection studies

The pGFP-hnRNP A1 expression vector has been previously described (92) and the pCMV-Flag-p38 plasmid was kindly provided by Dr. Roger Davis and has been previously described (161). The pFLAG-CMV™ and pFLAG-CMV-BAP™ (bacterial alkaline phosphatase) control vectors were obtained from Sigma™. These were transformed into One Shot® TOP 10 Competent cells from Invitrogen™ using the manufacturer's protocol, briefly: 1 ul of each plasmid was added to 50 ul of One Shot®

cells, incubated on ice for 30 minutes, incubated for 30 seconds in a 42°C water bath. 250 ul of pre-warmed S.O.C. medium was added to each reaction and incubated at 37°C for 1 hour at 225 rpm. 100 ul from each transformation reaction was plated onto LB agar plates with either 50 ug/ml kanamycin (pGFP-hnRNP A1) or 100 ug/ml ampicillin (pCMV-Flag-p38) to verify the absence of antibiotic resistant contamination. Plates were incubated overnight at 37°C and individual colonies were picked for minipreps. Plasmid DNA was isolated using QIAprep® miniprep kit (Qiagen™). Plasmid samples were eluted into 100 ul EB buffer (10mMTris-Cl, pH 8.5) and stored at 4°C.

**2.14 Transfection protocol**

Young IMR-90 HDF cultured in 100mm Petri dishes were transfected with pGFP, pGFP-hnRNP A1, pCMV-Flag-p38, pFLAG-CMV™ or pFLAG-CMV-BAP™ using Lipofectamine™2000 (Invitrogen™) according to manufacturer's protocol. Briefly, cells were plated in antibiotic free media supplemented with 10% FBS and grown to 90% confluency. Complexes were prepared at a ratio of 1:2.5 (ug DNA to Lipofectamine2000™) and complexes were added to plates and incubated at 37°C in a $CO_2$ incubator for 6 hours after which media was removed and 10 ml antibiotic-free media supplemented with 10% FBS was added to each plate and incubated for 48 hours. Plates were washed 3 times with 1X PBS and lysed under both denaturing and non-denaturing lysis conditions. Exogenously expressed GFP- hnRNPA1 was detected using a GFP mouse monoclonal antibody (BD Bioscience™) and the 4B10 antibody. A mouse monoclonal antibody against the FLAG epitope, M-2 antibody (Sigma™) was used to immunoprecipitate pCMV-FLAG, pCMV-FLAG-BAP, and pCMV-p38-Flag.

**2.15 Antibody Panel**

| Antibody | Specificity |
|---|---|
| 4B10 | hnRNP A1 |
| 4F4 | hnRNP C |
| 7G2 | nucleolin |
| p38 MAP kinase | total p38 MAP kinase (phosphorylated and unphosphorylated) |
| Phos p38 MAP kinase | phosphorylated p38 MAP kinase (Thr180/Tyr182) |
| GFP | green fluorescent protein (both N- and C- terminal fusion proteins) |
| M-2 anti-FLAG | FLAG epitope (recognizes FLAG peptide sequence at the N-, C-, or Met-N- terminus) |
| BAX | BAX |
| GAPDH | GAPDH |
| Endonuclease G | Endonuclease G |
| Actin | Actin |

4B10, 4F4, and 7G2 antibodies were all generously provided by Dr. Serafin Pinol-Roma

# Chapter 3.

# Phosphorylation of hnRNP A1 and its subcellular distribution in human diploid fibroblasts as a function of *in vitro* age

## 3.1 Introduction

Normal human diploid fibroblasts (HDF) in culture undergo a limited number of cell divisions before entering a terminal and irreversible growth phase termed replicative senescence (1). These cells arrest in the G-1 phase of the cell cycle and while they remain viable in culture there are associated changes in morphology and gene expression (15,18). The changes include an enlarged cell size, increases acidic β-galactosidase activity and decreased expression of numerous transcripition factors such as c-fos, Jun-B, and E2F-1 (18). There is concomitant upregulation of cyclin dependant kinase inhibitors (CDKI) p21 and p16 (24,28,29). Senescent fibroblasts are unresponsive to serum stimulation and fail to phosphorylate the retinoblastoma protein (pRb) which prevents the release of the E2F transcription factors which are required for entry into the S-phase of the cell cycle (50).

Posttranslational modification of proteins has a major role in the regulation of protein binding to nucleic acids whereby reversible phosphorylation regulates in part key cellular processes such as cell cycle growth, differentiation, and apoptosis (123,126,160). The tranverse through the cell cycle is controlled by cyclin-CDK interactions that are mediated by reversible phosphorylation. Major signaling pathways are regulated by phosphorylation and other posttranslational mechanisms that underlie important homeostatic mechanisms.

## 3.2 Results

### A. Comparison of protein expression of hnRNP A1 in IMR-90 log phase, $G_0$-arrest, and senescent HDF.

Hubbard et al., 1995 had determined previously that in HS-74 human diploid fibroblasts the levels of hnRNP A1 were lower in senescent HDF when compared to young HDF (116). To determine whether this was the case for IMR-90 fibroblasts, immunoblot analysis was performed using cultures of young, $G_0$-arrest, and senescent IMR-90 fibroblasts.

Since hnRNP A1 is in a complex with at least 20 other hnRNP proteins, the effective disruption of this complex during lysis was an essential step for determination of antibody specificity (49). Therefore, lysates were prepared using 1% Empigen BB lysis buffer, a zwitterionic detergent previously characterized for disruption of the hnRNP core complex (119). We performed differential immunoblot analysis of whole cell lysates of hnRNP A1, hnRNP C, and nucleolin in order to test 4B10 specificity for the hnRNP A1 protein in IMR-90 HDF lysates.

The results for differential immunoblottting reveal distinct molecular weight bands for hnRNP A1, (34 kDa), hnRNP C, (40-45 kDa) (fig.11, panels a and b) , and nucleolin, 100kDa, (fig. 11, panel c) in identical whole cell lysates prepared in either Triton X-100, Empigen BB, or SDS lysis buffer.

Next we tested 4B10 immunoprecipitates by probing with either 4B10-hnRNP A1 or 4F4-hnRNP C antibodies and the results strongly suggest that the 4B10 antibody binds to only hnRNP A1 and not hnRNP C in the 4B10 immunoprecipitates (fig.12, lanes 2,3,4,&5).

These results strongly suggest that hnRNP A1 is preferentially selected in IMR-90 fibroblasts on immunoprecipitation with 4B10, an antibody specific for hnRNP A1. In addition a 34kDa band does not appear in the 4F4-hnRNP C blot. Therefore the hnRNP complexes were sufficiently disrupted with EmpigenBB, a detergent characterized for such purposes.

These studies were followed with immunoblot analysis of hnRNP A1 protein levels in log phase, $G_0$-arrest, and senescent IMR-90. The results suggest that hnRNP A1 protein levels are highly diminished in senescent IMR-90 HDF compared to log phase and $G_0$-arrested HDF, (fig.13, panel a, lanes 1-3) and actin levels confirm normalization of sample load (fig. 13, panel b, lanes 1-3). These results are consistent with that observed in HS-74 fibroblasts (116).

To further characterize A1 protein levels, we performed immunoblot analysis of 4B10-hnRNP A1 immunoprecipitates from all three growth states. These IP's were resolved by SDS-PAGE followed by SDS-PAGE. The gel was stained with SYPRO™ total protein stain to visualize protein bands. The findings presented suggest that immunoprecipitated hnRNP A1 protein levels are highly diminished in senescent HDF compare to both log phase and $G_0$ arrest immunoprecipitates (fig. 14, lanes 1-3).

**B. Relative levels of phosphorylated hnRNP A1 in senescent HDF**

We have previously hypothesized that the altered nucleic acid binding activities and localization pattern of hnRNP A1 might be due to post-translational modifications in HS-74 (88). Modification through phosphorylation was assessed in HS-74 fibroblasts in those studies. Log phase, $G_0$-arrest, and senescent HS-74 HDF were labeled with $^{32}$P

ortho-phosphate, lysed, immunoprecipitated with 4B10-hnRNP A1, and subjected to SDS-PAGE. Preliminary findings with metabolic labeling of young and senescent HS-74 suggests that phosphorylation of A1 is increased in senescent fibroblasts (fig. 15, lanes 1-3). Since total protein levels of hnRNP A1 are diminished in these senescent cells the results suggest that the majority of A1 is in the phosphorylated form in senescent fibroblasts. All subsequent phosphorylation studies were carried out in IMR-90 HDF using non- radioactive detection methods.

The rationale for all subsequent studies in IMR-90 HDF is that gene expression during senescence in IMR-90 fibroblasts have been well documented, these cells proliferate more readily than HS-74 and as discussed above, immunoblot analysis showed that A1 levels had similar protein expression patterns as has been observed in HS-74 fibroblasts.

To determine the detection sensitivity of the anti-phosphoserine antibody for phosphorylated serine residues, whole lysates from HeLa cells were prepared under conditions that would disrupt hnRNP core complexes (119). Lysates were prepared with and without phosphatase inhibitors. Extracts were immunoprecipitated using 4F4, an antibody specific for hnRNP C. hnRNP C in HeLa cells is highly phosphorylated *in vivo* (130) and thus served as a positive control for immunodetection of phosphorylated protein. The immunoprecipitates were subjected to SDS-PAGE and probed using anti-phosphoserine antibody (fig. 16, panel a, lanes 1 & 2). The same membrane was stripped and reprobed for total hnRNP C protein levels (fig. 16, panel b, lanes 1 & 2). The results suggest that in the presence of phosphatase inhibitors the signal representing phosphorylated hnRNP C in HeLa extracts was detectable compared to extracts prepared

in the absence of phosphatase inhibitors which lacked a detectable signal (fig. 16 panel a, compare lanes 2 and 3). The subsequent reprobing of the membrane with 4F4-hnRNP C reveal heavy bands corresponding to total hnRNP C which confirmed the immunoprecipitated fraction of the protein (fig. 16, panel b). Based on these results, the addition of phosphatase inhibitors to the lysis buffer was consistently performed in all future phosphorylation studies.

The next step was to perform phosphoserine immunoblot analysis using Hela extracts immunoprecipitated with 4B10 antibody to test relative levels of hnRNP A1 phosphophorylation to total hnRNP A1 protein levels. A band corresponding to a 34kDa protein in the phosphoserine immunoblot is suggestive of the phosphorylated fraction of hnRNP A1 protein in this sample which included a whole cell lysate (fig. 7, panel a). The mock 4B10 IP was used to establish the relative molecular weights of the heavy and the light chain IgG and to rule out false positive signals (fig.17, panel a, lane 2).

The membrane was stripped and reprobed with 4B10 antibody to determine total protein levels of hnRNP A1 and results suggest an abundance of this protein immunoprecipitated in this sample (fig. 17, panel b, lane 3). The collective results for immunodetection of both hnRNP C and hnRNP A1 proteins in Hela extracts strongly suggest that immunodetection of phosphorylated serine residues on hnRNP A1 is a valid method.

The levels of phosphorylated hnRNP A1 were tested in log phase and senescent HDF using anti-phosphoserine antibodies. Whole cell lysates were prepared in 1% Empigen BB lysis buffer, immunoprecipitated with 4B10, and subjected to SDS-PAGE.

This blot was probed first with anti-phosphoserine antibody (fig. 18, panel a), then stripped and reprobed with 4B10 in order to test total protein levels of hnRNP A1 (fig.18, panel b). Relative levels of phosphorylated hnRNP A1 are apparent in the log phase sample but are highly diminished in the senescent IP sample (fig. 18, panel **a**, lanes 2 and 3) due to the low overall protein levels (fig.18 panel b, lanes 2 and 3). A mock IP reaction containing 4B10 antibody and beads was included to establish the molecular weight of the heavy and light chains of the antibody which are also phosphorylated and to exclude the possibility of false positive bands. In this experiment we were unable to detect phosphorylated hnRNP A1 in the senescent lysate (fig. 18, panel a, lane 1).

The lysis conditions were further optimized and this experiment was repeated. The phosphorylated form of hnRNP A1 in the senescent IP sample was visualized as a faint band in the 34kDa range (fig. 19, panel a, lane 3) and the subsequent reprobing of the membrane with 4B10 confirms the presence of total hnRNP A1 in the senescent sample (fig. 19, panel b, lane 3). This suggests that while the overall levels of A1 are diminished in senescent IMR-90 fibroblasts the detection of this post-translationally modified protein may represent increased levels of the phosphorylated form of the protein.

**C. Detectable levels of phosphorylated hnRNP A1 are diminished with Protein Phosphastase 2A treatment (PP2A).**

To further confirm that we were detecting phosphorylated A1, experiments were performed in the presence of protein phosphatase 2A (PP2A) which specifically dephosphorylates serine/threonine residues. Figure 20 represents immunoblot analysis of phosphorylated hnRNP A1 in young IMR-90 HDF after treatment with PP2A.

In lanes 3, 5, and 7 0.4U of PP2A was added to 400 ug of IMR-90 extracts prepared in Empigen lysis buffer with or without phosphatase inhibitors (PI), immunoprecipitated with 4B10 and immunoblotted with anti- phosphoserine antibodies.

Lanes 4 & 5 plates were incubated with 10 nM okadaic acid and prepared in Empigen BB lysis buffer in the the absence of phosphatase inhibitors. Okadaic acid is a potent inhibitor of PP2A which dephosphorylates at ser/thr residues (131). These lysates were incubated with 0.4U of PP2A, immunoprecipitated with 4B10 antibody and immunoblotted with anti-phosphoserine antibodies.

These results show that hnRNP A1 is partially dephosphorylated by treatment with PP2A (lane 7) and this dephosphorylation appears to be inhibited by the addition of either phosphatase inhibitors in the lysis buffer or with *in vivo* treatment with 10nM okadaic acid (lanes 2 & 3, 4 & 5). The samples were tested for equivalent hnRNP A1 protein loads by subsequent reprobing of the membranes with hnRNP A1 antibody. However, this resulted in heavy overlapping signals for hnRNP A1 which were rendered unsuitable for analysis (data not shown).

Our findings are consistent with those previously observed which found that PP2A dephosphorylates hnRNP A1 at specific serine residues and these residues may

represent the dephosphorylated serine sites in this experiment (97). These results further validate the feasibility of the immunodetection of phosphorylated hnRNP proteins using anti-phosphoserine specific antibodies.

**D. Semi-quantitation of phosphorylated hnRNP A1 levels in IMR-90 HDF**

Four experiments were analyzed for the relative levels of phosphorylation by densitometry and were calculated for log and senescent HDF as the signal intensity of phosphorylated hnRNP A1 divided by the signal intensity of the total hnRNP A1 protein level (fig. 21). Our analysis suggests that relative phosphorylation of hnRNP A1 in IMR-90 HDF is higher in senescent HDF compared to young HDF.

**E. Subcellular distribution of hnRNP A1 and nucleolin in IMR-90 HDF as a function of *in vitro* age.**

hnRNP A1 has both nuclear and cytoplasmic localization patterns and is known to accumulate in the cytoplasm in response to osmotic shock (93). To determine whether hnRNP A1 localization in senescent IMR-90 was similar to what we had previously observed in HS-74 (88), the nucleocytoplasmic distribution of hnRNP A1 was examined as a function of *in vitro* age.

Results reveal a predominantly nuclear localization in log phase and $G_0$-arrest HDF (fig. 22, panels 1 & 2) compared to a more diffuse distribution of hnRNP A1 into the cytoplasm (fig. 22, panel 3). Interestingly it is absent in the nucleoli in all three phases.

*In situ* immunofluorescence analysis using the secondary anti-mouse antibody as a control for non-specific binding, were negative for immunofluorescence (data not shown).

These findings are consistent with our previous findings which reported a predominantly nuclear distribution of hnRNP A1 compared to a more diffuse distribution in senescent HS-74 HDF (88).

Nucleolin is a 100 kDa protein which has been shown to shuttle between the nucleus and cytoplasm and is found in the nucleoli (73). As an internal control the subcellular distribution of nucleolin was also examined (fig. 23, panels 1-3). While nucleolin was found dispersed throughout the cell, it was also consistently found in the nucleoli of all three phases indicating that it has a distinct localization profile compared to hnRNP A1.

**Differential immunoblot analysis of 4B10-hnRNP A1 antibody specificity**

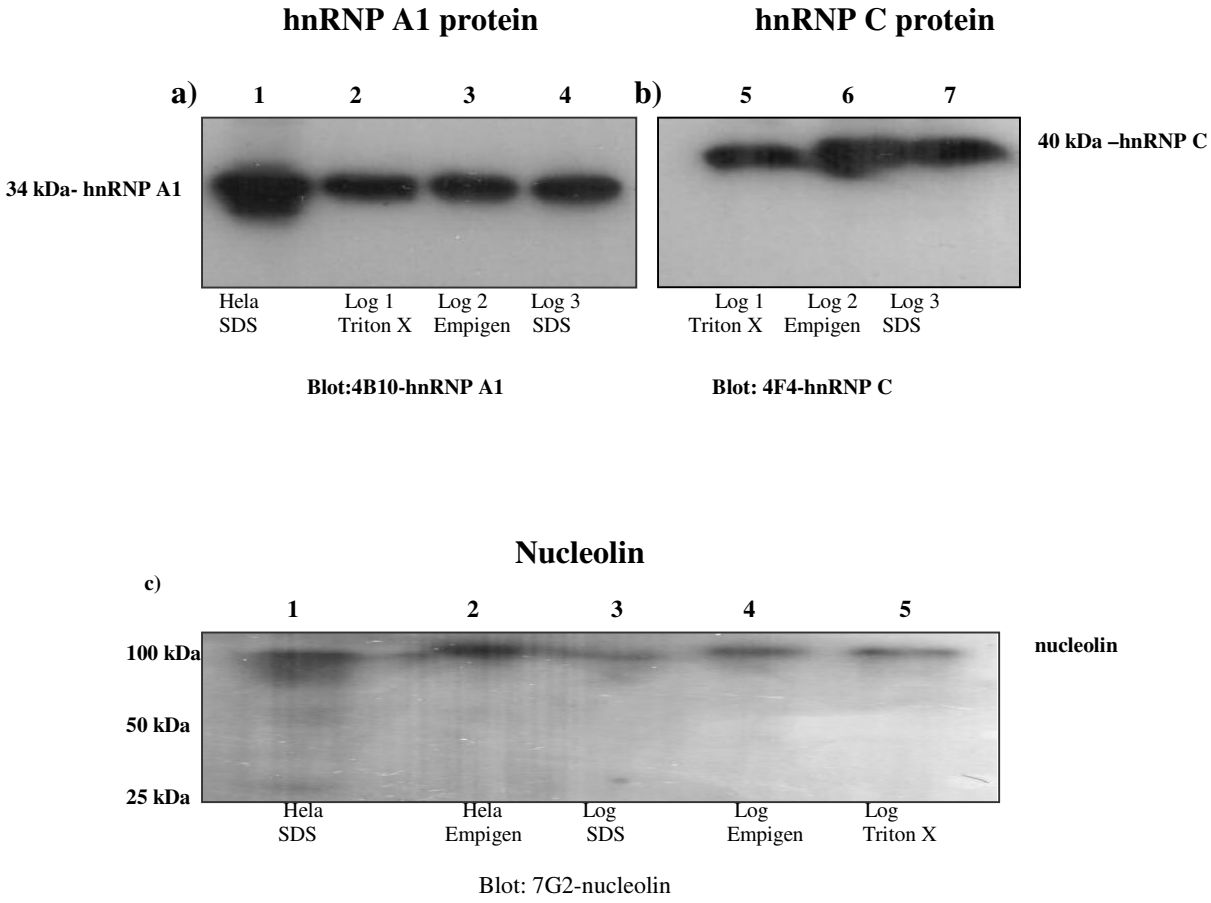


**Figure 11. Differential immunoblot analysis of 4B10 specificity.** Whole cell lysates were prepared in Hela cells or log phase IMR-90 HDF using SDS, Triton X, or Empigen BB lysis buffer and protein concentrations were normalized. 10ug of lysates were simultaneously subjected to 12.5% SDS-PAGE and immunoblotted with either **panel a)** 4B10, hnRNP A1 specific or **panel b**) 4F4, hnRNP C, **or panel c)** 7G2, nucleolin specific antibodies. These experiments were performed in duplicate.

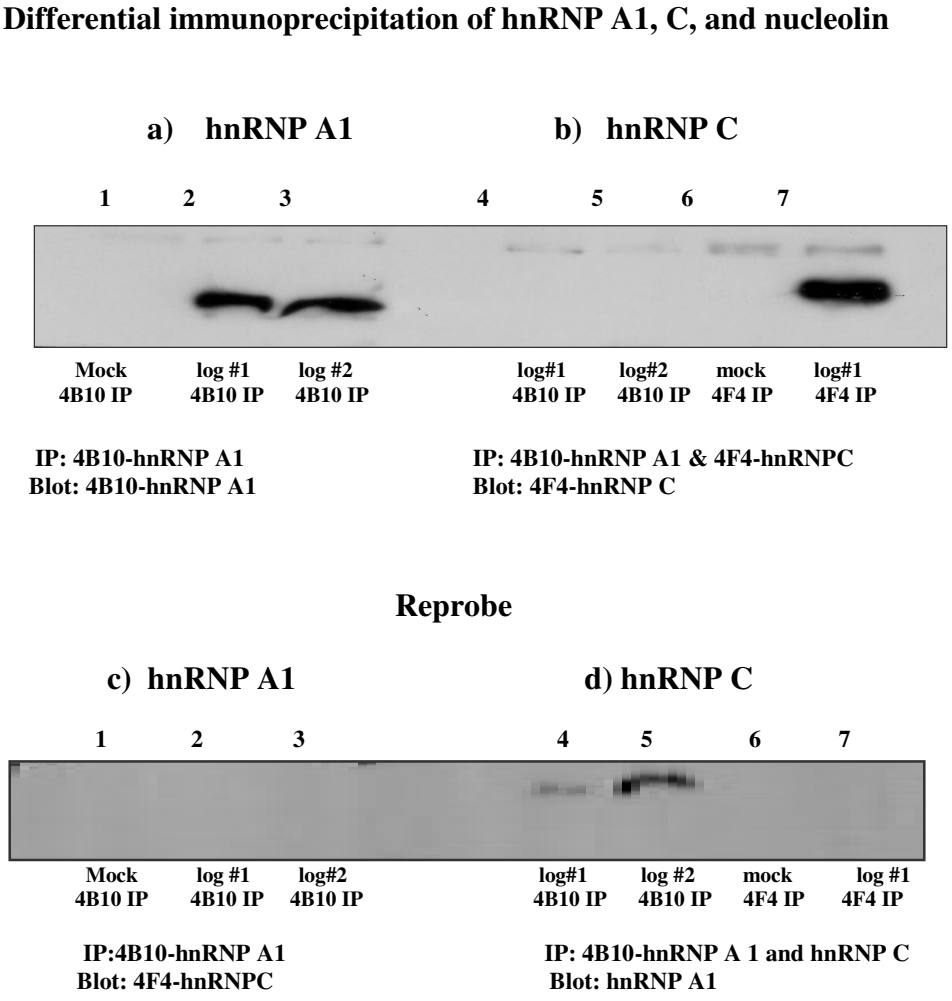


**Figure 12. Differential immunoblot analysis of hnRNP A1 and hnRNP C immunoprecipitate**s. Log phase samples were prepared in Empigen BB 1% lysis buffer. 400ug of total protein were used to immunoprecipitate with either 4B10 or 4F4 primary antibody, then subjected to 12.5% SDS-PAGE. Proteins were transferred to PVDF membrane and probed with **panel a)** 4B10 or **panel b**) 4F4 antibodies, hnRNP A1 or hnRNP C, respectively. Blots were then stripped and reprobed with the either hnRNP A or hnRNP C antibodies to confirm the absence of hnRNP C in the 4B10 IP's ( panel c, lanes 2&3) and presence of hnRNP A1 in the 4B10 IP's ( panel d, lanes 4 and 5). This experiment was performed in duplicate.

**hnRNP A1 protein levels in IMR-90 HDF**

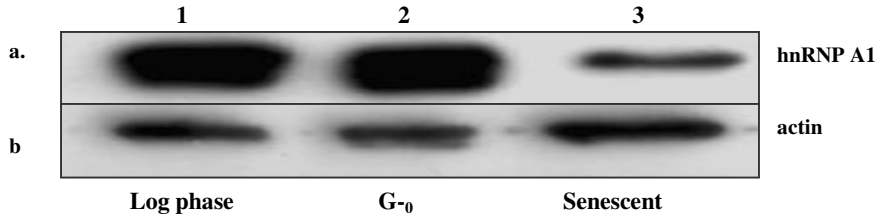


**Figure 13. Immunoblot analysis of hnRNP A1 protein levels in IMR-90 log phase and senescent whole cell lysates. Panel a)** 10ug of whole lysates were electrophoresed on a 12% SDS-PAGE and probed with 4B10 a monoclonal antibody specific for hnRNP A1. **Panel b**) The blot was then stripped and reprobed for total actin levels. This experiment was performed in triplicate.

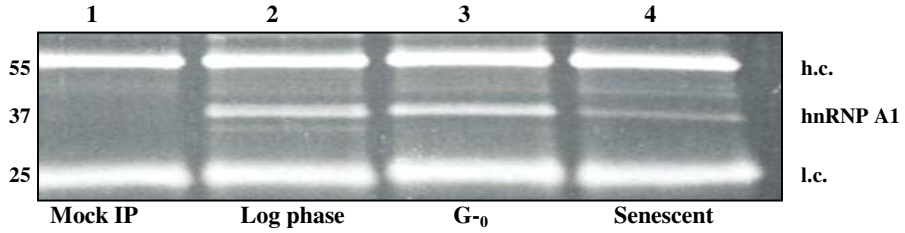


**Figure14. Immunoblot analysis of immunoprecipitated hnRNP A1 in log phase, G0 arrest and senescent IMR-90 HDF.** 500ug of whole lysates were immunoprecipitated with 4B10-hnRNP A1 antibody and subjected to 15% SDS-PAGE. Mock IP was included to establish molecular weight of heavy and light chains (55 and 25 kDa, respectively). This reaction contained antibody and beads only. Bands were visualized using SYPRO-Total protein stain. This experiment was performed four times.

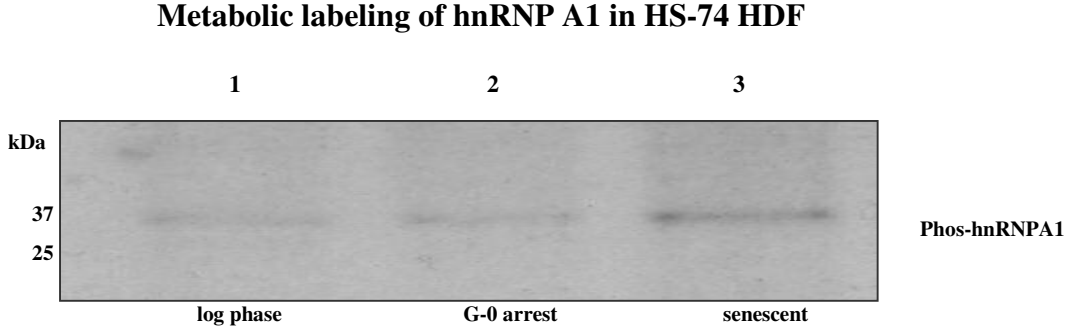


**Figure 15.** ***In vivo*** **$^{32}$P radiolabeling of log phase, G-0 arrest, and senescent HS74 fibroblasts.** Cells were incubated overnight in 0.5mCi/ml $^{32}$P-ortho-phosphate. Total protein was isolated and endogeneous hnRNP A1 was immunoprecipitated using 4B10 antibody. hnRNP A1 phosphorylation levels were determined by autoradiography following 12% SDS-PAGE. This experiment was performed four times.

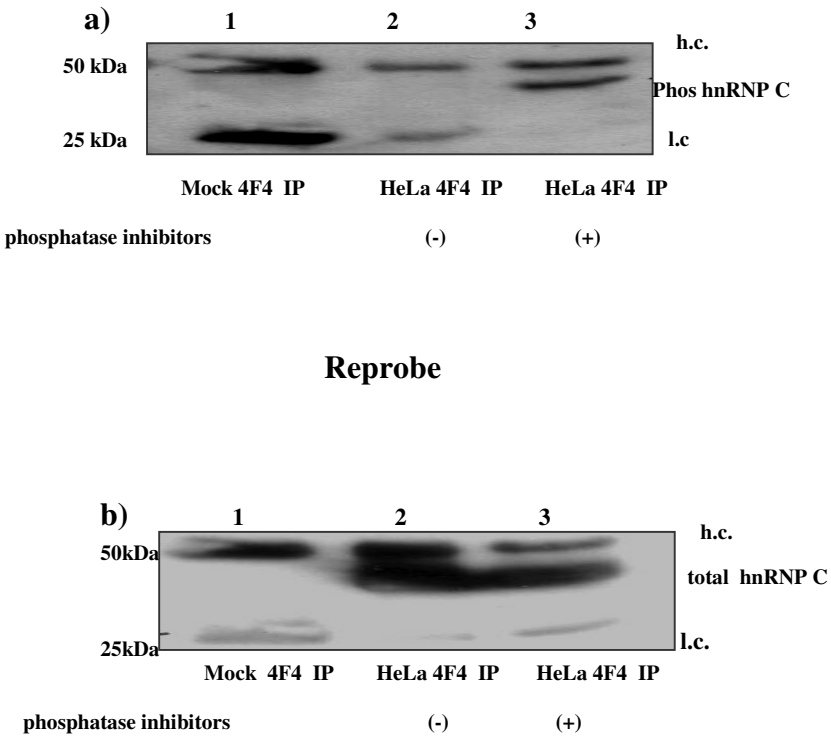


**Figure 16. Immunoblot analysis of phosphorylated hnRNP C in Hela extracts.** **Panel a**) 700 ul of HeLa extracts with and without phosphatase inhibitors were immunoprecipitated with 4F4 primary antibody, subjected to SDS-PAGE and immunoblotted with antiphosphoserine antibody to determine the levels of phosphorylated hnRNP C protein (lanes 2 & 3). Mock IP reaction was included to establish antibody heavy and light chain molecular weight, 55 and 25 kDa, respectively (lane 1). This reaction contained antibody and beads only.
**Panel b**) Blots were stripped and reprobed using 4F4 primary antibody to determine the total protein levels of hnRNP C (lanes 2 & 3). This experiment was repeated two times.

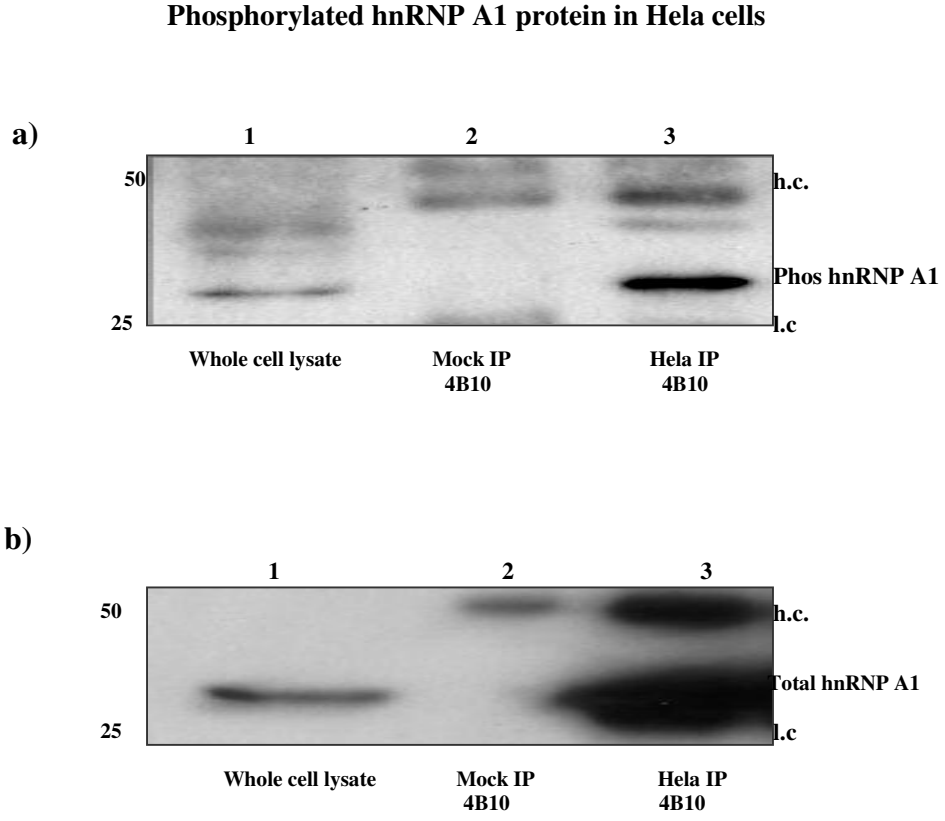


**Figure 17. Immunoblot analysis of phosphorylated hnRNP A1 in HeLa extracts.**
**Panel a)** 700ul of HeLa extracts lysed in the presence phosphatase inhibitors were immunoprecipitated with 4B10-hnRNP A1 antibody, subjected to SDS-PAGE and immunoblotted with anti-phosphoserine antibody to determine the level of phosphorylated hnRNP A1 protein ( lane 3). Mock IP reaction was included to establish molecular weight of antibody heavy and light chain, 55 and 25 kDa, respectively (lane 2). This reaction contained antibody and beads only.
**Panel b)** Blots were stripped and reprobed using 4B10-hnRNP A1 antibody to determine the total protein levels of hnRNP A1 (lane3). This experiment was repeated two times.

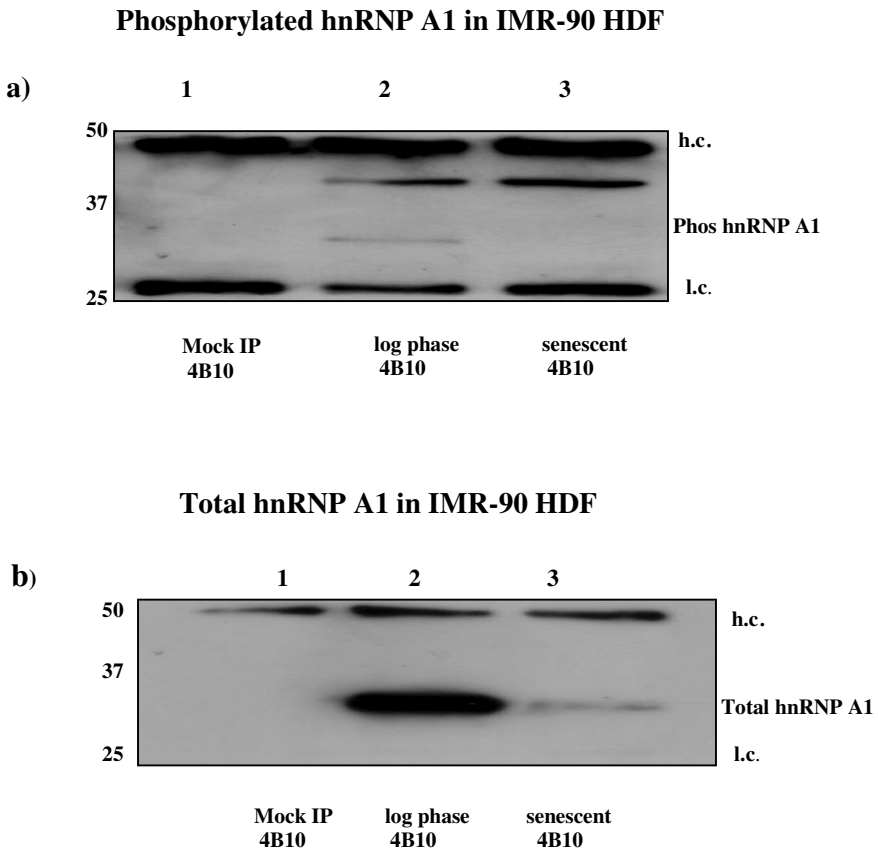


**Figure 18. Immunoblot analysis of phosphorylated hnRNP A1 in log phase and senescent fibroblasts.** ≈700ug of total cell lysates prepared in Empigen lysis buffer were immunoprecipitated using 4B10 primary antibody, reactions were extensively washed and separated by 12.5% SDS-PAGE (lanes 2 & 3). Mock IP reaction was included to establish molecular weight of heavy and light chain, 55 and 25 kD, respectively, (lane 1). This reaction contained antibody and beads only.
**Panel a)** Proteins were transferred to PVDF membrane, and probed with anti-phosphoserine primary antibody. **Panel b**) Blots were then stripped and reprobed for total hnRNP A1 levels using 4B10 primary antibody. This experiment was performed in triplicate.

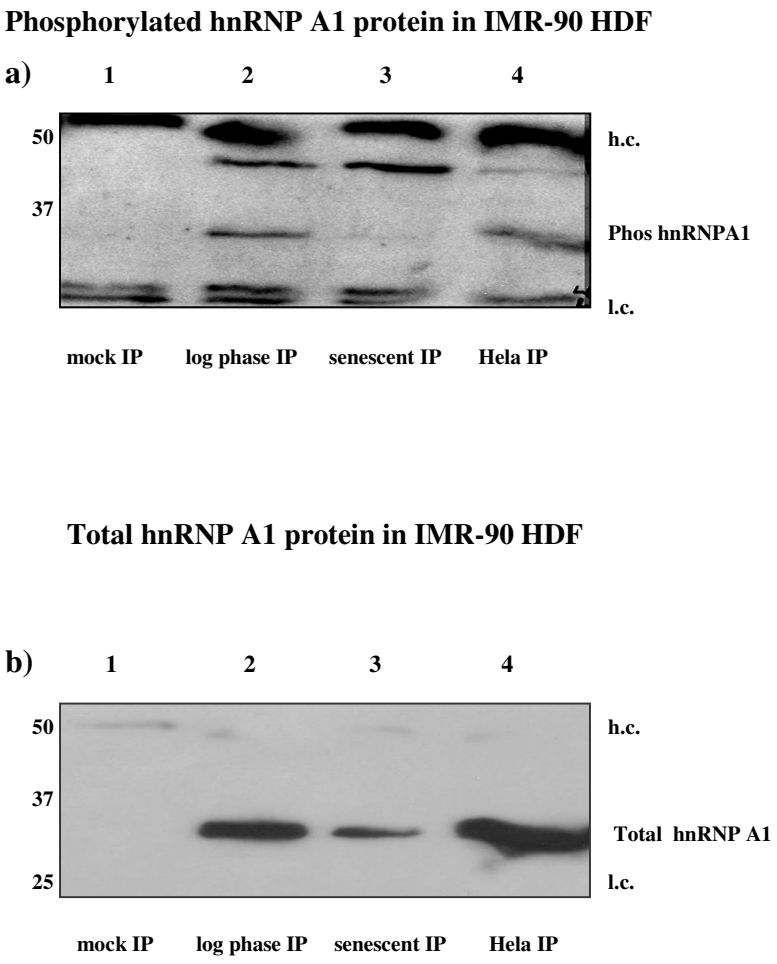


**Figure 19. Immunoblot analysis of phosphorylated hnRNP A1 in log phase and senescent fibroblasts**. ≈750ug of total cell lysates prepared in Empigen lysis buffer were immunoprecipitated using 4B10 primary antibody, reactions were extensively washed and separated by 12.5% SDS-PAGE (lanes 2, 3, &4). Mock IP reaction was included to establish molecular weight of antibody heavy and light chain, 55 and 25 kDa, respectively (lane 1). **Panel a**) Proteins were transferred to PVDF membrane, and probed with a 1ug/ml dilution of anti-phosphoserine primary antibody.
**Panel b)** Blots were then stripped and reprobed for total hnRNP A1 levels using 4B10 primary antibody. This experiment is representative of four independent experiments.

**Dephosphorylation of hnRNP A1 with Protein Phosphatase 2A**

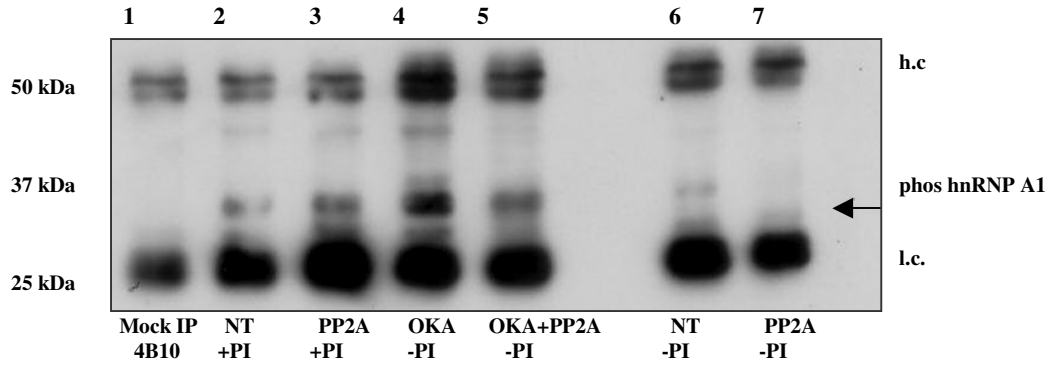


**Figure 20. Immunoblot analysis of phosphorylated hnRNP A1 in young IMR-90 after treatment with PP2A and/or okadaic acid.**

a) Lane 2 was untreated and lysed in the presence of phosphatase inhibitors, (PI).

b) Lanes 3, 5, and 7: 0.4U of PP2A was added to 400ug of young IMR-90 extracts prepared in Empigen lysis buffer with or without phosphatase inhibitors, (PI), incubated at 30$^{o}$C for two minutes, immunoprecipitated with 4B10, subjected to SDS-PAGE, and immunoblotted with anti-phosphoserine antibody to detect phosphorylated hnRNP A1.

c) Lanes 4 and 5 plates were incubated *in vivo* with 10mM okadaic acid for 2 hours at 37$^{o}$C and lysed in the absence of phosphatase inhibitors. These extracts were processed as above. Mock IP reaction was included to establish molecular weight of antibody heavy and light chain, 55 & 25 kDa, respectively, (lane 1). This experiment was performed in duplicate.

| Cell line IMR-90 | Phosphorylated hnRNP A1/Total hnRNP A1 Protein levels | | | | |
|---|---|---|---|---|---|
| | 1 | 2 | 3 | 4 | S.E. ± |
| Log phase | 0.034 | 0.013 | 0 .037 | 0.105 | 0.02 |
| Senescent | 0.021 | 0.035 | 0.21 | 0.04 | 0.04 |

Table 1. Relative ratios of hnRNP A1 phosphorylation in log phase and senescent IMR-90 HDF were calculated by dividing the signal intensity of phosphorylation levels by signal intensity of total protein levels. Signals were obtained using ImageQuant ™ software on scanned blots. Membranes were first probed with anti-phosphoserine antibody, processed and scanned and signal intensity was quantitated. Membranes were subsequently reprobed with anti-hnRNP A1 antibody, processed and the signal intensity was quantitated. The relative signal for phosphorylated hnRNP A1 was calculated. Ratio values from four independent experiments were tabulated and summarized above. Standard error was calculated as the standard deviation/√N where = sample number. Refer to figure 21 for graph.

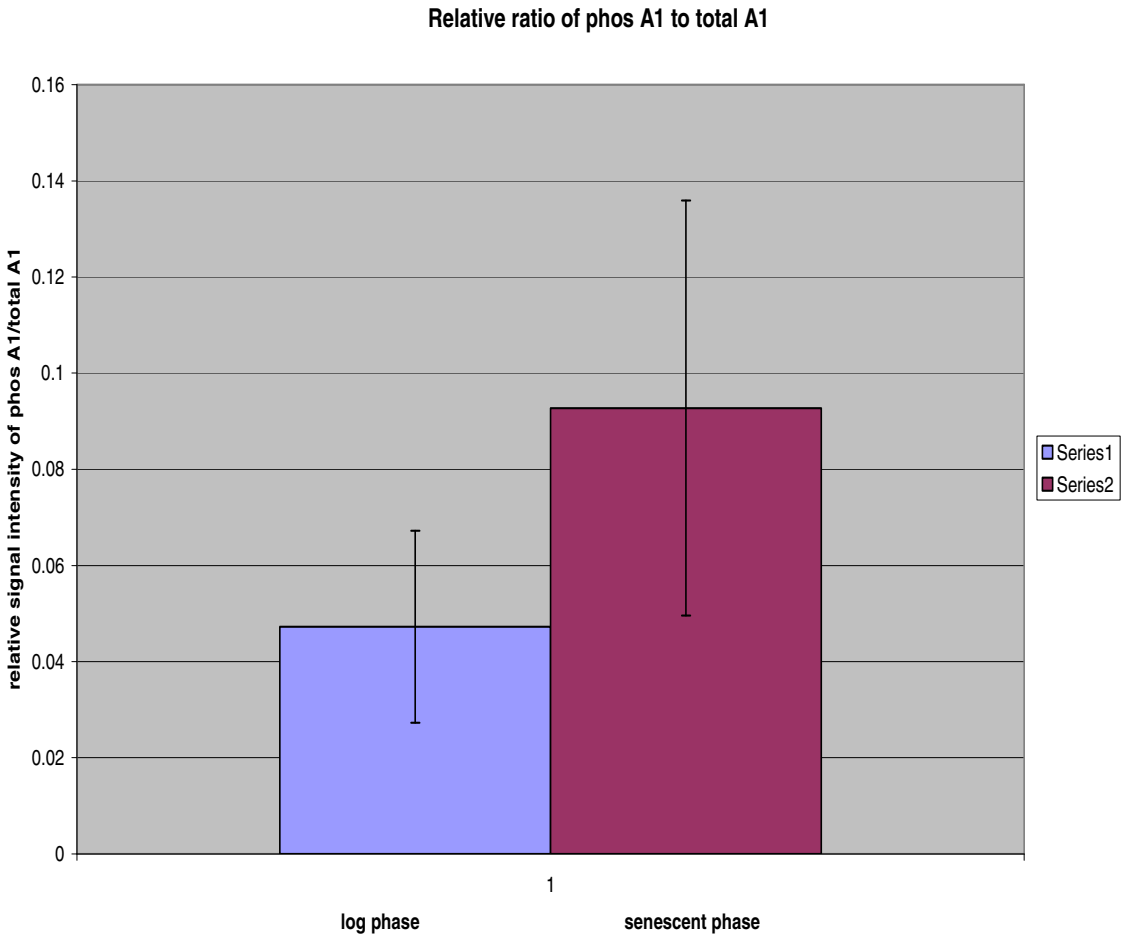


**Figure 21. Graphical representation of the relative ratios of phosphorylated hnRNP A1.** The relative ratios for phosphorylated hnRNP A1:total hnRNP A1 protein in log phase and senescent IMR-90 were quantitated using ImageQuant™ analysis and is presented as relative ratio of signal intensity. Data are presented as mean S.E.± densitometric values from four independent experiments.

***In situ* immunofluorescence of hnRNP A1 in log phase, $G_0$-arrest, and senescent IMR-90 HDF**

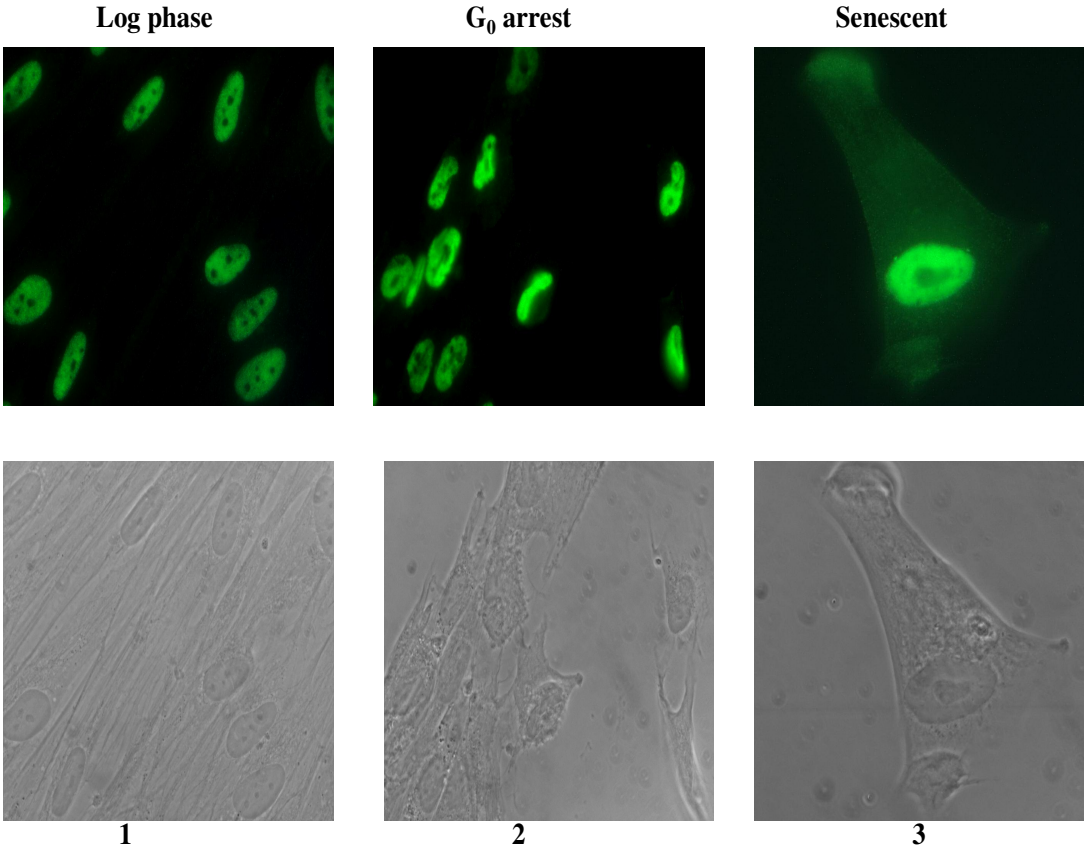


**Figure 22. *In situ* immunofluorescence of hnRNP A1 in log phase, $G_0$-arrest, and senescent IMR-90 HDF.** In panels 1-3 IMR-90 HDF were fixed, permeabilized, and incubated first with 4B10-hnRNP A1 primary antibody followed by anti-mouse secondary antibody. All fields are shown at a magnification of 400x. This experiment was performed in triplicate.

***In situ* immunofluorescence of nucleolin in log phase, $G_0$-arrest, and senescent IMR-90 HDF**

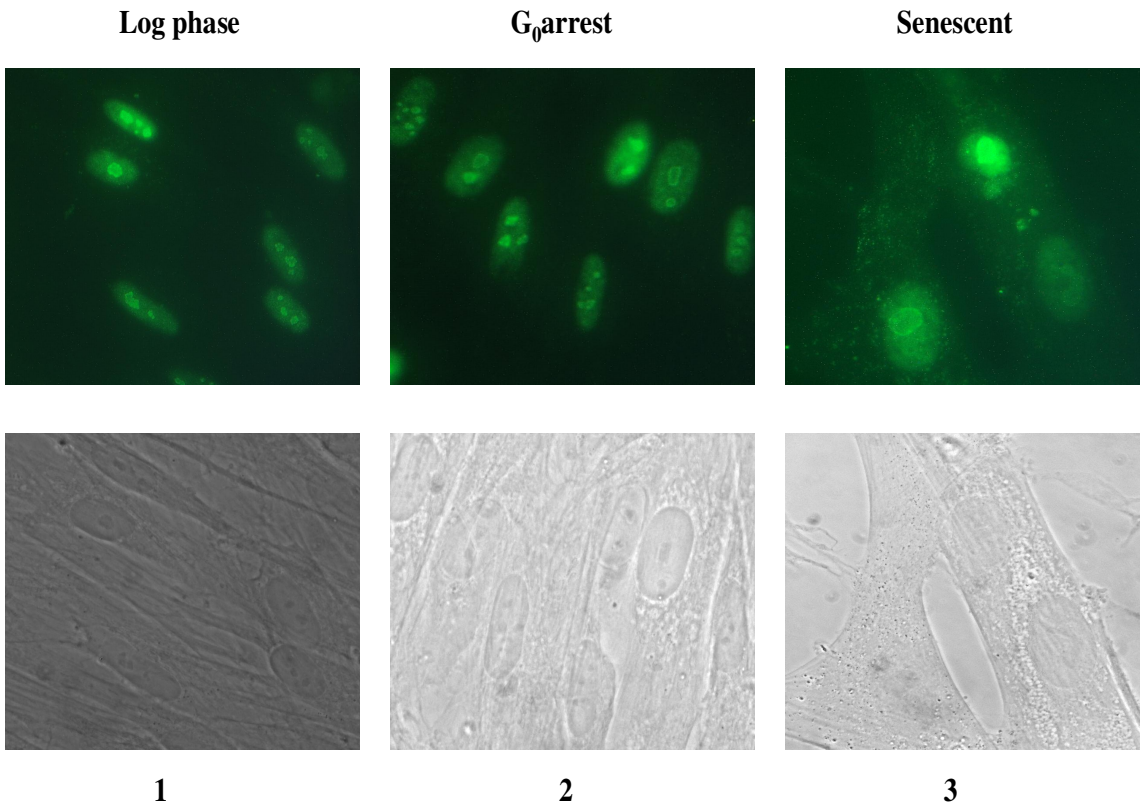


**Figure 23. In situ immunofluorescence of nucleolin in IMR-90 log phase, $G_0$-arrest, and senescent HDF.** In panels 1-3 IMR-90 HDF were fixed, permeabilized, and incubated first with 7G2-nucleolin primary antibody followed by anti-mouse secondary antibody. All fields are shown at a magnification of 400x. This experiment was performed in triplicate.

## 3.3 Discussion

**Expression of hnRNP A1 in IMR-90 HDF**

In this study we measured the relative levels of phosphorylated hnRNP A1 as compared to total hnRNP A1 protein levels as a function of *in vitro* age in IMR-90 HDF, a human diploid fibroblast derived from fetal lung tissue. Our findings suggest that relative levels of phosphorylated hnRNP A1 are increased in senescent HDF. Subsequent immunofluorescence analysis of the subcellular distribution of hnRNP A1 reveal a predominantly nuclear localization in young HDF compared to a diffuse cytoplasmic distribution in senescent HDF. Consistent with increased phosphorylated hnRNP A1 shown by others, the cytoplasmic accumulation of hnRNP A1 has been shown to be modulated by the p38 MAP kinase pathway in response to osmotic shock with a concomitant increase in phosphorylation (93). These initial findings collectively suggest that post-translational modifications may have a regulatory role during senescence.

hnRNP's are proteins that bind RNA polymerase II transcripts which are termed hnRNA's (heterogeneous nuclear RNA). Over 24 major proteins designated A1-U (34kDa-120 kDa) have been identified in hnRNP complexes (49) and among the proteins found in the core hnRNP complex are hnRNP's A, B, and C in the 30-43kDa range. Since hnRNP A1 exists in this multiprotein complex, we sought to efficiently disrupt the core complex in order to efficiently immunodetect and immunoprecpitate hnRNP A1 using the 4B10 monoclonal antibody which has been previously characterized for the immunodetection of hnRNP A1 (119).

We tested the specificity of the 4B10 monoclonal antibody for hnRNP A1 in lysates prepared from IMR-90 HDF under conditions known to disrupt the hnRNP core complex. These studies were initiated in order to ensure that: a) the hnRNP core complex was sufficiently disrupted in our samples and b) to confirm that only hnRNP A1 and no other hnRNP protein was immunodetected with the 4B10 antibody.

In order to test the relative levels of hnRNP A1 phosphorylation as a function of *in vitro* age the total hnRNP A1 levels were first examined by immunoblot analysis. Total protein levels of hnRNP A1 were highly diminished in senescent IMR-90 HDF compared to young and $G_0$-arrest HDF. These findings are consistent with Hubbard et al., 1995 which report that protein levels of hnRNP's A1, A2/B1, and C are decreased in senescent HS-74 HDF. Furthermore, decreased protein levels of hnRNPA1 in senescent HDF parallel the observed decrease in its mRNA levels in senescent HDF as indicated by Northern analysis (88).

The observation that protein levels of hnRNP A1 decrease in senescent HDF also parallels the observed alteration of its nucleic acid binding properties. Previous studies have shown that in senescent fibroblasts the RNA binding activity to a model RNA substrate diminishes as opposed to *in vitro* telomeric DNA binding activities which increase (132). hnRNP A1 protein can counteract the effect of SR proteins by promoting distal 5' splice site utilization *in vitro* and *in vivo* and the decreased hnRNP A1 protein levels would potentially result in the selection of proximal 5' splice sites (56,133,134,135). Indeed earlier studies demonstrated that the ratio of hnRNP A1 to the splicing factor, SF2 decreases in senescent HDF with the resulting decrease in the ratio of p14 $^{ARF}$ to p16 $^{INK4A}$ (132). More recent studies have implicated hnRNP A1 in the

alternative splicing of c-H-ras mRNA which renders two proteins, p21-H-Ras and p19-H-RasIDX (136). hnRNP A1 was found to have an inhibitory role in IDX splicing, thus a decrease in hnRNP A1 protein levels may potentially alter the expression of p21-H-*ras*. Overexpression of *ras* is known to induce a premature senescent phenotype and this effect is mediated through the p38 MAP kinase signaling pathway (137).

Since hnRNP A1 is involved in a range of pre-mRNA processing functions as well as mRNA transport and stability, the decreased protein levels and altered binding activities observed in senescent fibroblasts may affect the levels of expression of mature mRNA's and contribute to the senescent phenotype.

**Phosphorylation of hnRNP A1**

Reversible phosphorylation has a regulatory role in modulating the activity of several DNA-RNA binding proteins as well as modulating protein-protein interactions. The kinases known to phosphorylate hnRNP A1 *in vitro* and *in vivo* at serine/threonine residues *in vitro* are Protein kinase C ζ, (PKCζ), Protein Kinase A (PKA), Casein Kinase II, (CKII) and Mnk (96,97,115). Phosphorylation of hnRNP A1 by protein kinase Cζ occurs at three major sites, ser $^{95}$,ser $^{192}$, and ser $^{199}$ which correlates with an inhibition of its strand annealing activity (97). These sites are also dephosphorylated by protein phosphatase 2A which restores the strand annealing activity. Studies by Hamilton et al., 1997 indicated that modulation of serine-threonine phosphorylation of hnRNP A1 regulated its' binding to AU-rich elements (ARE's), which are *cis*-acting elements that modulate mRNA stability and turnover (25)**.**

hnRNP A1 is dephosphorylated by Protein Phosphatase 2A (PP2A) which is the class of phosphatases that dephosphorylates serine residues (96,97). Cytoplasmic hnRNP A1 binds to A-U rich elements (ARE) which are found in the 3-untranslated region (UTR) of many unstable RNA's (85). ARE's are conserved sequences which promote the removal of the poly-A tail and destabilizes mRNA. Binding of these ARE's by hnRNP A1 confers mRNA stability *in vivo* (86). It has been previously reported that phosphorylation of hnRNP A1 by MNK1/2 decreased its binding to TNFα mRNA 3'UTR which contributed to the de-repression of the translation of TNF α mRNA (115). This data is consistent with Idriss et al., 1994 which reported that phosphorylation of hnRNP A1 at three major sites, ser $^{95,}$ ser $^{192}$, and ser $^{199}$ by Protein Kinase C ξ diminished its *in vitro* strand annealing activity of hnRNP A1 and subsequent dephosphorylation with protein phosphatase 2A restored its strand annealing activity (85,97). Thus the reversible phosphorylation of hnRNP A1 modulates its affinity for specific sequences on labile mRNA's which ultimately affects gene expression.

The preliminary analysis of phoshorylated hnRNP A1 was examined in HS-74 HDF, a human diploid fetal bone fibroblast cell strain with hnRNP A1 expression profiles similar to IMR-90 HDF. The *in vivo* phosphorylation of hnRNP A1 was tested by metabolic labeling in HS-74, and since hnRNP A1 is only weakly phosphorylated under steady state conditions (93), the results suggest that the phosphorylation of hnRNP A1 was higher in senescent HS-74 HDF compared to young and $G_0$-arrest HS-74 HDF (fig.15). Previous attempts to test the levels of phosphorylated hnRNP A1 in senescent HDF by 2D gel electrophoresis were largely unsuccessful owing to very low protein recovery in senescent HDF.

Furthermore these results are consistent with recent findings of Allemand et al., 2005 who detected relatively low levels of phosphorylated hnRNP A1 in Hela cells with an anti-phosphoserine antibody (71).

A more stringent analysis of the specificity of the phosphoserine antibody was performed using protein phosphatase 2A (PP2A) in conjunction with immunoblot analysis. Cell lysates when treated with PP2A, a protein phosphatase which dephosphorylates at serine/threonine residues, demonstrated a diminished detection of phosphorylated hnRNP A1 compared to the untreated samples and this may suggest that hnRNP A1 was dephosphorylated by PP2A. The results suggest that in PP2A-treated lysates prepared in the presence of phosphatase inhibitors the level of detectable phosphorylation increased compared to the PP2A treated samples prepared in the absence of phosphatase inhibitors. These findings are consistent with those of Cobianchi et al., 1993 who reported that phosphorylated hnRNP A1 was recovered from labeled Hela cells only in the presence of okadaic acid which is potent inhibitor of PP2A (131).

The relative levels of phosphorylated hnRNP A1 in young and senescent IMR-90 HDF were tested using the anti-phosphoserine antibody and calculated as the ratio of phosphorylated hnRNP A1 to total hnRNP A1 protein level as quantitated by ImageQuant ™ software (fig. 21). Hamilton et al., 1997 quantitated phosphorylated hnRNP A1 in human lymphocytes using the same parameters. Given that the total protein level of hnRNP A1 is highly diminished in senescent HDF, the overall phosphorylated fraction of this protein appears to be higher in senescent HDF compared to young HDF where hnRNP A1 is highly expressed. However, since hnRNP A1 is only

weakly phosphorylated under steady state conditions it remains difficult to detect the phosphorylated form of this protein.

*In vitro* studies have shown that both PKC ζ and PKA kinases phosphorylate hnRNP A1 at serine [199] and recently Mnk 1 has been shown to phosphorylate hnRNP A1 (94, 96, 115). We know from previous studies that hnRNP A1 is involved in the annealing of complementary RNA molecules *in vitro* which may serve to enhance base pairing interactions (74,75). As a splicing factor it has been shown to modulate the effects of another splicing factor, SF2/ASF (serine-arginine splicing factor 2) and promote distal 5' splice site selection (56). A shift in the concentration of nuclear hnRNP A1:SF2/ASF results in the selection of proximal 5' splice sites which is counteracted in a concentration dependant manner by increasing the ratio of hnRNPA1. Cytoplasmic accumulation of hnRNP A1 has been shown to alter its alternative splicing properties (93). Thus decreasing the ratio of hnRNP A1 in the nucleus can affect RNA processing.

**Subcellular localization of hnRNP A1 in IMR-90 HDF**

hnRNP A1 shuttles between the nucleus and cytoplasm in a transcription-dependant and independent manner (79). Under steady state conditions and in the absence of stress stimuli hnRNP A1 is predominantly nuclear in young HDF and our results in IMR-90 are suggestive of distinct nucleo-cytoplasmic localization profiles between young and senescent HDF.

Our findings show that the subcellular distribution in IMR-90 log phase and $G_0$-arrest HDF is predominantly nuclear compared to senescent HDF where it diffuses into

the cytoplasm, suggesting a distinct localization profile both young and log phase HDF (figs.22 panel 1-3). hnRNP A1 is noticeably absent from the nucleoli in all three cell phases. *In situ* localization of nucleolin, another shuttling protein revealed a distinct localization in the nucleoli of all three cell phases and dispersed into the cytoplasm of senescent HDF (fig. 23 panels 1-3).

One important consequence of accumulating hnRNP A1 in the cytoplasm is the potential effect on the regulation of alternative splicing in senescent cells. Nuclear ratios of hnRNP A1 can modulate splice site usage. hnRNP A1 can also modulate alternative splicing of its own pre-mRNA (166). Thus both the decreased protein levels and altered subcellular distribution of hnRNP A1 observed in senescent IMR-90 HDF may affect gene expression.

These findings in IMR-90 HDF are consistent with Zhu et al., 2002 where it was reported that hnRNP A1 localized to the cytoplasm in senescent HS-74 fibroblasts while remaining predominantly nuclear in young and $G_0$ arrested fibroblasts (88). Collectively these results suggest that the increase in phosphorylated hnRNP A1 observed in senescent HDF may mediate the cytoplasmic accumulation of hnRNP A1 in senescent HDF. This is supported by recent findings that phosphorylation of the F-peptide in the C -terminus of hnRNP A1 regulated the cytoplasmic accumulation of hnRNP A1 by reducing its interaction with the transportin receptors, Trn1 and Trn2b (71). In addition both PKC ζ and PKA can induce cytoplasmic accumulation of hnRNP A1 (94, 96). Whether the import/export signals of hnRNP A1 are altered in senescent HDF or whether nuclear membranes are compromised in senescent HDF remains to be elucidated, however the end result of cytoplasmic accumulation of hnRNP A1 is known to affect its alternative

splicing properties and these effects may be extrapolated to senescent HDF. Thus, the cytoplasmic accumulation of hnRNP A1 appears to increase due to phosphorylation and may provide a significant contribution towards altering the level of gene expression during senescence.

### 3.4 Conclusion

We initially sought to examine potential kinase/phosphatase modulators of hnRNP A1 phosphorylation in senescent HDF. Studies which reported modulation of hnRNP A1 by the p38 MAPK signaling pathway in response to osmotic shock also observed a concomitant increase in phosphorylation levels of hnRNP A1. This effect was abrogated by the overexpression of a MKK3/6 dominant negative mutant which prevented the upstream activation of p38 MAPK. In their report, the cytoplasmic accumulation of hnRNP A1 affected its alternative splicing activity (93).

These studies implicated the involvement of activated p38 MAP kinase in the regulation of hnRNP A1 and thus warranted further investigation in IMR-90 HDF. An examination of p38 MAP kinase as a putative modulator of either hnRNP A1 protein levels or localization was initiated in IMR-90 HDF and is discussed in chapter 4.

# Chapter 4.

# p38 MAP kinase studies

## 4.1 Introduction

p38 MAP Kinase is a serine/threonine kinase that is activated in response to a variety of cellular stress signals including UV light, lipopolysaccharides, inflammatory cytokines-TNFα, IL-1, and osmotic shock (153,154,155). The p38 MAPK family consists of at least 4 isoforms, α,β,γ,δ, the first two of which are inhibited by a pyridinyl imadazole, SB203580 (138). p38 MAPK is activated upon phosphorylation at $Thr^{180}/Tyr^{182}$ residues by at least three upstream MAP kinase kinases, MKK3,6, and 4 mostly in response to non-mitogenic signals (106). Activated p38 MAPK kinase phosphorylates numerous downstream substrates which include transcription factors and downstream kinases (139,140,141,142,93). The dual specificity phosphatases MAP Kinase Phosphatase, (MKP) dephosphorylates and inactivates p38 MAP kinase (110).

In this study we examined the steady state levels of activated p38 MAPK in IMR-90 HDF in the absence of external stress stimuli and quantitated its relative kinase activity as a function of *in vitro* age. Here we show that in senescent HDF both the activated form of p38 MAPK and its kinase activity are increased compared to young HDF.

Replicative senescence is accompanied by a sequence of changes which include altered expression of cell-cycle proteins, upregulation of p53, $p16^{INK4a}$, and $p21^{CIP1/WAF-1/SD1}$; these changes distinguish senescence from quiescence or differentiation. (22,23,24,29).

We know from previous studies that oncogenic *ras* induces premature senescence in primary mammalian cells and this effect is mediated by an active mitogenic MEK-ERK pathway (137,143). Stress activated p38 MAP kinase is also activated during the

onset of *ras*-induced senescence and studies have shown that constitutively active p38 MAP kinase induces premature senescence (137). In addition these studies demonstrated that inhibition of p38 MAP kinase prevented oncogenic *ras*-induced premature senescence. This growth arrest is associated with growth inhibitors such as p16 $^{Ink4a}$ and p53 (143). The cascade of signaling events in *ras* induced-premature senescence is as follows:

Oncogenic ras activates the MEK-ERK pathway which activates MKK3/6 activates p38 MAP kinase pathway in normal primary cells:

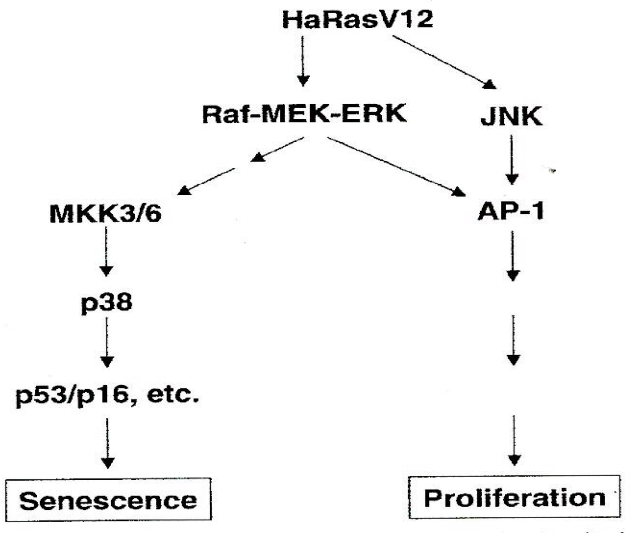


**Figure 24.** Schematic representation of the role of p38 MAP kinase in oncogenic ras-induced premature senescence in primary fibroblasts (137)

Oncogenic-*ras* induced premature senescence differs from replicative senescence in that it is telomere-independent, the latter resulting from serial passaging of primary fibroblasts. Secondly, in primary fibroblasts premature senescence is a late response to oncogenic *ras* expression, the immediate consequence of *ras* activation is growth stimulation (137). Elevated p38 MAPK activity has been reported in senescent W138

fibroblasts (156). This group also reported that p38 MAPK was activated by shortened telomeres in MRC-5 fibroblasts. Furthermore the BrdU labeling efficiency rates of senescent WI38 fibroblasts cultured in media containing SB203580 (a specific inhibitor of p38 MAPK) was increased to 30%. A dominant negative form of MKK6 (MKK6AA), the kinase upstream of p38 MAPK was introduced into young WI38 cells and found to increase the life span of these cells by 7 population doublings suggesting that p38 MAP kinase activity is necessary for telomere dependent senescence.

Our recent findings suggest that in addition to increased levels of activated (phosphorylated) p38 MAPK, there is also a concomitant increase in kinase activity in senescent fibroblasts as shown by phosphorylation of a ATF-2 substrate.

The subcellular localization profile of hnRNP A1 in IMR-90 fibroblasts reflects a predominantly nuclear localization in log phase cells compared to a diffuse cytoplasmic localization in senescent cells as discussed in chapter 3. While hnRNP A1 is not directly phosphorylated *in vitro* by p38 MAP kinase (115, 93) it has shown to be a substrate for another p38 MAPK target, Mnk1 (115). Rousseau et al., 2002 identified hnRNP $A_0$ as a major substrate for MAPKAP-K2, a kinase phosphorylated by p38MAPK (144). Other kinases known to be phosphorylated by p38 MAPK are MNK1/2, MSK2, MAPKAP-K3, and MSK1 (145).

## 4.2 Results

### A. Expression levels of H-*ras* and p38 MAP kinase signaling proteins in IMR-90 HDF.

Previous studies in WI38 HDF have shown that H-*ras* mRNA levels were elevated in senescent cells (128). We determined whether the pattern of protein expression was increased in senescent IMR-90. Endogenous protein levels of H-*ras* were analyzed by immunoblotting and found to be elevated in senescent HDF as compared to log phase fibroblasts (fig. 25, panel a). The resulting actin analysis confirms normalization of the total protein load in each sample (fig.25, panel b).

Cell lysates from log phase, $G_0$-arrest, and senescent HDF were immunoblotted with antibodies to both total p38 MAP kinase and to phosphorylated p38 MAP kinase (Pp38 MAP kinase) which is the activated form of the kinase. The results suggest that while the total protein levels of p38 MAP kinase were relatively unchanged (fig. 26, panels a, lanes 1-3), the phosphorylated form, Pp38 MAP kinase, was highly expressed in senescent HDF compared to the log phase and $G_0$ arrest HDF( fig. 26, panel b, lane3). A positive control for p38 MAP kinase and the phosphorylated p38 MAP kinase were included (fig. 26, panels a and b, lane 4). Protein loading was normalized was by actin analysis (fig. 26, panel c).

### B. p38 MAP kinase activity in IMR-90 HDF

ATF-2 is a transcription factor which is phosphorylated by activated p38 MAP kinase and frequently used as a substrate to measure p38 MAP kinase activity (146). Dual phosphorylation at two sites, $Thr^{180}$ and $Tyr^{182}$ activates p38 MAPK to

phosphorylate numerous downstream targets (106). We next examined the kinase activity in order to assay the catalytic activity of p38 MAPK. The kinase activity of this protein was found to be markedly elevated in senescent HDF (fig. 27, lane 5) compared to log phase and $G_0$-arrest HDF, this suggests that p38 MAP kinase was functional in senescent HDF.

We measured kinase activity six times and normalized the relative activity in $G_0$-arrest and senescent IMR-90 HDF to the relative activity in log phase IMR-90. Our results suggest that p38 MAP kinase activity is elevated in senescent IMR-90 HDF compared to log phase or $G_0$-arrest HDF (fig. 28). This elevated kinase activity reflects the observed increase in the activated protein form of the kinase in senescent HDF (fig. 26, panel b, lane 3).

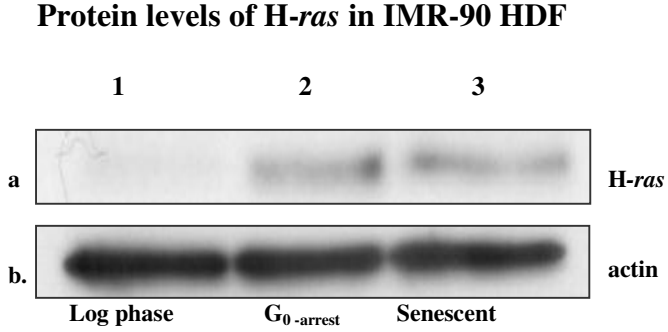


**Figure 25. Immunoblot analysis of H-*ras* levels in log, $G_0$-arrest, and senescent IMR-90 fibroblasts.** 50ug of whole cell lysates were subjected to 15% SDS-PAGE and H-ras levels were determined by immunoblotting ( panel a, lanes 1,2,3).
Membrane was stripped and reprobed with actin antibody as a loading control (panel b, lanes 1,2,3). This experiment was repeated three times.

**Protein levels of p38 MAPK and phosphorylated p38 MAPK in IMR-90 HDF**

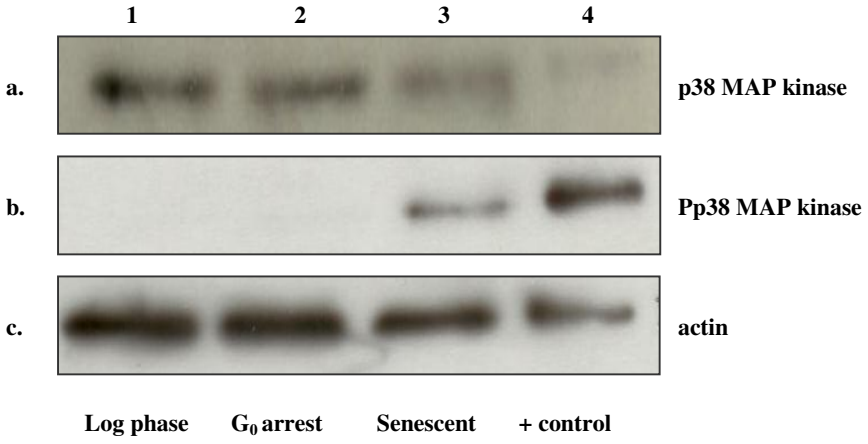


**Figure 26. Immunoblot analysis of p38 MAP kinase and phosphorylated p38 MAP kinase levels in log phase, $G_0$ arrest, and senescent IMR-90 extracts**. 25 ug of whole cell lysates were electrophoresed on a 12% SDS-PAGE and probed with antibodies to p38 MAP kinase,( panel a, lanes 1-3), phosphorylated p38 MAP kinase (panel b, lanes 1-3), and actin, (panel c, lanes 1-3). This experiment was repeated three times.

**p38 MAP kinase assay in IMR-90 HDF**

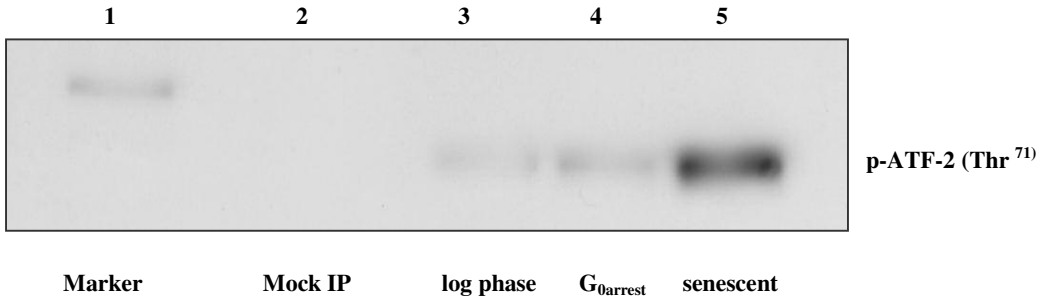


**Figure 27. p38 MAP kinase activity in IMR-90 HDF.** 400ug of whole cell lysate from log phase, $G_0$-arrest, and senescent fibroblasts were incubated with Immobilized anti-phosphorylated p38 MAP kinase beads, subjected to kinase assay conditions, and kinase activity was measured using a fusion ATF-2 protein with a single site for phosphorylation at $Thr^{71}$. A mock IP reaction was included as a negative control and contained antibody and beads only. This experiment was repeated six times.

| Cell line IMR-90 | Signal Intensity( ImageQuant™) for Kinase Activity | | | | | | |
|---|---|---|---|---|---|---|---|
| | 1 | 2 | 3 | 4 | 5 | 6 | S.E.± |
| Log phase | 36.0 | 32.0 | 24.2 | 81.3 | 10.6 | 17.6 | 0 |
| G-0 arrest | 44.8 | 26.8 | 66.5 | 62.0 | 40.4 | 28.7 | 0.49 |
| Senescent | 91.7 | 73.5 | 151.6 | 99.9 | 60.0 | 159.6 | 1.18 |
| Ratios: | 1.0 : 1.25 : 2.6 | 1.0 : 0.84 : 2.3 | 1.0 : 2.7 : 6.2 | 1.0 : 0.76 : 1.2 | 1.0 : 3.8 : 5.3 | 1.0 : 1.6 : 9.1 | |

Table 2. Relative kinase activity of p38 MAP kinase in log phase,$G_0$-arrest and senescent IMR-90 HDF. ImageQuant analysis was used to calculate the ratios of signal intensity by dividing the values for $G_0$-arrest and senescent samples by the the value obtained for the log phase sample (log phase normalized to 1) for each experimental set.
Six independent experiments were analyzed. Standard error was calculated as the standard deviation/√N where = sample number. Refer to figure 28 for graph.

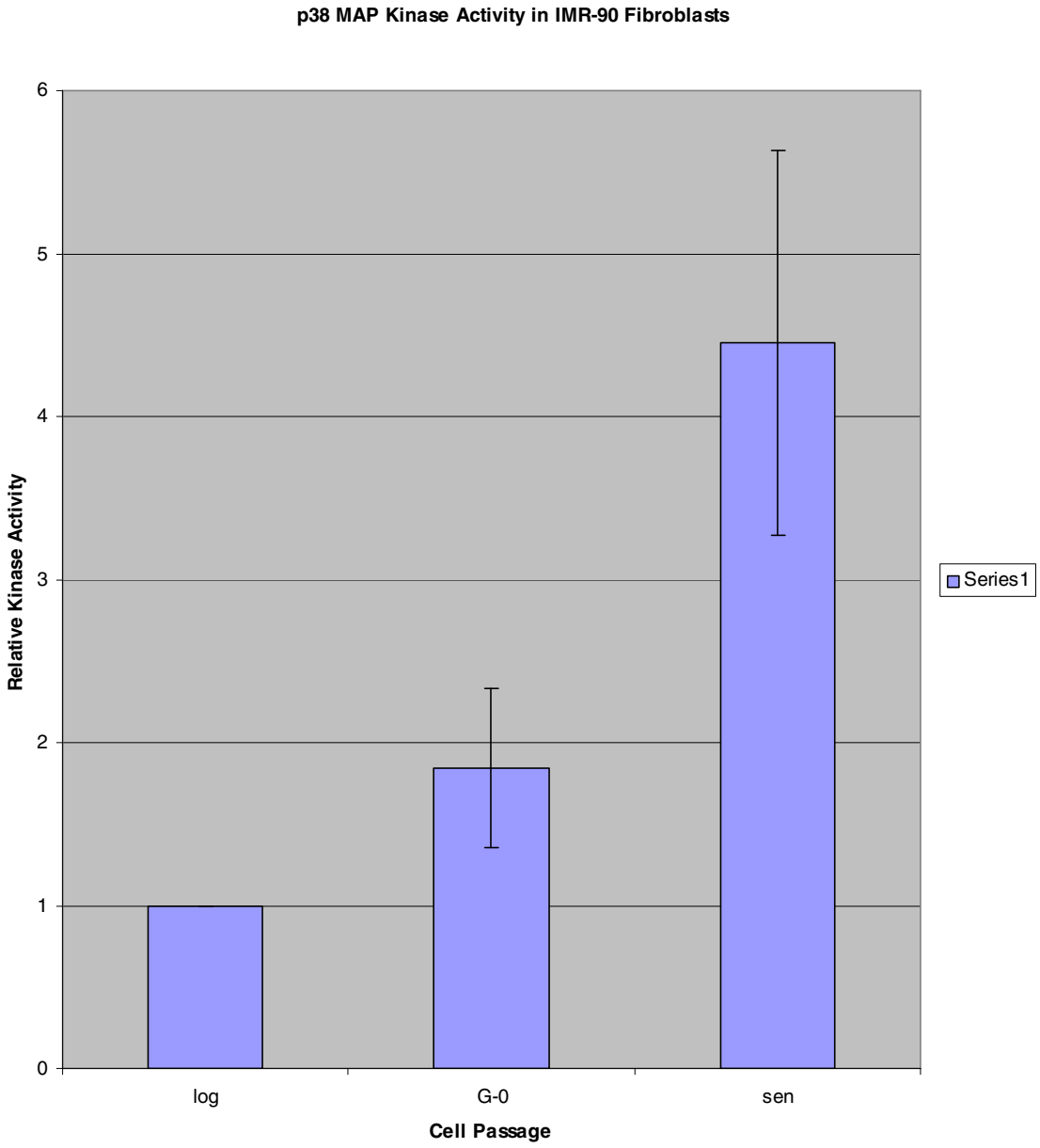


**Figure 28. Relative p38 MAP kinase activity in young $G_0$- arrest, and senescent IMR-90.** p38 MAP kinase activity is elevated in senescent IMR-90 HDF as measured by phosphorylation of a fusion ATF-2 protein with a single site for phosphorylation at Thr[71]. This graph represents the relative kinase activity in $G_0$-arrest and senescent HDF as compared to log phase HDF. Relative ratios were quantitated using ImageQuant™ analysis. Data are presented as mean S.E.± densitometric values from six independent experiments.

## 4.3 Discussion

The Ras family of proto-oncogenes consists of three GTP-binding proteins, c-H-*ras*, K-*ras,* and, N-*ras* and all are involved in the transduction of external mitogenic signals (reviewed in 147): These proteins play a key role in controlling proliferation and differentation**.** *Ras* is a GDP/GTP switch located in the inner surface of the plasma membrane which tranduces signals from receptors to the cytoplasm. By altering the catalytic activity of *ras*, activated *ras* oncogenes amplify the downstream signals which drive the cell towards proliferation and malignant transformation. In addition to proliferative functions normal *ras* also has both pro-apoptotic and onco-suppressor properties. The expression of a wild-type H-*ras* gene can suppress transformation by mutant H-*ras* in tumor cell lines and the observation that oncogenic-*ras* induces a state of permanent growth -arrest supports these onco-suppressor properties (147).

This may in part explain that while the initial cellular response to *ras* overexpression is cell proliferation, the end result is premature senescence. Our analysis of endogeneous H-*ras* indicate that levels are elevated in senescent IMR-90 HDF and are consistent with previous findings by Deng et al., 2004 which reported that the differential effects of *ras* depended upon its signaling intensity. High intensity *ras* signaling activated the p38 MAP kinase pathway and resulted in the accumulation of p53 and $p16^{INK4}$, thereby contributing to cell cycle arrest (28).

A major role of p38 MAP kinase is the regulation of inflammatory cytokine gene expression. More recent studies have revealed that in addition to modulating the cellular stress response it also negatively regulates cell growth (28, 35, 93). The overexpression

of oncogenic *ras* results in premature senescence which is mediated by the p38 MAP kinase signaling pathway (137.

The ability of oncogenic *ras* to induce premature senescence in primary mammalian cells is mediated by an active MEK-ERK-p38 MAP kinase pathway and dominant negative p38 MAP kinase mutant abrogates this effect and prevents premature senescence (137). The observation that p38 MAPK activation is necessary and sufficient for the induction of hnRNP A1 cytoplasmic accumulation in response to osmotic shock along with a concomitant increase in phosphorylation (93) prompted us to test if the p38MAP kinase signaling pathway was upregulated in senescent HDF. So we asked whether levels of activated p38 MAP kinase increased in senescent IMR-90 HDF compared to young HDF. We sought to examine the levels of activated p38 MAPK in IMR-90 by analyzing the endogeneous levels of total p38 MAPK followed by the assesment of the activated form of the kinase in log phase, $G_0$ -arrest, and senescent HDF. Our findings suggest that while the total protein levels of p38 MAPK were relatively unchanged in all three phases, the phosphorylated form of p38 MAPK was markedly upregulated in senescent HDF (fig. 26). These findings were consistent with those in WI38 HDF by Iwasa et al., 2003. This group also found that the inhibition of p38 MAP kinase activity in WI38 HDF resulted in a decrease in β galactosidase activity and an increase in population doublings. Other recent studies have shown that inactivation of p38 MAP kinase resulted in the stimulation of proliferation and a delay in the onset of senescence in rabbit articular chondrocytes (162).

There exist at least three possible mechanisms to describe the ability of p38 MAP kinase to act as a growth inhibitor:

1) p38 MAP kinase has been established as an inhibitor of cyclin D gene expression (148)
2) Secondly, p38 MAP kinase can phosphorylate and inhibit cdc25B and cdc25c, two protein phosphatases that activate cyclin dependent protein kinase activities (149).
3) p38 MAP kinase phosphorylates p53 tumor suppressor protein on two activating sites and causes p53-dependent growth arrest (150 ).

These targets of p38 MAPK may collectively function to negatively regulate the cell cycle. Our studies show that p38 MAP kinase is elevated and functional in senescent IMR-90 (fig. 24). This activity may induce the accumulation of hnRNP A1 in the cytoplasm of senescent cells. As discussed above, p38 MAP kinase signaling cascade mediates cytoplasmic accumulation of hnRNP A1 (93). This increase in phosphorylation was attributed to the reduced interaction of the M-9 motif with the transportin which resulted in A1's cytoplasmic accumulation (71).

## 4.4 Conclusion

Our results show that H-*ras* protein levels and the p38 MAP kinase activity are elevated in senescent IMR-90 HDF. These proteins are also activated in response to external stress stimuli such as osmotic shock, UV radiation, and pro-inflammatory cytokines (153,154,155). Moreover intrinsic stress stimuli such as ROS (reactive oxygen species) which are byproducts of cellular metabolic pathways is a form of cellular stress which is believed to play a regulatory role in the aging process. (157).

These findings are consistent with published reports of elevated p38 MAP kinase activity in senescent WI38 HDF (157). Our observations that there are increased levels of phosphorylated A1 in senescent IMR-90 HDF taken together with the increase in p38 MAPK activity and A1's cytoplasmic accumulation indicates an *in vivo* interaction between these two proteins.

# Chapter 5.

# p38 MAP kinase-hnRNP A1 interaction studies

## 5.1 Introduction

Our data suggests that while hnRNP A1 levels are diminished in senescent IMR-90 HDF, its relative phosphorylation increases compared to young HDF. Our observations also suggest that activated p38 MAP kinase protein levels as well kinase activity are elevated in senescent HDF. Given these findings we asked whether hnRNP A1 interacts with activated p38 MAPK in IMR-90 HDF. We performed co-immunoprecipitation analysis of hnRNP A1- p38 MAP kinase interaction in young, $G_0$-arrest, and senescent IMR-90 and found that hnRNP A1 co-precipitates with p38 MAP kinase in young and $G_0$-arrest fibroblasts but this interaction was not observed in senescent fibroblasts. This may be due to the highly diminished protein levels of hnRNP A1 in senescent IMR-90 HDF and requires further investigation. As a result, however, we focused our analysis of the hnRNP A1-p38 MAP kinase interaction in young IMR-90 HDF.

Here we present in differential co-immunoprecipitation analysis that these two proteins interact *in vivo*. In addition, our data show that exogenously expressed hnRNP A1 also co-precipitates with activated p38 MAPK which further supports our protein interaction studies. These findings suggest that there may be a putative *in vivo* interaction between hnRNP A1 and the activated form of p38 MAP kinase. We further investigated whether p38 MAP kinase inhibition modulates hnRNP A1 protein levels and/or diminishes the putative association between these two proteins using a specific p38 MAP kinase inhibitor.

The analysis demonstrates that *in vivo* inhibition of p38 MAP kinase activity in young IMR-90 HDF modulates the total protein levels of hnRNP A1 in young IMR-90

HDF as well as the protein levels of hnRNP A1 associating with activated p38 MAP kinase.

## 5.2 Results

### A. hnRNP A1 co-immunoprecipitates with p38 MAP kinase

We determined whether A1 and p38 MAP kinase formed a complex by performing co-immunoprecipitation assays. Cell lysates from log phase and $G_0$-arrest IMR-90 HDF were prepared under non-denaturing lysis conditions followed by immunoprecipitation with Phos-p38 MAP kinase antibody. The blot was probed with 4B10-hnRNP A1 and results show that 34 kDa bands representing hnRNP A1 were present (fig. 29, lanes 2 and 3). This study shows that hnRNP A1 can be co-immunoprecipitated with phosphorylated p38 MAP kinase. As a control for specificity, log phase lysates were incubated with actin antibody beads and immunoblotted with hnRNP A1 (fig. 29, lane 1). These experiments were repeated three times using log phase and $G_0$-arrest lysates.

We also tested the ability of hnRNP A1 to co-precipitate with Pp38 MAP kinase in senescent IMR-90 lysates but were unable to detect a 34kDa band (results not shown). The lack of detectable signal may be accounted for by the diminished protein levels of A1 in senescent cells. It was problematic to obtain sufficiently high protein yields to fully characterize *in vivo* interactions of A1 and p38 MAP kinase during senescence. However, this lack of evidence does not rule out a potential p38 MAPK-hnRNP A1 interaction in senescent HDF. All subsequent experiments were carried out with young HDF where the levels of hnRNP A1 are highly expressed.

We next performed the reciprocal analysis to determine whether p38 MAP kinase and phosphorylated p38 MAP kinase co-immunoprecipitated with hnRNP A1. Figure 30 shows that both p38 MAP kinase and phosphorylated p38 MAP kinase co-

immunoprecipitate with hnRNP A1 as indicated by the 38 kDa bands in (fig. 30, panels a and c). Included in each blot was a positive control extract for p38 MAP kinase and phosphorylated p38 MAP kinase (fig. 30, panels a and c, lane 3). These blots was then stripped and reprobed with hnRNP A1 to ensure that hnRNP A1 immunoprecipitated with the 4B10 antibody (fig. 30, panels b and d.). These results show an *in vivo* protein interaction between activated p38 MAP kinase and hnRNP A1. Furthermore the very low levels of co-precipitated phosphorylated p38 MAPK may reflect its diminished protein levels observed in young IMR-90 (fig. 30, panel c). These blots were reprobed with 4B10 antibody which confirmed the immunoprecipitated levels of hnRNP A1 in these lysates (fig. 30, panels b and c). Our results are highly suggestive of a reciprocal interaction between hnRNP A1-Pp38 MAP kinase.

To examine the binding specificity of the activated p38 MAPK antibody used in co-immunoprecipitate studies, we tested whether proteins others than hnRNP A1 co-precipitated with the Pp38 MAP kinase antibody under the conditions examined. We immunoprecpitated phosphorylated p38 MAPK from young HDF lysate and probed with antibodies for GAPDH, BAX, and Endonuclease G (fig.31, lanes 1,3,5, & 7). Whole cell lysates were included in the immunoblot analysis as positive controls for the GAPDH, BAX, and Endonuclease G antibodies (fig. 31, lanes 2, 4, & 8).

Our results show that neither GAPDH, Bax, or endonuclease G co-precipitated with the Pp38 MAP kinase immunoprecipitates (fig. 31, lanes 1, 3, & 7). Furthermore, the identical lysates were also immunoprecipitated with Pp38 MAPK beads and probed with 4B10-hnRNP A1 to detect the simultaneous co-precipitation of hnRNP A1 (fig. 31, lanes 5, 6, & 9). This differential co-precipitation analysis may suggest that the Pp38

MAPK- hnRNP A1 interaction is not the result of non-specific binding of the Pp38-MAP kinase antibody.

**B. Further characterization of hnRNP A1-p38 MAP kinase interaction**

Although our initial experiments suggested that the endogeneous forms of these proteins interact *in vivo*, we tested further the putative hnRNP A1-Pp38 MAP kinase interaction. We performed a transient transfection of the GFP-hnRNP A1 expression vector into young IMR-90 HDF to exogenously express hnRNP A1 for co-precipitation analysis. Immunoblot analysis of lysates prepared from HDF transfected with either pGFP, pGFP-hnRNP A1, or left untreated (NT) indicate that the GFP-hnRNP A1 fusion protein was exogeneously expressed only in the pGFP-hnRNP A1 transfectants as demonstrated by the 65kDa band (34kDa hnRNP A1 + 30 kDa GFP) present in the blot probed with hnRNP A1 antibodies (fig. 32, lanes 3 and 6). In addition both GFP (30kDa) and GFP-hnRNP A1 (65kDa) proteins were detected when the blots were probed with anti-GFP antibodies (fig. 33, lanes 2, 3 and 5, 6). As a control, we transfected an empty GFP vector (lanes 2 and 5) which indicated that the other bands observed in lanes 1 and 4 as well as the additional bands in which cells were transfected with the fusion vector (lanes 3 and 6) were due to non-specific binding. These results strongly suggest that both the GFP and GFP-hnRNP A1 fusion proteins were sufficiently expressed in young IMR-90 HDF.

To determine whether the GFP-hnRNP A1 fusion protein co-precipitated with Pp38 MAP kinase, lysates were prepared from NT, pGFP, and pGFP-hnRNP A1 transfected HDF and immunoprecipitated with Phos-p38 MAP kinase antibody. The

immunoprecipitates were subjected to SDS-PAGE and followed by hybridization with either 4B10-hnRNP A1 or Phos-p38 MAP kinase antibodies

Our findings show that the GFP-hnRNP A1 fusion protein (64kDA) co-precipitated with endogeneous P-p38 MAP kinase (fig.34, panel a, lane 3). The fusion protein was not detected in the NT or pGFP lanes (fig. 34, panel a, lanes 1 and 2). These results suggest an *in vivo* interaction between the exogenous hnRNP A1 and phosphorylated p38 MAP kinase and support our initial studies discussed earlier in this chapter in section A.1. In addition endogenous hnRNP A1,(34kDa) also co-immunoprecipitates with Pp38 MAP kinase in all lanes, as expected, (fig. 34, panel a, lanes 1-3).

In order to confirm the presence of the appropriate co-precipitated protein the same blot was stripped and reprobed with either 4B10-hnRNP A1 or Pp38 MAPK. Both hnRNP A1 and Pp38 MAPK are present in their respective IP's (fig. 34, panel b, lanes 1-3, 5).

Reciprocal experiments were performed using exogeneously expressed p38 MAP kinase in young IMR-90 HDF. We exogeneously expressed the p38 -Flag fusion protein in young HDF and the presence of both exogeneous and endogenous p38 MAP kinase was confirmed by immunoblot analysis using the p38 MAP kinase antibody. The p38-Flag fusion protein has a slightly higher molecular weight compared to endogenous p38 MAP kinase (fig. 35, lanes 3 and 7).

We then assessed the presence of the exogenous p38-Flag fusion protein using the monoclonal M2 Anti-FLAG antibody that binds to fusion proteins containing a FLAG peptide sequence. We were unable to detect p38-Flag fusion protein in these samples

(data not shown) so we immunoprecipitated the lysates using the M2 antibody and probed with p38 MAP kinase antibody (fig. 36). In this manner we were able to enrich for the p38-Flag fusion protein and therefore detect exogeneous p38-Flag using the p38 MAP kinase antibody (fig. 36, lane 5). As expected we did not detect the exogeneous p38-Flag fusion protein in the untreated (NT), pCMV-FLAG, or pCMV-FLAG-BAP transfected HDF (fig.36, lanes 1-4).

We followed up with co-precipitation analysis of these lysates using the M2 anti-FLAG immunoprecipitates in order to precipitate exogenous p38 MAP kinase only. In this manner we tested whether endogenous hnRNP A1 associates with the p38 MAP kinase-Flag fusion protein in the sample. We obtained mixed results for this experiment: the subsequent probing of the M2-anti FLAG immunoprecipitates with 4B10-hnRNP A1 revealed endogenous hnRNP A1 bands for all the samples, NT, pCMV, pCMV-BAP, and pCMV-p38-Flag (data not shown). These findings most likely represent either an overload of the M2-antibody used in the immunoprecipitation reaction or cross-reactivity between the M-2 anti-FLAG antibody and hnRNP A1 since both are monoclonal. However, the earlier experiments whereby hnRNP A1 was co-precipitated with p38 MAP kinase are sufficient to demonstrate the interaction.

We then asked whether levels of endogeneous A1 co-precipitating with Pp38 MAPK IP's increase in HDF expressing exogeneous the p38 –Flag fusion protein. These transfected HDF express two fractions of p38 MAPK, endogenous and exogeneous and presumably both forms are also present in the phosophorylated state. Using the Pp38 MAPK antibody we immunoprecpitated lysates prepared from untreated HDF, pCMV-BAP, pCMV-FLAG-BAP, and pCMV-p38-Flag transfected HDF. These

immunoprecipitates were subjected to SDS-PAGE and immunoblotted with 4B10-hnRNP A1 antibodies (fig. 37).

Our results show that the endogenous level of hnRNP A1 co-precipitated with Pp38 MAP kinase is increased in the pCMV-p38-Flag transfected HDF (fig.37, lane 4) compared to the NT, pCMV-FLAG, and pCMV-FLAG-BAP transfected HDF ( fig.37, lanes 1-3). This is consistent with the collective association of hnRNP A1 with both endogeneous and exogeneous p38 MAP kinase and should show an increase in signal on co-immunoprecipitation.

### C. Inhibition of *in vivo* p38 MAP kinase activity in IMR -90 HDF using SB203580

We next sought to determine whether we could inhibit the phosphorylation of hnRNP A1 by p38 MAP kinase using a specific inhibitor of this enzyme. Therefore we used the pyridinyl imadazole, SB203580 ($IC_{50}$ value= 600nm for *in vivo* inhibition), a well characterized inhibitor of p38 MAP kinase to inhibit p38 MAP kinase activity *in vivo* (72). The lowest concentration required for partial inhibition of kinase activity in IMR-90 HDF was empirically determined at 2.5uM:

Log phase, $G_0$-arrest, and senescent IMR-90 HDF were treated with 2.5uM SB203580 or DMSO equivalent and immunoprecipitated with phos-p38 MAP kinase beads followed by kinase assay with ATF-2 ($Thr^{71}$) as the substrate (fig. 38).

Results suggest that kinase activity was partially blocked in log phase, $G_0$-arrest, and senescent HDF treated with 2.5uM SB203580 compared to the HDF treated with DMSO equivalent (fig. 38, lanes 2,4,6). SB203580 specifically inhibits the p38 MAP kinase isoforms, α and β while the remaining two isoforms γ δ are unaffected (151).

We then examined the effects of inhibiting the basal activation of p38 MAP kinase *in vivo* using the p38 MAP kinase inhibitor SB203580 on the phosphorylation levels of hnRNP A1 in young HDF. Young IMR-90 HDF were incubated in 2.5uM of SB203580 or DMSO equivalent and subjected to immunoblot analysis using antibodies to hnRNP A1. Results suggest that the endogeneous levels of hnRNP A1 are upregulated in the SB203580 treated young HDF compared to the DMSO treated HDF (fig. 39, lanes 2 and 4). We were surprised to find that the total protein levels of hnRNP A1 was modulated through inhibition of the p38 MAP kinase pathway. This experiment was repeated three times and graphical analysis of these results suggest that there is a 1.5 fold increase in the upregulation of total hnRNP A1 protein levels in HDF treated with SB203580 (fig. 42).

Subsequent analysis using SB203580 was performed only in young HDF due to the observation in immunoblot analysis which showed that protein levels of hnRNP A1 in senescent HDF remain relatively unaffected bytreatment with SB203580 as compared to DMSO treated senescent HDF (fig. 39). Our data suggests that inhibition of p38 MAP kinase upregulates the hnRNP A1 protein levels in young HDF. However, this does not exclude the possibility that hnRNP A1 protein levels in senescent HDF may be affected by concentration and exposure times not examined in this study and requires further testing.

The modulation of protein levels of hnRNP A1 by p38 MAP kinase prompted us to next examine the effects of p38 MAPK inhibition on the co-precipitation of hnRNP A1. Young IMR-90 HDF were incubated with 2.5uM SB203580 or DMSO equivalent and immunoprecpitated with Pp38 MAPK kinase antibody. These IP reactions were then

subjected to SDS-PAGE and immunoblotted with antibodies to hnRNP A1. The results suggest that the levels of hnRNP A1 co-precipitating with Pp38 MAP kinase are increased in HDF treated with SB203580 compared to DMSO treated HDF (fig. 41, lanes 2 and 4). Graphical analysis of these results suggests a 4.0 fold increase in the level of co-precipitating hnRNP A1 in these Pp38 MAPK immunoprecipitates (fig. 43).

**hnRNP A1 co-immunoprecipitates with phosphorylated p38 MAP kinase**

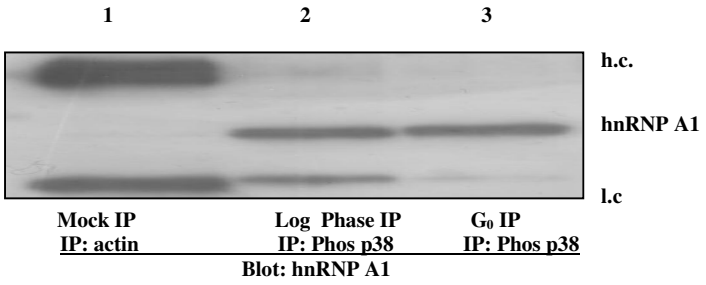


**Figure 29. Cө immunoprecipitation of hnRNP A1 in Pp38 MAP kinase immunprecipitates.** 300ug of log phase and $G_0$-arrest lysates were immunoprecipitated with 20ul immobilized Phospho-p38 MAP kinase ($Thr^{180}/Tyr^{182}$) monoclonal antibody beads, subjected to 12% SDS-PAGE and subsequently immunoblotted with 4B10-hnRNP A1 antibody. A mock IP reaction was included to establish the molecular weight of the antibody heavy and light chain, 55 & 25 kDa, respectively. This experiment was repeated three times.

**Reciprocal analysis**

**p38 MAP kinase and phosphorylated p38 MAP kinase co-immunoprecipitate with hnRNP A1**

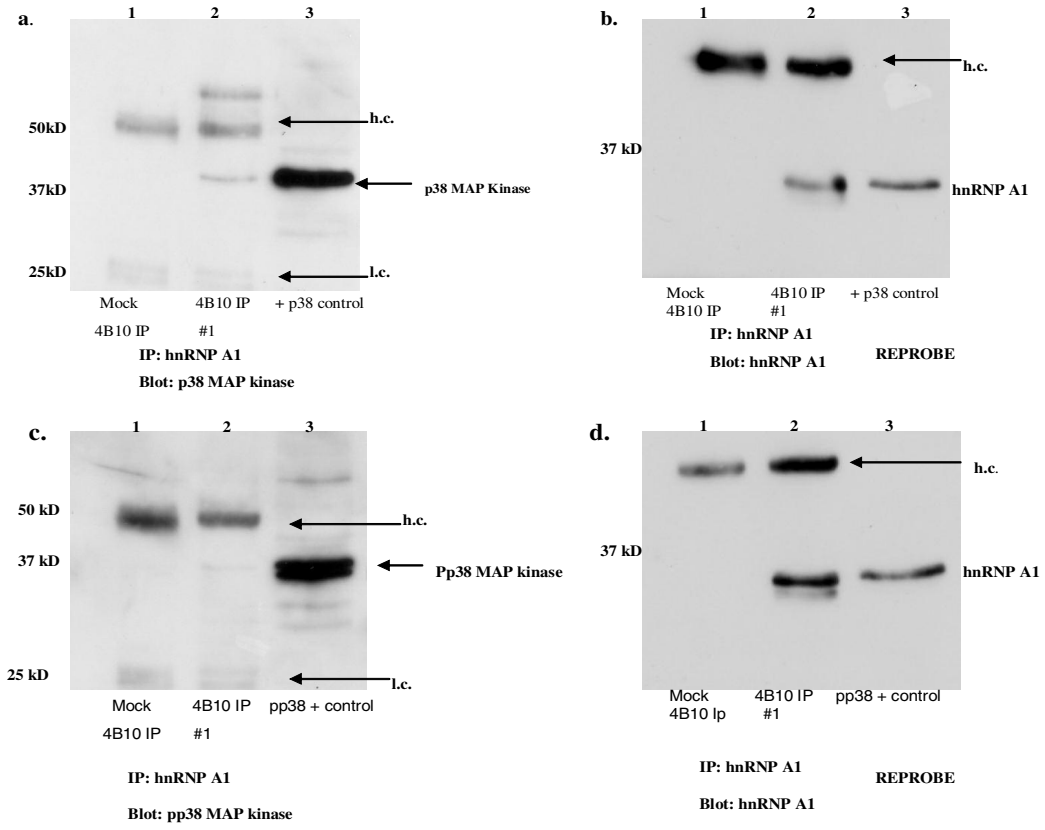


**Figure 30. Co-immunoprecipitation of p38 MAPK and phosphorylated p38 MAPK with hnRNP A1.** 300 ug of total lysate isolated from log phase IMR-90 HDF were immunoprecipitated using 4B10-hnRNP A1 antibody, subjected to 12.5% SDS-PAGE and immunoblotted with either **panel a**) p38 MAP kinase or **panel c**) Pp38 MAP kinase to detect co-precipitation of these proteins. Both blots were stripped and reprobed with 4B10 monoclonal antibody to detect total hnRNP A1**, panels b**) and **d**). Mock IP reactions were included to establish the molecular weight of the antibody heavy and light chain, 55 & 25 kDa, respectively. This reaction contained antibody and beads only.

**Differential co-immunoprecipitation of GAPDH, BAX, and Endonuclease G**

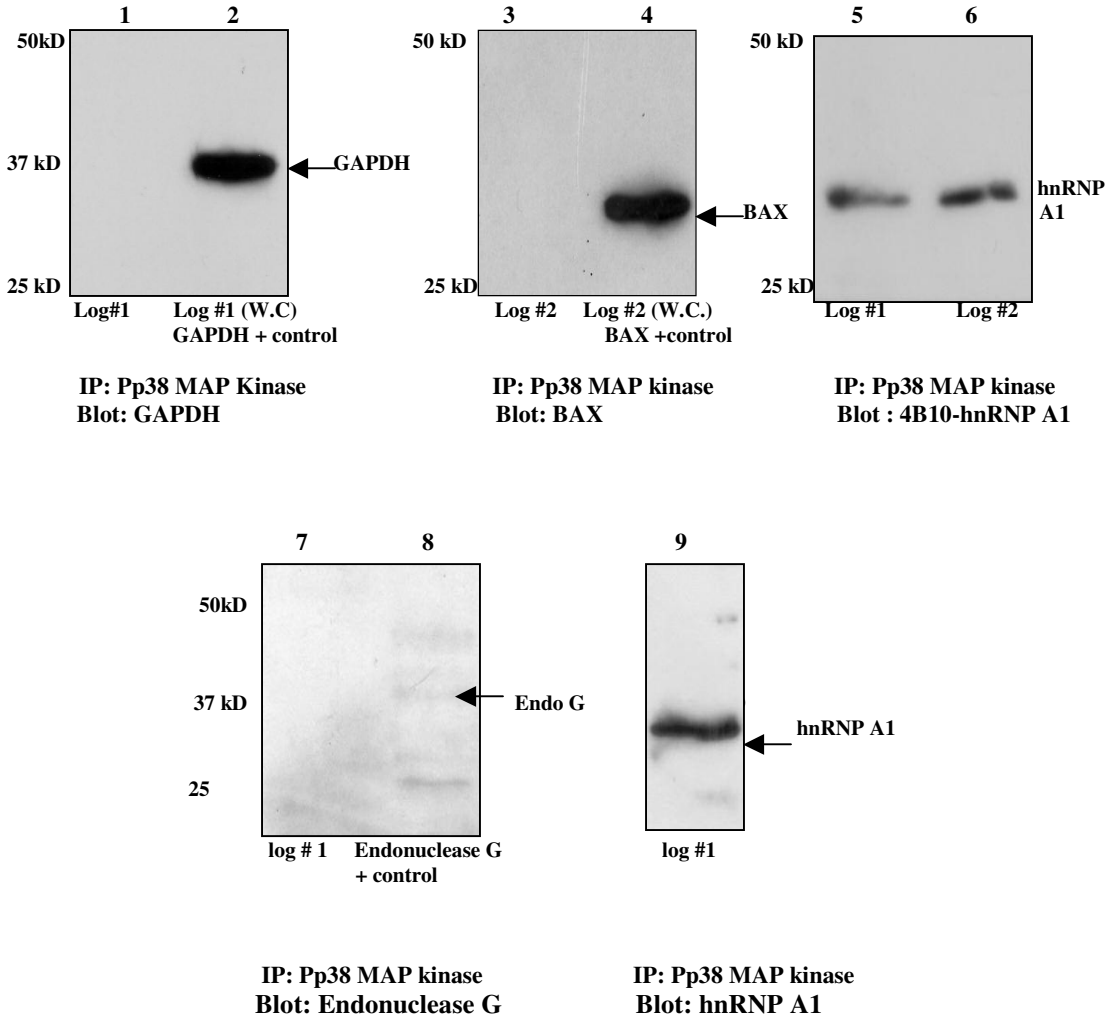


**Figure 31. Differential co-immunoprecipitation of Bax, GAPDH, and endonuclease G with Pp38 MAP kinase IP's.** 300 ug of total cell lysate from log phase IMR-90 HDF were immunoprecipitated with Immobilized Phos-p38 MAP kinase antibody beads, subjected to 12% SDS-PAGE, transferred to PVDF membrane, and probed with either GAPDH, ( lanes 1&2), BAX, ( lanes 3& 4), endonuclease G, ( lanes 7&8), or hnRNP A1, (lanes 5, 6, & 9). Positive controls for GAPDH, Bax, and endonuclease G were included in lanes 2, 4, and 8 respectively. These experiments were performed in duplicate.

**Immunoblot analysis of pGFP-hnRNP A1 fusion protein**

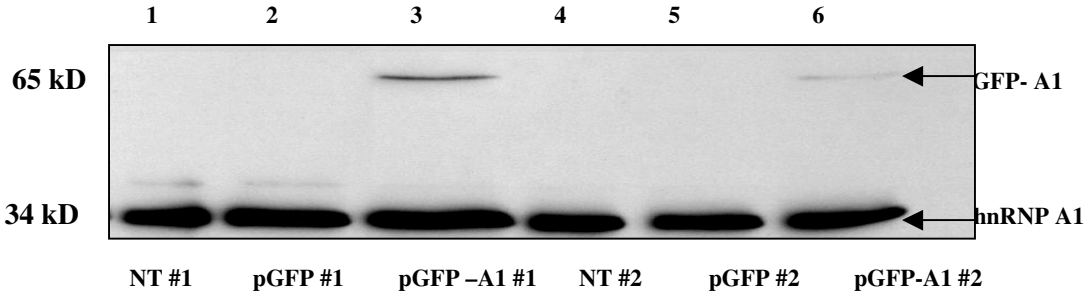


**Figure 32 . Immunoblot analysis of pGFP-hnRNP A1 fusion protein levels**. IMR-90 fibroblasts were transfected with pGFP (empty vector), pGFP-A1, or left untreated (NT). 20 and 30 ug of total lysates were collected 48 hrs later, resolved by 12% SDS-PAGE and immunoblotted with 4B10-hnRNP A1 antibody. This experiment was performed in duplicate.

**GFP and GFP-A1 protein levels**

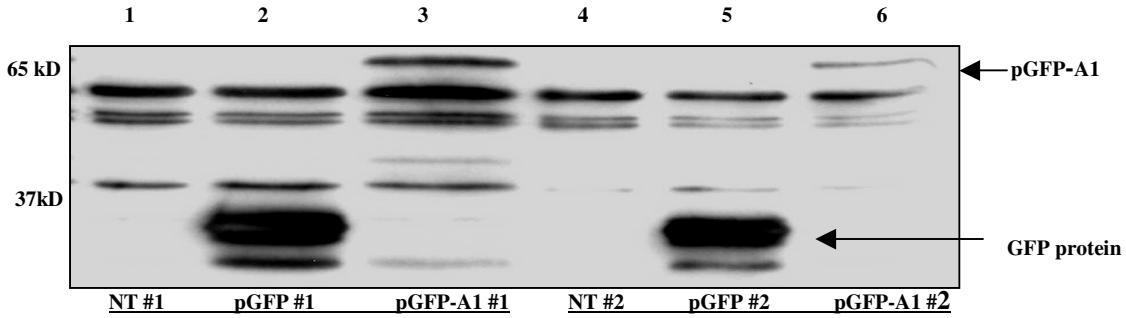


**Figure 33. Immunoblot analysis of the Green Fluorescent Protein.** IMR-90 fibroblasts were transfected with pGFP (empty vector), pGFP-A1, or left untreated (NT). Lysates were collected 48hrs later, resolved by 12% SDS-PAGE and immunoblotted with a monoclonal GFP antibody. This experiment was repeated two times.

**Pp38 MAP kinase-GFP-A1 co-immunoprecipitation analysis**

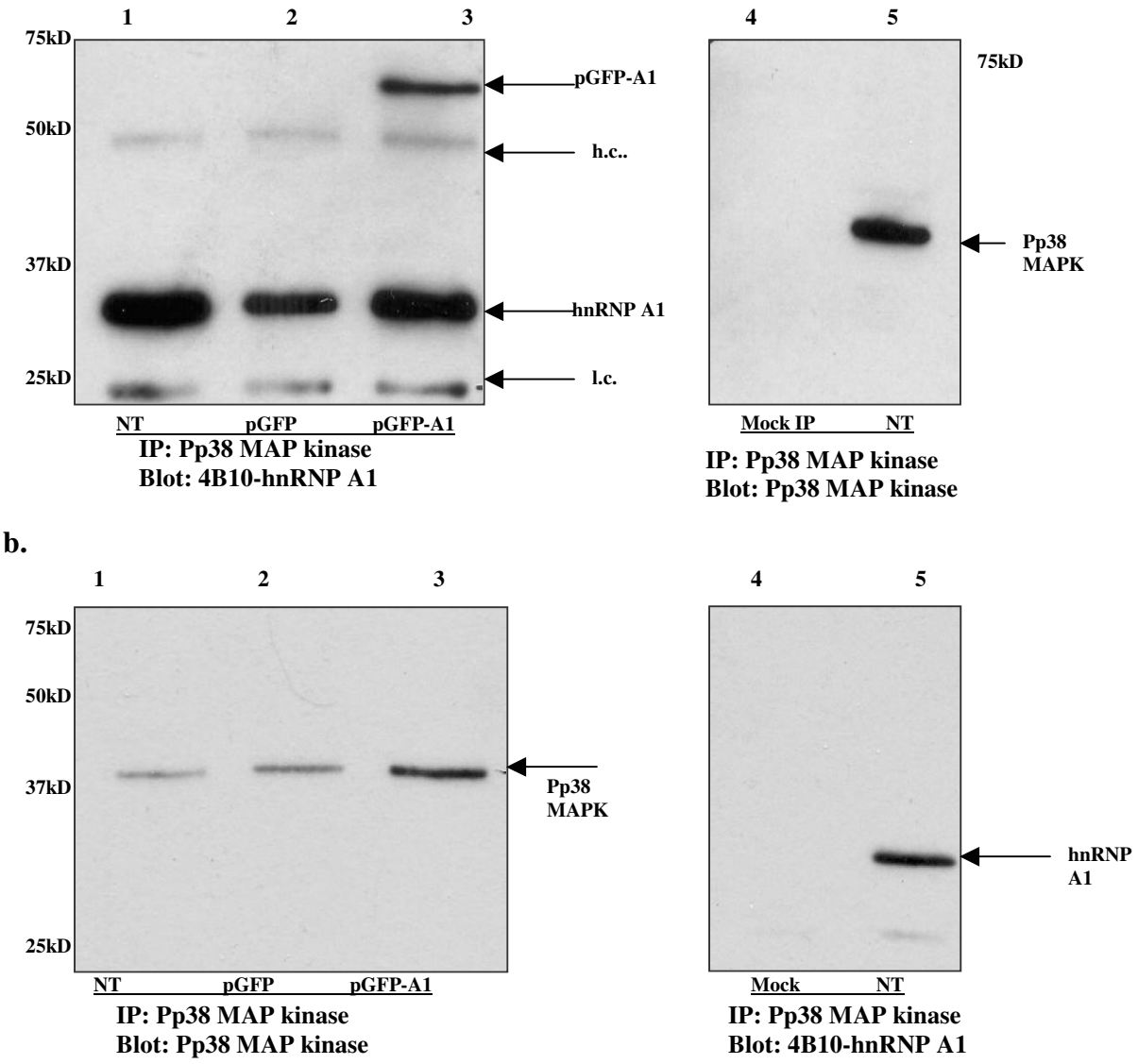


**Figure 34. Co-precipitation analysis of Pp38 MAP kinase-exogenous hnRNP A1 interaction** was examined once the expression of pGFP-A1 was confirmed by western analysis. **Panel a)** Lysates prepared from pGFP, pGFP-A1, or untreated (NT) were immunoprecipitated with Pp38 MAP kinase, subjected to 12,5% SDS-PAGE, transferred to PVDF,and probed with either 4B10 –hnRNP A1 or Pp38 MAP kinase as a positive control for the immunoprecipitation reaction. **Panel b)** Reprobe of Pp38 MAP kinase-hnRNP A1 blot with Pp38 MAP kinase or hnRNP A1. This experiment was repeated two times.

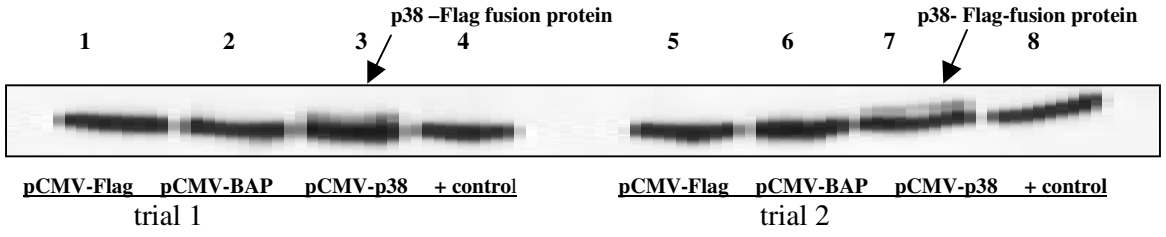


**Figure 35. Immunoblot analysis of exogenous p38 MAP kinase in transfected IMR-90 HDF.**
Log phase HDF were transfected with pCMV-Flag (empty vector, lanes 1 & 5), pCMV-Flag-BAP (lanes 2 & 6), or pCMV-p38-Flag ( lanes 3 & 7).
Lysates were collected 48 hours later, resolved by 12% SDS-PAGE, and followed with immunoblotting with p38 MAP kinase antibody. A positive control for endogenous p38 MAP kinase was loaded in lanes 4 & 8). This experiment was repeated two times.

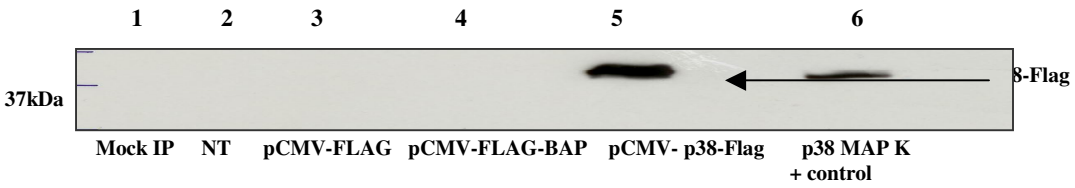


**Figure 36. Immunoprecipitation of p38-Flag with M2 anti-FLAG antibody to detect exogeneous p38 MAP kinase.** Immunoblot analysis of exogeneous p38 MAP kinase-Flag fusion protein using the M2 antibody which detects fusion proteins containing a FLAG peptide. 600ug of lysate was collected from NT, or pCMV-FLAG, pCMV-FLAG-BAP, and pCMV-p38-Flag transfected IMR-90 HDF (lanes 2,3,4, &5) and immunoprecipitated with the M2 anti-Flag antibody . The IP reactions were subjected to 12.5% SDS-PAGE, transferred to PVDF, and immunoblotted with p38 MAP kinase antibody. 30ug of a positive control lysate for endogenous p38 MAP kinase was included in lane 6. This experiment was repeated in duplicate.

**hnRNP A1 co-immunoprecipitation of phos p38 MAP kinase IP's**

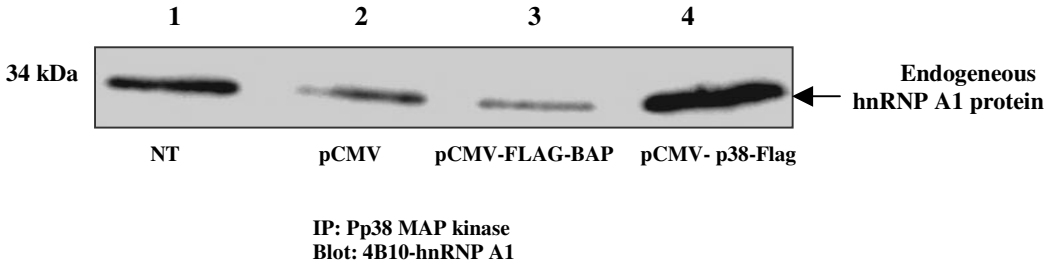


**Figure 37. hnRNP A1 co-precipitation of phosphorylated 38 MAP kinase IP's in pCMV-p38-Flag transfected IMR-90.** 300 ug of lysate collected from NT (No treatment) pCMV, pCMV-FLAG-BAP, pCMV-p38 Flag, were immunoprecipitated with pp38 MAP kinase antibody, subjected to 12.5% SDS-PAGE and immunoblotted with 4B10 which detects total levels of hnRNP A1 co-immunoprecipitating with Pp38 MAP kinase in these samples. This experiment was repeated two times.

**p38 MAP kinase assay in IMR-90 HDF treated with SB203580**

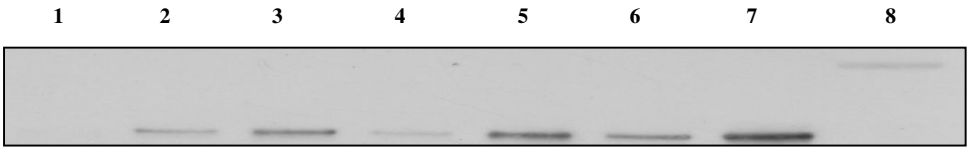


**Figure 38. p38 MAP Kinase Assay in IMR-90 HDF treated with 2.5uM SB203580.** 200ug of total cell lysate prepared from log phase ( lanes 2 & 3), $G_0$ arrest ( lanes 4 & 5), and senescent HDF (lanes 6 & 7) treated with 2.5uM SB203580 (SB) or DMSO (DM) equivalent were immunoprecipitated with Pp38 MAP kinase antibody and a kinase assay was performed using a synthetic pATF-2 (71) peptide as the substrate. This experiment was repeated two times. A positive control for phosphorylated ATF-2 was included in lane 8.

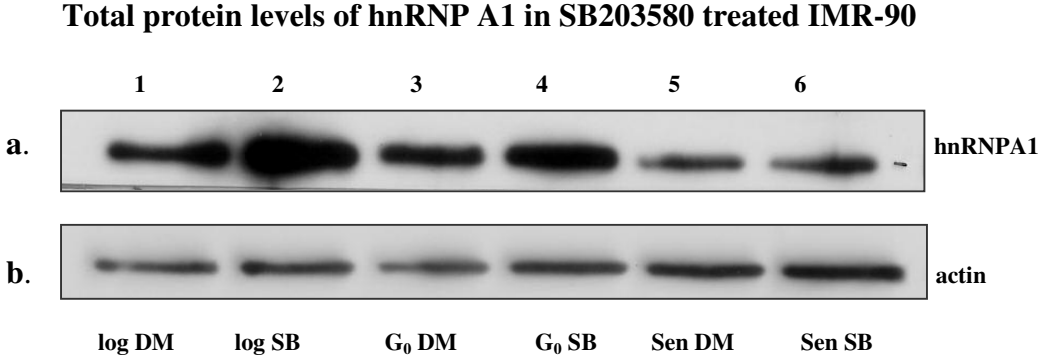


**Figure 39. Immunoblot analysis of total hnRNP A1 protein levels. Panel a)** 20 ug of lysate prepared from log phase ( lanes 1 & 2), $G_0$-arrest (lanes 3 & 4), and senescent HDF (lanes 5 & 6) treated with 15uM SB203580 or DMSO equivalent were subjected to 12% SDS-PAGE, transferred to PVDF and probed with 4B10-hnRNP A1 antibody. **Panel b)** Membrane was stripped and reprobed with actin as a loading control. This experiment was repeated in triplicate.

***In vivo*** **p38 MAP kinase inhibition using SB203580**

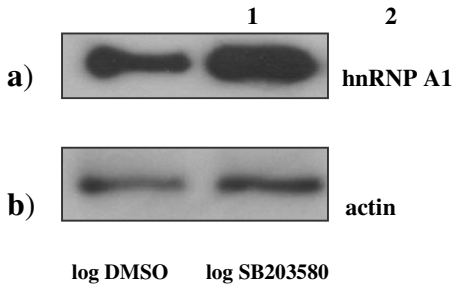


**Figure 40. Immunoblot analysis of hnRNP A1 protein levels in SB203580 treated young HDF.** 15 ug of total cell lysate prepared from SB203580 (2.5uM) treated (panel a, lane 2) or DMSO equivalent HDF (panel a, lane 1) were subjected to 12% SDS-PAGE,and immunoblotted with 4B10- hnRNP A1 antibody to detect total protein levels of hnRNP A1. Membranes were stripped and reprobed for actin levels. These experiments were performed three times.

**Co-immunoprecipitation of hnRNP A1 with Pp38 MAP kinase in SB203580 treated IMR-90 HDF**

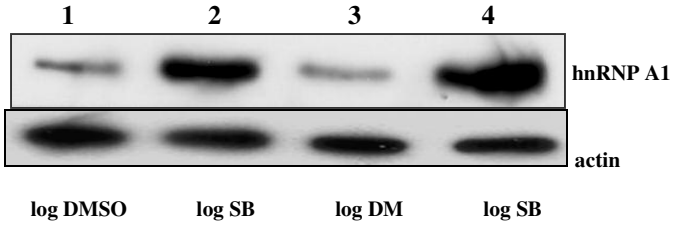


**Figure 41. Co-immunoprecipitation of hnRNP A1 with Pp38 MAP kinase**. 200ug of total cell lysate collected from SB203580 (2.5uM) treated or DMSO equivalent HDF were immunoprecipitated with Pp38 MAP kinase, subjected to 12.5% SDS-PAGE, transferred to PVDF membrane, and immunoblotted with 4B10-hnRNP A1 antibody. 5 ug of collected supernatant from each reaction were immunoblotted for actin levels. These experiments were performed three times.

| Cell Line | Signal Intensity ( ImageQuant™) | | |
|---|---|---|---|
| | 1 | 2 | 3 |
| Log phase IMR-90 SB203580 | 188.7 | 200.0 | 148.3 |
| Log phase IMR-90 DMSO | 63.9 | 132.3 | 118.3 |
| Ratios: | 2.95:1 | 1.5:1 | 1.25:1 |
| | | S.E.± 0.54 | |

Table 3. Ratios of signal intensities for total protein levels of hnRNP A1 in SB203580 treated IMR-90 HDF. Control lysates were treated with DMSO (dimethylsulfoxide) equivalent. ImageQuant™ analysis was used to calculate the ratios (of signal intensity) by dividing the intensity of the whole protein levels in the treated samples by the intensity obtained in the control samples which were normalized to 1. Three independent experiments were analyzed. Standard error was calculated as the standard deviation/√N where = sample number. Refer to figure 42 for graph.

**Graphical analysis of hnRNP A1 protein levels in SB203580 treated IMR-90 HDF**

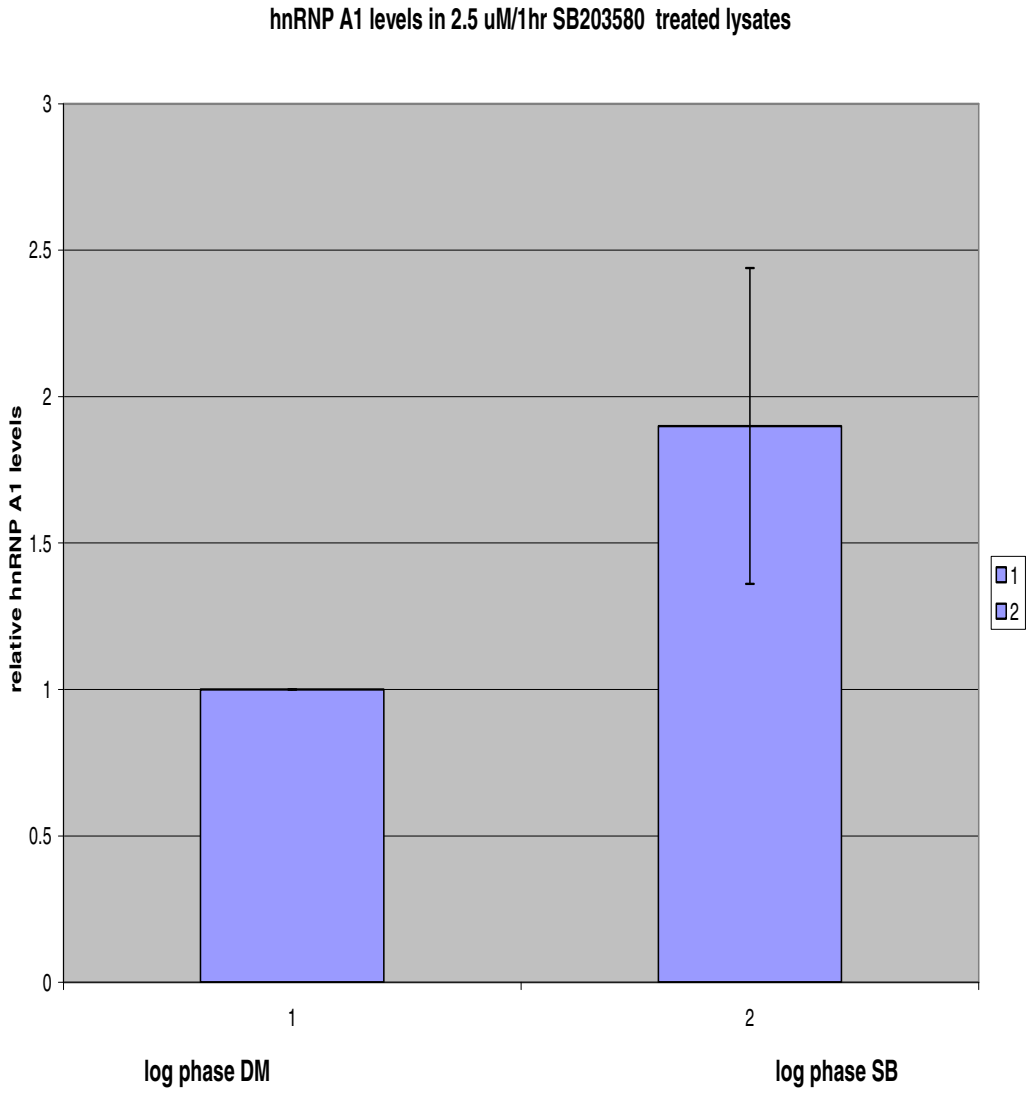


**Figure 42. Graphical analysis of hnRNP A1 protein levels in SB203580 treated IMR-90 HDF. a**) hnRNP A1 protein levels in whole cell lysate Results were presented as hnRNP A1 protein levels relative to the protein levels in the presence of SB203580. Data are presented as S.E.± densitometeric values from 3 independent experiments.

| Cell line | Signal Intensity ( ImageQuant™) | | |
|---|---|---|---|
| | 1 | 2 | 3 |
| **Log phase IMR-90 SB203580** | **165.3** | **163.6** | **185.6** |
| **Log phase DMSO** | **49.3** | **31.7** | **46.1** |
| **Ratios:** | **3.35:1** | **5.15:1** | **4.0:1** |
| | **S.E.± 0.53** | | |

Table 4. Ratios of signal intensities for co- immunoprecipitated hnRNP A1 protein levels in SB203580 treated IMR-90 HDF. Control lysates were treated with DMSO (dimethylsulfoxide) equivalent. ImageQuant ™ analysis was used to calculate the ratios (signal intensity) by dividing the intensity of the co-immunoprecipitated protein levels in the treated samples by the intensity obtained in the control samples which were normalized to 1. Three independent experiements were analyzed. Standard error was calculated as the standard deviation/√N where = sample number. Refer to figure 43 for graph.

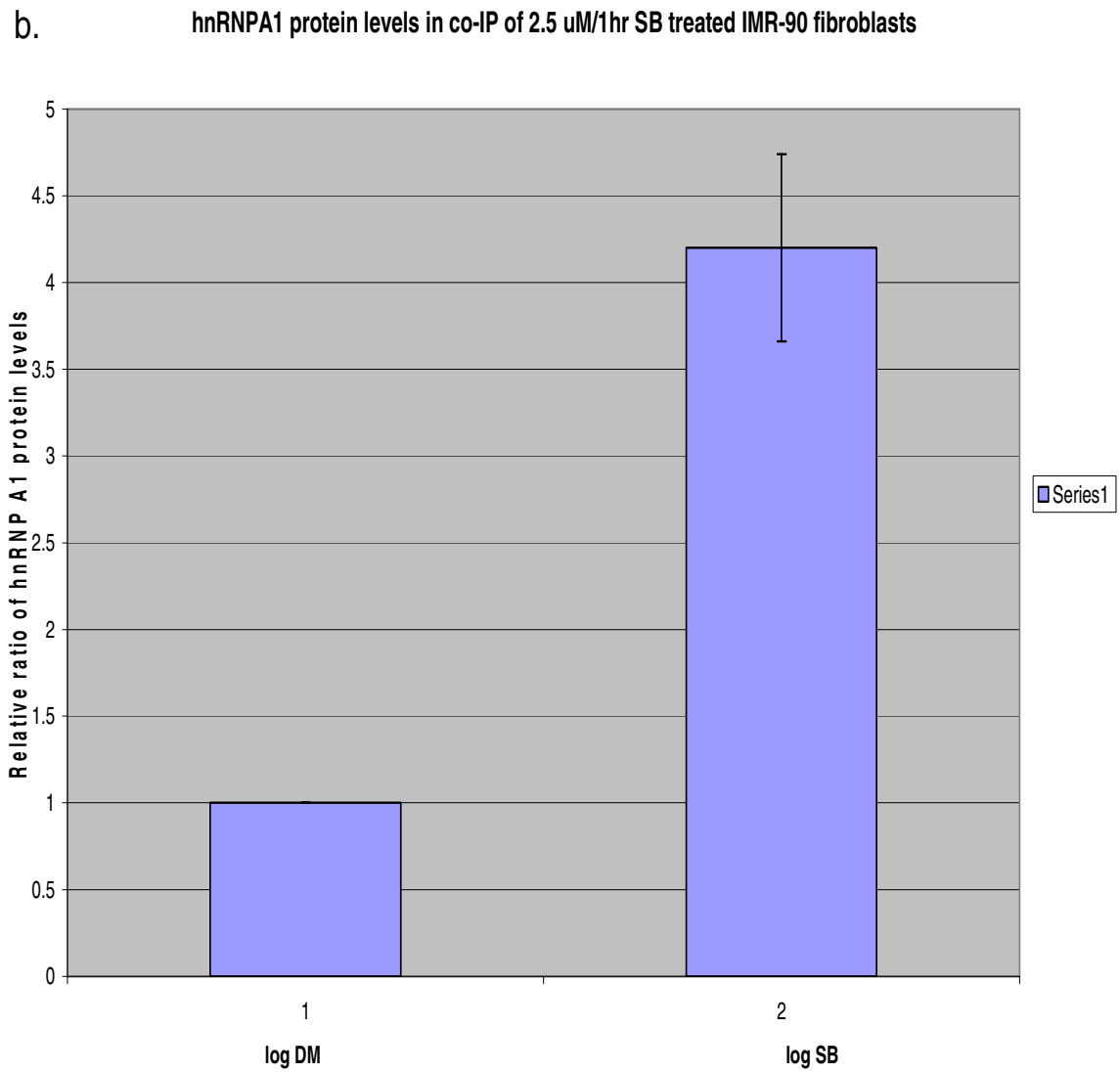


**Figure 43. Graphical analysis of hnRNP A1 protein levels in SB203580 treated IMR-90 HDF**. hnRNP A1 co-precipitating with Pp38 MAP kinase.
Results were presented as hnRNP A1 protein levels relative to the protein levels in the presence of SB203580. Data are presented as S.E.± densitometeric values from 3 independent experiments.

## 5.3 Discussion

### p38 MAP kinase- hnRNP A1 interaction studies

Our preliminary studies strongly suggest that hnRNP A1 co-precipitates with activated p38 MAP kinase in young IMR-90 HDF. We attempted to test this putative interaction in senescent HDF but were unable to detect co-precipitating hnRNP A1 at the protein concentrations examined (results not shown). While the activated form of p38 MAP kinase is elevated in senescent IMR-90 HDF, the protein level of hnRNP A1 is highly diminished and may account for the lack of detection. As a result we focused instead on testing this interaction in young IMR-90 HDF. Our co-immunoprecipitation analysis of the putative hnRNP A1-phosphorylated p38 MAP kinase interaction suggests that in young IMR-90 HDF, hnRNP A1 co-precipitates with phosphorylated p38 MAP kinase (fig. 29) and this interaction is not observed in Pp38 MAP kinase precipitates probed with irrevelant antibodies. Additional co-precipitation experiments using young IMR-90 lysates immunoprecipitated with the hnRNP A1 antibody demonstrated that both p38 MAPK and Pp38 MAPK co-precipitated with hnRNP A1.

Analysis of the putative p38 MAP kinase-hnRNP A1 interaction using exogenously expressed hnRNP A1 protein demonstrated that a GFP-A1 fusion protein also co-immunoprecipitates with p38 MAP kinase.

Our findings of a putative protein interaction are supported by recent studies which show that hnRNP A1 is phosphorylated by Mnk 1, a kinase substrate of p38 MAP kinase (115). Earlier studies by others found that while hnRNP A1 phosphorylation was

mediated by the p38 MAP kinase pathway , it was not shown to directly phosphorylate hnRNP A1 either *in vitro* or *in vivo* (93). Our data suggests a reciprocal hnRNP A1-p38 MAP kinase interaction and thus an indirect phosphorylation event via the p38 MAP kinase pathway in IMR-90 HDF cannot be excluded.

We questioned if the levels of hnRNP A1 co-precipitating with phosphorylated p38 MAP kinase increase in IMR-90 HDF which exogeneously express p38 MAP kinase. The rationale was that there should be more substrate (endogeneous and exogeneous p38 MAPK) available for this binding interaction and thus more hnRNP A1 co-precipitating with phosphorylated p38 MAPK. Our findings suggest that more hnRNP A1 co-precipitated in the cells transfected with pCMV-p38-Flag compared to the untreated, pCMV, or pCMV-FLAG-BAP transfected cells. This is consistent with the exogeneous expression of p38 MAP kinase which may result in an increased level of the phosphorylated form of kinase present in the immunoprecipitation reaction and in the collective amounts of hnRNP A1 co-precipitating with these IP's.

**p38 MAP kinase activity inhibition studies**

p38 MAP kinase has been previously shown by others to modulate both the accumulation and phosphorylation of hnRNP A1 in response to osmotic shock. Their *in vitro* analysis suggested that kinase substrates of p38 MAP but not p38 MAPK itself interacted with hnRNP A1 (93). Other studies have shown that its splice form $A_0$ is phosphorylated by MAPKAP2, a substrate for p38 MAPK α (144). Mnk 1 has been shown more recently to directly phosphorylate hnRNP A1 thus establishing p38 MAPK as upstream effector of hnRNP A1 phosphorylation (115). Iwasa et al., 2003

demonstrated that in senescent WI38 HDF the inhibition of p38 MAP kinase correlated with a decrease in B-galactosidase activity and an increase in population doublings.

In light of our recent findings which suggests an *in vivo* phosphorylated p38 MAPK-hnRNP A1 interaction in IMR-90 HDF, we asked whether inhibition of the p38 MAP kinase would modulate a) the phosphorylation levels of hnRNP A1 and/or b) the association of hnRNP A1 with Pp38 MAPK IP's.

*In vivo* inhibition of p38 MAP kinase activity using SB203580 has been extensively documented (151). Enslen et al., 1998 reported effective but not total inhibition of p38 MAP kinase isoforms α and β2 using 1uM SB203580 (106). This is a well characterized pyridinyl imidazole inhibitor which has been shown to compete for the ATP- binding site of p38 MAP kinase (158). Thus it only inhibits the catalytic activity of p38 MAP kinase and not its own phosphorylation.

Kinase assays were performed in order to determine the degree of inhibition as measured by phosphorylation of a synthetic ATF-2 substrate. Our results suggest that a concentration of 2.5uM SB203580 partially inhibited the catalytic activity of p38 MAP kinase in young, $G_0$ arrest, and senescent IMR-90 (fig.39). The partial inhibition of the kinase activity may be attributed to several factors. First, the precise concentration of inhibition can vary from cell to cell, cell type to cell type, and from cell phase to cell phase. We observed that one concentration did not inhibit total p38 MAP kinase activity in all three cell phases. Secondly, SB203580 specifically inhibits the p38 MAP kinase isoforms α and β so that the remaining two isoforms, γ and σ putatively retain their catalytic activity and could potentially phosphorylate the ATF-2 substrate used in the kinase assay. Given these caveats, we empirically determined an optimum concentration

of 2.5 uM and an exposure time of 1hr to partially inhibit p38 MAP kinase activity in young, $G_0$ arrest and senescent HDF IMR-90 HDF.

However, when we inhibited p38 MAP kinase activity in young IMR-90 HDF and examined the endogenous protein levels of hnRNP A1 we unexpectedly found that total hnRNP A1 protein levels were upregulated by 1.5 fold in the HDF treated with 2.5uM SB203580 compared to the DMSO treated HDF (figs.35 and 36). We limited our inhibition studies to young IMR-90 HDF due to the observation that protein levels of hnRNP A1 in senescent HDF treated with SB203580 were relatively unchanged (fig. 35).

Additionally, co-precipitation analysis of the hnRNP A1-phos p38 MAP kinase interaction suggests that inhibition of p38 MAP kinase activity modulates the protein levels of hnRNP A1 associating with phosphorylated p38 MAP kinase. Our results suggest that there was a 4.0 fold increase in the protein levels of hnRNP A1 co-precipitating with Pp38 MAP kinase in HDF treated with 2.5uM SB203580 compared to the DMSO treated HDF (fig 37). These studies also indicate that the hypophosphorylated form of hnRNP A1 binds to p38 MAP kinase preferentially. The results of the co-immunoprecipitation experiments also suggest that inhibition of p38 MAP kinase activity increases the ability of p38 MAP kinase to interact with hnRNP A1. Thus, it may be that the unphosphorylated form hnRNP A1 binds preferentially in the complex with subsequent phosphorylation by p38 MAP kinase or a kinase downstream in its pathway. Phosphorylation of another well known splicing factor, SF2/ASF, regulates its binding to SR protein –specific kinase (SRPK) (163). Serine/Arginine splicing factors (SR) are posttranslationally modified by phosphorylation on serine residues (164) Unphosphorylated SF2/ASF binds to SRPK whereas phosphorylated SF2/ASF does not

(163). It cannot be excluded however, that the increase in hnRNP A1 protein co-precipitating in these experiments is due to the better accessibility of the antibody for precipitation of the complex.

These findings also do not exclude the possibility that hnRNP A1 protein levels in senescent HDF are potentially modulated by p38 MAPK inhibition especially given that phosphorylated p38 MAPK protein levels are elevated in senescent HDF. Further analysis with time-course and dose-response studies are required in order to effectively analyze this question.

Modulation of protein levels has been well documented for other proteins via phosphorylation/dephophorylation (159.). The p38 MAP kinase pathway can regulate protein stability via phosphorylation, for example in the ubiquitination and degradation of cyclin D1 protein which is triggered by direct phosphorylation on Thr 286 by p38 MAP kinase (114) Phosphorylation has been shown to effect the protein levels of hnRNP A1 through the ubiquitin pathway (92).

Our data suggests that steady state endogenous levels of hnRNP A1 in IMR-90 HDF may be regulated by signaling mediated by the p38 MAP kinase pathway Collectively, these results suggest that in young IMR-90 HDF 1) inhibition of p38 MAP kinase activity upregulates total hnRNP A1 protein levels and 2) protein levels of hnRNP A1 in young IMR-90 HDF are potentially modulated by the p38 MAP kinase signaling pathway and 3) the putative Pp38 MAPK –hnRNP A1 interaction is modulated by inhibition of p38 MAP kinase activity. The mechanism whereby inhibition of p38 MAP kinase results in the apparent modulation of hnRNP A1 protein levels is presently unknown. It may be due to the effects of indirectly inhibiting Mnk phosphorylation

Mnk1/2 which are substrates for p38 MAP kinase, have been recently shown to phosphorylate hnRNP A1 *in vitro* and *in vivo* (115).

## 5.4 Conclusion

One important consequence of the observed diminished protein levels and cytoplasmic accumulation of hnRNP A1 in senescent HDF is the alteration of nuclear ratios of hnRNP A1 to antagonistic splicing factors. Both hnRNP's and SR proteins vary in concentration between different cell types and differential expression of these proteins in concert may affect the alternative splicing of select pre-mRNA's (165). Recent data suggests that ratios of hnRNP A1 to antagonistic splicing factors in the nucleus have a role in c-H-ras alternative splicing and thus acts as a *trans*-acting factor (136). Our data suggests that c-H-*ras* protein levels are elevated in senescent HDF which may be consistent with the diminished hnRNP A1 protein levels and cytoplasmic accumulation observed in senescent HDF. Activated p38 MAP kinase protein levels and kinase activity are also elevated in senescent HDF. Two major observations underlie the involvement of both nuclear and cytoplasmic hnRNP A1 in RNA metabolism: 1) the p38 MAPK- mediated cytoplasmic accumulation of hnRNP A1 resulted in its altered alternative splicing activity, (93), and 2) Mnk1- mediated phosphorylation of hnRNP A1 reduced its binding to TNF α AU-rich sequences (ARE) both *in vitro* and *vivo*, (115). Furthermore our studies suggest that 1) p38 MAP kinase and hnRNP A1 associate *in vivo* and) inhibition of p38 MAP kinase activity modulates hnRNP A1 protein levels. Collectively these findings suggest potential mechanisms to link the p38 MAP kinase-hnRNP A1 interaction to either the induction or maintenance of the senescent phenotype through the altered regulation of post-transcriptional processing.

## 5.5 Future Experiments

Follow up studies in IMR-90 HDF to further examine the modulation of hnRNPA1 protein levels and the hnRNP A1-p38 MAPK protein interaction studies include:

**A. p38 MAP kinase- hnRNP A1 n senescent IMR-90 HDF:**

1. To test the putative p38 MAP kinase –hnRNP A1 interaction in senescent HDF. This experiment involves optimization of protein recovery in senescent HDF.
2. To determine optimum inhibition of p38 MAP kinase in senescent HDF using time course studies with SB203580.
3. Test the modulation of hnRNP A1 protein levels by inhibition of p38 MAP kinase

**B. *In situ* immunofluorescence studies:**

1. Examine p38 Map kinase inhibition in senescent HDF. Will it induce a nuclear relocalization of hnRNP A1?
2. Transiently transfect p38- Flag in young IMR-90 HDF. Will this alter the subcellular distribution of hnRNP A1?

**C. Phosphorylation assays:**

Examine MNK as a putative regulator of hnRNP A1 phosphorylation protein levels:

1- Test Mnk1/2 kinase activity in IMR-90 HDF. Is it upregulated in senescence?

2- Examine whether Mnk inhibition modulates phosphorylation of hnRNP A1 in log phase, $G_{0-}$ arrest, and senescent HDF.

3- Test whether inhibition of p38 MAP kinase activity inhibits the Mnk1/2 kinase activity in young and senescent HDF.

## References


1. Hayflick, L., Moorehead, P.S., 1961. The serial cultivation of human diploid cell strains. Exp. Cell. Res. 25, 585-621.
2. Cristofalo, V.J., Pignolo, R.J., 1993. Replicative senescence of human fibroblast-like cells in culture. Physio. Rev. 73, 617-638.
3. Harley, C.B., Futcher, A.B., Greider, C.W., 1990. Telomeres shorten during aging of human fibroblasts. Nature. 345, 458-460.
4. deLange, T. 2001. Telomere capping one strand fits all. Science. 292, 1075-1076.
5. Witkowski, J.A., 1987. Cell Aging in vitro: A historical perspective. Exp.Gerontol. 22, 231-248.
6. Arking, R. Biology of Aging: Observations and Principles: 2nd Edition copyright 1998 by Sinauer Associates. Pages 448-451.
7. Jha, K, K., Banga, S., Palejwala, V., Ozer, H.L., 1988. SV-40-mediated immortalization. Exp. Cell.Res. 245, 1-7.
8. Neufeld, D.S., Ripley, S., Henderson, A., Ozer, H.L., 1987. Immortilization of human fibroblasts transformed by origin defective simian virus 40. Mol. Cell. Biol. 7, 2794-2802.
9. Wei, W., and Sedivy, J.M. 1999. Differentiation between senescence (M1) and crisis (M2) in human fibroblast cultures. Exp. Cell. Res. 253, 519- 522.
10. Chin, C.P., Harley, C.B., 1997. Replicative senescence and cell immortality: The role of telomeres and telomerase. Exp. Bio. Med. 99-106.
11. Hornsby. P.J., 2002. Cellular senescence and tissue aging in vivo. J. Geront.Bio. Sci. 57A, 251-256.

12. Berube, N.G,, Smith, J.R., Pereira-Smith O.M., 1998. Insights from model systems: the genetics of cellular senescence. Am. J. Hum.Genet. 62, 1015-1019

13. Hubbard, K., Ozer, H.L., 1999. Senescence & immortalization of human cells. In: Studsinski: GP, editor. Cell growth, differentiation, & senescence. New York: Oxford University Press. pp 281- 300.

14. Campisi, J., 1997. Aging and cancer: The double-edged sword of replicative senescence. JAGS.45, 482-488.

15. Matsamura, T., Zerrudo, Z., Hayflick, L., 1979. Senescent human diploid cell in culture: survival, DNA synthesis, and morphology. J. Gerontol. 34, 328-334.

16. Cristofalo, V.J., Lorenzini, A., Allen, R.J., Torres, C., Tresini, M.,2004. Replicative senescence: a critical review. Mech, Ageing Dev. 125, 827-848.

17. Sitte, N., Merker, K., von Zglinicki, T., Grune, T., Davies, K.J.A., 2000. Protein oxidation and degradation during cellular senescence of human BJ fibroblasts; part I-effects of proliferative senescence. FASEB. 14, 2495- 2502.

18. Cristafalo, V.J., Volker, C., Francis, M.K., Tresini, M.,. 1998. Age-dependant modifications of gene expression in human fibroblasts. Critical Rev. Euk. Gene Exp. 1: 43-80.

19. Seshadri, T., Campisi, J., 1990. Repression of c-fos transcription and altered genetic program in senescent fibroblasts. Science. 247,205-209.

20. DiPaolo, B.R., Pignolo, R.J., Cristafalo, V.J.,1995. Identification of proteins differentially expressed in quiescent and proliferatively senescent fibroblast cultures. Exp. Cell. Res. 220, 178-185.

21. Noda, A., Ning, Y., Venable, S.F., Pereira-Smith, O.M., Smith, J.R., 1994. Cloning of senescent cell-derived inhibitors of DNA synthesis in an expression screen. Exp. Cell.Res. 211, 90-98.

22. Atadja, P., Wong, H., Garkavtsev, C., Veillette, C., Riabowal, K., 1995. Increased activity of p53 in senescing fibroblasts. Acad. Sci. USA. 92, 8348-52.

23. Dimri, G.P., Lee, X., Basile, G., et al. 1995. A novel biomarker identifies senescent cell in culture and aging skin in vivo. Proc. Natl. Acad. Sci. USA 92:9363-9367.

24. Alcorta, D.A., Xiong, Y., Phelps, D., Hannon, G., Beach, D., Barrett, J.C., 1996. Involvement of the cyclin-dependent kinase inhibitor p16(INK4A) in replicative senescence of normal fibroblasts. Proc. Natl. Acad. Sci. USA 93: 13742-13747.

25. West, M.D., Pereira-Smith, O.M., Smith, J.R., 1989. Replicative senescence of human skin fibroblasts correlates with a loss of regulation and overexpression of collagenase activity. Exp. Cell.Res. 184, 138-147.

26. Millis, A.J., McCue, H.M., Kumar, S., Baglioni, C., 1992. Metalloproteinase and TMP-1 gene expression during replicative senescence. Exp. Gerontol. 27, 425-428.

27. Lorenzini, A., Tresini, M., Mawal-Dewan, M., Frisoni, L., Zhang, H., Allen, R.G., Sell, C., Cristafalo, V.J., 2002. Role of the Raf/MEK/ERK and the PI3K/AKT(PKB) pathways in fibroblast senescence. Exp. Gerontol. 37, 1149-1156.

28. Deng, Q., Liao, R., Wu, B.-L., Sun, P., 2004. High intensity ras signaling induces premature senescence by activating p38 pathway in primary human fibroblasts, 9, 1050-1059.

29. Stein, G., Drullinger,L.F., Soulard, A., Dalic, V.,1999. Differential roles for cyclin-dependant kinase inhibitors p21 and p16 in the mechanism of senescence and differentiation in human fibroblasts. Mol.Cell. Biol. 19, 2109-2117.

30. Nevins ,J.R., 2001 The Rb/E2F pathway and cancer. Hum. Mol. Genet. 10:699-703.

31. Pomerantz, J., Schreiber-Agus, N., Ligeois, N.J., Silverman, A., Alland, L., Chin, L., Potes, J., Chen, I., Orlow, H., Lee, W., Cardon-Cardo, C., DePinho, R.A., 1998. The INK4A tumor suppressor gene product , p19ARF interacts with MDM2 and neutralizes MDM2's inhibition of p53. Cell. 92, 713-723.

32. Zhang, Y., Xiong, Y., Yarbrough, W.G., 1998. ARF promotes MDM2 degradation and stabilizes p53: ARF-INK4a locus deletion impairs both the Rb-p53 tumor suppressor pathways. Cell. 92, 725-734.

33. Kastan, M.B., 1993. p53: A determinant of the cell cycle response to DNA damage. Adv. Exp. Med. Biol. 339, 291-293.

34. Graeber, T.G., Osmanian., C., Jacks, T., Housman, D.E., Koch, C.J., Lowe, S.W., Giaccia, A.J., 1996. Hypoxia-mediated selection of cells with diminished apoptotic potential in solid tumors. Nature. 379, 88-91.

35. Lin, A.W., Barradas, M., Stone, J.C., van Aelst, L., Serrano, M., Lowe, S.W., 1998. Premature senescence involving p53 and p16 is activated in response to constitutive MEK/MAPK mitogenic signaling. Genes and Dev. 12, 3008-3019.

36. Garfinkel, S., Wessendorf, J.H., X, Hu., Maciag, T., 1996. The human diploid fibroblast senescence pathway is independent of interleukin-1α mRNA levels and tyrosine phosphorylation of FGFR-1 substrates. Bichim. Biophys. Acta. 1314: 109-119.

37. Zambetti, G., Dell'Orco, R., Stein, G., Stein, J., 1987. Histone gene expression remains coupled to DNA synthesis during in vitro cellular senescence. Exp. Cell. Res. 172, 397-403.

38. Chang, C.D., Phillips, P., Lipson, K.E., Cristofalo, V.J., Baserga, R.,1991. Senescent human fibroblasts have a post-transcriptional block in the expression of the proliferating cell nuclear antigen gene. J. Biol.Chem. 266, 8663-8666.

39. Pendergrass W.R., Angello, J.C., Saglewicz, A.C., Norwood, T.H., 1991. DNA polymerase alpha and regulation of entry into S-phase in heterokaryons. Exp. Cell.Res. 192, 426-32.

40. Beausejour, C.M., Krtolica, A., Galini, F., Narita, M., Lowe, S.W., Yaswen, P., Campisi, J., 2003. Reversal of human cellular senescence: roles of the p53 and p16 pathways. EMBO J. 22, 4212,-4222.

41. Bukrinsky, M.I. et al 1993. A nuclear localization signal with HIV-1 matrix protein that governs infection of non-dividing cells. Nature. 365, 666-669.

42. Cristofalo, V.J., Tresini, M., 1998. Defects in signal transduction during replicative senescence of diploid human fibroblasts in vitro. Aging. 2, 151-152.

43. Goldstein, G., 1978 Lymphocyte differentiation induced by thymopoietin, bursopoietin, and ubiquitin. Symp. Soc. Dev. Bio. 35, 197-202.

44. Krecic, A.M., Swanson, M.S., 1999. hnRNP complexes: composition, structure, and function. Curr. Opin. Cell. Bio. 11, 363-371.

45. McAfee, J.G., Huang, M, et al: The packaging of pre-mRNA. In Eukaryotic mRNA processing. Edited by Krainer AR. IRL Press at Oxford University Press, 68-102, 1997.

46. Nakielny, S., Dreyfuss, G., 1997. Nuclear export of proteins and mRNAs. Curr. Opin Cell. Bio. 9, 42-429.

47. Timchenko, L.T., Miller, J.W., et al. 1996. Identification of a (CUG)n triplet repeat RNA-binding protein and its expression in myotonic dystrophy. 1996. Nuc. Acid Res. 24, 4407-4414.

48. Philps, A.V., Timchenko, L.T., Cooper, T.A., 1998. Disruption of splicing regulated by a CUG-binding protein in myotonic dystrophy. Science. 280, 737-741.

49. Dreyfuss, G., Matunis, M.J., Pinol-Roma, S., Burd, C.G., 1993 hnRNP proteins and the biogenesis of mRNA. Annu Rev Biochem, 62:289-321.

50. Pinol-Roma, S., Choi,Y.D., Matunis, M.J., Dreyfuss, G. 1988. Immunopurification of heterogeneous nuclear ribonucleoprotein particles reveals an assortment of RNA-binding proteins. Genes & Dev. 2, 215-227.

51. Dreyfuss, G., Matunis, M.J., Pinol-Roma, S., Burd, C.G., 1993. hnRNP proteins and the biogenesis of mRNA. Annu. Rev.Bichem. 62, 289-321.

52. Mayeda, A., Munroe, S.H., Xu, R.M., Krainer, A., 1998. Distinct functions of the closely related tandem RNA-recognition motifs of hnRNP A1. RNA. 4, 1111-1123.

53. Kamma, H., Horiguchi, H., Wan, L., et al. 1999. Molecular characterization of hnRNP A2/B1 proteins:tissue specific expression and novel isoforms. Exp. Cell. Res. 246, 399-411.

54. Weighardt, F., Biamonti, G., Silvano, R., 1996. The roles of heterogeneous nuclear ribonucleoproteins (hnRNP) in RNA metabolism. Bio Essay. 18, 747-755.

55. Wilk, H.E., Werr, H., Friedrich, D.,et al. 1985. The core proteins of 35 S hnRNP complexes, the characterization of nine different species. Eur. J. Biochem. 146: 71-81.

56. Mayeda, A., Munroe, S., Caceres, J.F., Krainer, A.R., 1994. Functions of conserved domains of hnRNP A1 and other hnRNP A/B proteins. 13, 5483-5495.

57. Adams, S.A., Nakagawa, T.Y., Swanson. M.S., Woodruff, T., Dreyfuss, G., 1986. Mol. Cell. Biol. 6, 2932-43.

58. Dreyfuss, G., Swanson, M.S., Pinol-Roma, S., 1988. Heterogenous nuclear ribonucleoprotein particles and the pathway of mRNA formation. Trends Biochem 13, 86-91.

59. Schwemmle, M., Gorlach, M., Bader, M., Sarre, T.F., Hilse, K., 1989. Binding of mRNA by a oligopeptide containing an evolutionarily conserved sequence from RNA binding proteins. FEBS Lett. 251, 117 120.

60. Merrill ,B., Stone, K.L., Cobianchi, F., Wilson, S.H., Williams, K.R., 1988. Phenylalanines that are conserved among several RNA-binding proteins form part of the nucleic acid binding pocket in the A1 heterogenous nuclear ribonucleoprotein. J. Bio. Chem. 263, 3307 -13.

61. Cartegni, L., Maconi, M., Morandi, E., Cobianchi, F., et al. 1996. hnRNP A1 selectively interacts through its Gly-rich domain with different RNA-binding proteins. J. Mol. Biol. 259, 337-348.

62. Leser, G.P., Escara-Wilke, J., Martin, T.E., 1984. Monoclonal antibodies to heterogenous nuclear RNA-protein complexes. The core group comprise a conserved group of related peptides .J Biol. Chem. 259:1827-1833.

63. Kumar, A., Williams, K.R.,, Szer, W., 1986. Purification and domain structure of core hnRNP proteins A1 and A2 and their relationship to single-stranded DNA binding proteinsJ. Biol. Chem. 261:11266-11273.

64. Michael, W.M., Choi, M., Dreyfuss, G., 1995. A nuclear export signal in hnRNP A1: a signal mediated, temperature dependent nuclear protein export pathway. Cell. 83, 415-422.

65. Siomi, H., Dreyfuss, G., 1995. A nuclear localization domain in the hnRNP A1 protein. J.Cell.Biol. 129, 551-560.

66. Michael, W.M., Siomi, H., Choi, M., Pinol-Roma, S., Nakielny, S., Liu, Q., Dreyfuss, G., 1995. Signal sequences that target nuclear import and nuclear export of pre-mRNA binding proteins. Cold Spring Harbor Symposium Quant. Biol. 60, 663-668.

67. Weinghardt, F., Biamonti, G., Riva, S., 1995. Nucleo-cytoplasmic distribution of human hnRNP proteins: a search for targeting domains in hnRNP A1. J. Cell Sci. 108, 545-555.

68. Pollard, V.W., Michael, W.M., Nakielny, S., Siomi, M.C., Wang, F., Dreyfuss, G. 1996. A novel receptor-mediated nuclear protein import pathway. Cell 86, 985-995.

69. Friedell, R.A., Truant, R., Thorne, L., Benson, R.E., Cullen, B.R., 1997. Nuclear import of hnRNP A1 is regulated by by a novel co-factor related to karyopherin-beta. J. Cell.Sci. 110, 1325-1331.

70. Rebane ,A., Aab, A., Steitz, A., 2004. Transportins 1 and 2 are redundant nuclear import factors for hnRNP A1 and HuR. RNA. 10, 590-9.

71. Allemand, E., Guil, S., Myers, M., Moscat, J., Caceres, J. F., Krainer, A.R., 2005. Regulation of heterogeneous nuclear ribonucleoprotein A1 transport by phosphorylation in cells stressed by osmotic shock. PNAS. 102, 3605-3610.

72. Mayeda, A., Krainer, A.R., 1992. Regulation of alternative pre-mRNA splicing by hnRNP A1 and splicing factors SF2. Cell 68 365-375.

73. Biamonti, G., Riva, S., 1994. New insights into the auxillary domain of eukarotic RNA binding proteins. FEBS Lett. 340: 1-8.

74. Kumar A, Wilson, S.H., 1990. Biochemistry 29: 10717-10722

75. Pontius, B., Berg, P., 1990. Renaturation of complementary DNA strands mediated by purified mammalian heterogeneous nuclear ribonucleoprotein A1 protein: Implications for a mechanism for rapid assembly. Proc. Natl. Acad. Sci. 87: 8403-8401.

76. Krainer, A.R., Conway, G.C., Kozak, D., 1990. The essential pre-mRNA splicing factor influences 5' splice site selection by activating proximal sites.Cell. 62, 35-42.

77. Burd, C.G., Dreyfuss, G., 1994. Conserved structures and diversity of functions of RNA-binding proteins. Science. 265, 615-621.

78. Dallaire, F., Dupuis, S., Fiset, S., Chabot, F., 2000. Heterogeneous nuclear ribonucleoprotein A1 andUP1 protect mammalian telomeric repeats and modulate telomere replication *in vitro*. J. Biol. Chem. 275, 14509-14516.

79. Pinol-Roma, S., Dreyfuss, G., 1991. Transcription-dependent and transcription independent nuclear transport of hnRNP proteins. Science 253, 312-253.

80. Greenberg, M.E., Belasco, J.G., In Control of Messenger RNA Stability (Belasco JG and Brawerman G, eds) pp199-218, Academic Press, New York.

81. Bohjanen, P.R., Petryniak, B., June. C,H., Thompson, C.B., Lindsten, T., 1991. AU-RNA binding factors differ in their binding specificity and affinity. Mol. Cell. Biol., 11, 3288-3295.

82. Brewer, G., 1991. An A+U-rich element RNA binding factor regulates c-myc mRNA stability in vivo.Mol Cell Biol 11: 2460-2466.

83. Levine, T.D., Gao, F., King, P.H., Andrews, L.G., Keene , J.D., Mol Cell Biol: 13: 3494-3504.

84. Malter, J.S., 1989. Identification of an AUUUA-specific messenger RNA binding protein. Science, 246: 664-666.

85. Hamilton, B.J., Burns, C.M., Nichols, R.C., Rigby, W.F.C., 1997. Modulation of AUUUA response element binding by heterogeneous nuclear ribonucleoprotein A1 in human T lymphocytes. J. Biol. Chem. 272, 28732-28741

86. Shyu, A.B., Greenberg, M.E., Belasco, J.G., 1989. The c-fos transcript is targeted for rapid decay by 2 distinct mRNA degradation pathways. Genes Dev 3: 60-72.

87. Eperon, I.C., Makarova, O.V., Mayeda, A., Munroe, S.H., Caceres, J.F., Hayward, D.G.,, Krainer, A.R., 2000. Selection of alternative 5'splice sites: role of U1 snRNP and models for the antagonistic effects of SF2/ASF and hnRNP A1. Mol. Cell. Bio. 20, 8303-8318.

88. Zhu, D., Ghandhi, S., Hubbard, K., 2002. Modulation of the expression of p16 ARF by hnRNP A1/A2 RNA binding proteins: implications for cellular senescence.. J. Cell. Phys. 193, 19-25.

89. Rooke, N., Markovtsov,V., Cagavi, E., Balck, O.L,. 2003. Role for SR Proteins and hnRNP A1 in the regulation of C-src Exon N1. Mol. Cell. Bio. 23, 1874:1884.

90. Kim, S., Merrill, B.M., Rajpurohit, R., Kumar, A., Stone, K.L., Papov,V.V., Schneiders, J.M., Szer, W., Wilson, S.H., Paik, W.K., et al. 1997. Bichemistry. 36, 5185-5192.

91. Li, T., Evdokimov, E., Shen., R.F., Chao, C.C., Tekle, E., Wang, T., Stadtman, E.R., Yang, D.C., Chock, P.B., 2004. Proc. Nat. Acad. Sci. USA. 101. 8551-8556.

92. Perrotti, D., Iervolino, A., Cesi, V., Cirinni, M., Lombardini, S., Grassilli, E., Bonatti, S., Claudio, P.P., Calebretta, B., 200o. Mol.Cell. Biol.20, 6159-6169.

93. van Oordt, W., Diaz-Meco, M.T., Lozano, J., Krainer, A.R., Moscat, J., Caceres, J.F. 2000. The MKK3/6-p38-signaling cascade alters the subcellular distribution of hnRNP A1 and modulates alternative splicing regulation. J. Cell Bio. 149,307-316.

94. Municio, M.M., Lozano, J., Sanchez, P., Moscat, J,, Diaz-Meco, M.T., 1995. Identification of heterogeneous ribonucleoprotein A1 has a novel substrate for Protein kinase C ζ. J.Biol.Chem. 270: 15884-15891.

95. Dreyfuss, G., Matunis, M.J., Pinol-Roma, S., Burd, C.G., 1993. hnRNP proteins and the biogenesis of mRNA. Annu. Rev. Biochem . 62, 289-321.

96. Cobianchi, F., Calvio, C., Stoppini, M., Buvoli, M., Riva, S., 1993. Phosphorylation of human hnRNP A1 protein abrogates *in vitro* strand annealing activity. Nuc. Acid Res. 21: 949-955.

97. Idriss, H., Kumar, A., Casas-Finet, J.R., Guo, H., Damuni, Z., Wilson, S.H., 1994. Regulation of in vitro nucleic acid strand annealing activity of heterogeneous nuclear ribonucleoprotein A1 by reversible phosphorylation. Biochem. 33, 11382-11390.

98. Guthrie, C., 1993. Messenger RNA splicing in yeast: clues to why the spliceosome is a ribonucleoprotein. Science 253: 157-163.

99. Pearsson, G., Robinson, F., Beers-Gibson, T., Xu, B.E., Karandikar, M., Berman, K., Cobb, M.H., 2001. Mitogen activated protein (MAP) kinase pathways: regulation and physiological functions. Endocr. Rev. 22, 153-183.

100. Enslen, H., Davis, R.J., 2001. Regulation of MAP kinases by docking domains. Biology of the Cell. 93, 5-14.

101. Dan, I., Watanabe, N.M, Kusumi, A., 2001. The Ste20 group kinase as regulators of MAP kinase cascades. Trends Cell. Bio. 11, 220-230.

102. Jiang, Y., Gram, H., Zhao, M., New, L., Gu,J., Feng, L., DiPadora, F., Ulevitch, R.J., Han, J., 1997. Characterization of the structure and function of the fourth member of the p38 group mitogen activated protein kinase, p38δ. J. Biol. Chem. 272, 30122-30128.

103. Lechner, C., Zahalka, M.A., Giot, J.F., Moller, N.P., Ullrich, A., 1996. ERK6, a mitogen-activated protein kinase involved in C2C12 myoblast differentiation. Proc.Natl.Acad. Sci. USA. 93, 4355-4359.

104. Mertens, S., Craxton, M., Goedert, M., 1996. SAP kinase-3, a new member of the family of mammalian stress-activated protein kinases. FEBS Lett. 383, 273-276.

105. Goedert, M., Cuenda, A., Craxton, M., Jakes, R., Cohen, P., 1997. Activation of novel stress-activated protein kinase SAPK4 by SKK3(MKK6): comparison of its substrate specificity with that of other SAP kinases. EMBO J. 16, 3563-3571

106. Enslen, H., Raingeaud, J., Davis, R.J., 1998. Selective activation of p38 mitogen-activated protein (MAP) kinase isoforms by the MAP kinase kinase MKK3 and MKK6. J. Biol.Chem. 273, 1741-1748.

107. Cohen, P., 1997. The search for physiological substrates of MAP and SAP kinases in mammalian cells. Trends Cell Biol. 7, 353-361.

108. Alonso, G., Ambrosino, C., Jones, M., Nebreda, A.R., 2000. Differential activation of p38 mitogen-activated protein kinase isoforms depending on signal strength. J.Biol.Chem. 275, 40641-40648.

109. Davis, R.J., 1994. MAPK's new JNK expands the group. Trends Biol. Sci 19, 470-473.

110. Camps, M., Nichols, A., Arkinstall, S., 2000. Dual specificity phoshatases: a gene family for control of MAP kinase function. FASEB J. 14, 6-16.

111. Brunet, A., Roux, D., Lenormand, P., Dowd, S., Keyse, S., Pouyssegur, J., 1999. Nuclear translocation of p42/p44 mitogen activated protein. EMBO J. 664-74.

112. Chen, R.H., Sarnecki, C., Blenis, J., 1992. Nuclear localization and regulation of ERK and Rsk encoded protein kinase. Mol.Cell.Biol. 12, 915-927.

113. Gonzalez, F.A., Seth, A., Reden, D.L., Bowman, D.S., Fay, F.S., Davis, R.J., 1993. Serum-induced translocation of mitogen activated protein kinase to the cell surface ruffling membrane and nucleus. J. Cell. Biol. 122,1089-1101.

114. Casanovas, O., Miro, F., Estanyol, J.M., Itarte, E., Agell, N., Bach, O., 2000. Osmotic stress regulates the stability of cyclin D1 in a p38SAPK2-dependent manner. J. Biol. Chem. 275, 35091-35097.

115. Buxade, M., Parra, J.L., Rousseau, S., Shpiro, N., Marquez, R., Morrie, N., Bain, J., Espel, E., Proud, C.G., 2005. The Mnks are novel components in the control of TNFα biosynthesis and phosphorylate and regulate hnRNP A1. Immunity. 23, 177-189.

116. Hubbard, K., Dhanaraj, S.N., Sethi, K.A., Rhodes, J., Wilusz, J., Small, M.B., Ozer, H.L., 1995. Alteration of DNA and RNA binding activity of human telomere binding proteins occurs during cellular senescence. Exp. Cell. Res. 218, 241-247.

117. Smith, H.S., Owens, R.B., Hiller, A.J., Nelson,-Rees, W.A, Johnston, J.O., 1976. The biology of human cells in tissue culture. I. characterization of cells derived from osteogenic sarcomas. Int. J. Cancer. 17, 219-234.

118. Neufeld, D.S., Ripley, S., Henderson, A., Ozer, H.L., 1987. Immortalization of human fibroblasts by origin-defective simian virus 40Mol. Cell. Bio. 7, 2794-2802.

119. Pinol-Roma, S., Choi, Y.D., Dreyfuss, G., 1986. Immunological methods for purification and characterization of heterogeneous nuclear ribonucleoprotein particles. Annu. Rev. Cell. Biol. 459, 317-324

120. Laemmli, U.K., 1970. Cleavage of structural proteins during the assembly of the head of bacteriophage T4. Nature (London). 227, 680-685.

121. Usui, et al., 1983. Phosphoprotein phosphatases in human erythrocytes cytosol. J.Biol. Chem. 258, 10,455-50.

122. Shenolikar, and Nairn, 1990. Protein phosphatases: recent progress. Adv. Sec. Messenger Phosphoprotein Res.

123. Edelman, A.M., Blumenthal, D.K., Krebs, E.G., 1987. Protein serine/threonine kinases. Annu. Rev. Biochem. 56, 567-613.

124. DeFranco, D.B., Qi, M., Borror, K.C., Garabedian, M.J., Brantigan, D.L., 1991. Protein phosphatases types 1 and/or 2A regulate nucleocytoplasmic shuttling of glucocorticoid receptors. Mole. Endocrinolog. 5, 1215-28

125. Reinhart,, P.H., Chung, S., Martin, B.L., Brautuigan, D.L.,Levitan, I.B., 1991. Modulation of calcium-activated potassium channels from rat brain by protein kinase A and phosphatase 2A. Neuroscience. 11, 1627-35.

126. Karin, M., Hunter, T., 1992. Transcriptional control by protein phosphorylation: signal transmission from the cell surface to the nucleus. Cell. 70, 375-387.

127. Xu, G., Construction of GFP vectors to study the localization of hnRNP A1 and A2 during cellular senescence. M.A. Thesis CCNY

128. Rittling, S.R., Brooks, K.M., Cristofalo, V.J., Baserga, R., 1986. Expression of cell cycle-dependent genes in young and senescent WI38 fibroblasts. Proc. Natl. Acad. Sci. U.S.A. 83, 3316-20.

129. Cohen, P., 1988. Protein phosphorylation and hormone action.. Proc. R. Soc. Lond. B. Biol. Sci. 234, 115-144.

130. Pinol-Roma, S., Dreyfuss, G., 1993. Cell cycle-regulated phosphorylation of the pre-mRNA-binding (heterogeneous nuclear ribonuclear) C protein. Mol. Cell. Bio. 13, 5762-5770.

131. Sheppeck, J.E., II, Gauss, C.M., Chamberlin, A.R., 1997. Inhibition of the ser/thr phosphatases PP1 and PP2A by naturally occurring toxins. Biorganic and Med. Chem. 5, 1739-1750.

132. Hubbard, K., Dhanara,j S.N., Sethi, K.A., Rhodes, J., Wilusz, J., Small, M.B., Ozer. H.L., 1995. Alteration of DNA and RNA binding activity of human telomere binding proteins occurs during cellular senescence. Exp Cell Res 218: 241-247.

133. Mayeda, A., Krainer, A.R., 1992. Regulation of alternative pre-mRNA splicing by hnRNP A1 and splicing factor SF2. Cell. 68, 365-375.

134. Caceres, J.F., Stamm, S., Helfman, D.M., Krainer, A.R., 1994. Regulation of alternative splicing in vivo by overexpression of antagonistic splicing factors. Science. 265, 1706-1709.

135. Yang, X., Bani, M.R., Lu, S.J., Rowan S., Ben-David, Y., Chabot, B., 1994. The A1 and A1B proteins of heterogeneous ribonucleoparticles modulate 5'splice site selection in vivo. Proc. Natl. Acad. Sci. USA. 91, 6924-6298.

136. Guil, S., Gattani, R., Carrascal, M., Abian, J., Stevenson, J., Bach, Elias, M., 2003. Roles of hnRNP A1, SR proteins, and p68 helicase in c-H-ras alternative splicing. Mol. Cell. Bio. 23, 2927-2941.

137. Wang, W., Chen, J.X., Liao, R., Deng, Q., Zhon, J.J., Huang,S ., Peiqing,S., 2002. The sequential activation of the MEK-Extracellular signal-regulated kinase & MKK3/6-p38 mitogen-activated protein kinase pathways mediates oncogenic ras-induced premature senescence. Molecular and Cellular Biology 22, 3389-3403

138. Lee, J.C., et al., 1999. p38 Mitogen-activated protein kinase inhibitors-mechanisms and therapeutic potentials. Pharmocol. Ther. 82, 389-397.

139. Raingeaud, J., et al, 1996. MKK3- and MKK6- regulated gene expression is mediated by the p38 mitogen-activated protein kinase signal transduction pathway. Mol. Cell. Biol. 16, 1247-1255.

140. Wang, X.Z., Ron, D. 1996. Stress induced phosphorylation and activation of the transcription factor CHOP (GADD153) by p38 MAP kinase. Science 272, 1347-1349.

141. Han, J., et al. 1997. Activation of the transcription factor MEF2C by the MAP kinase p38 in inflammation. Nature 386, 296-299.

142. Johnson, G.L., Lapadat, R., 2002. Mitogen activated protein kinase pathways mediated by EFK, JNK, and p38 protein kinases. Science, 298, 1911-1912.

143. Serrano, M., Lin, A.W., McCurrach M.E., Beach, D., Lowe, S.W., 1997. Oncogenic ras provokes premature senescence with accumulation of p53 and p16INK 4A. Cell. 88, 593-602.

144. Rousseau, S., Morric, N., Peggie, M., Campbell, D.G., Gaestel, M., Cohen. P., 2002. Inhibition of SAPK2a/p38 prevents hnRNP A0 phosphorylation by MAPKAP-K2 and its interaction with cytokine mRNA's. 23, 6505-6514.

145. Olson, .JM., Hallahan, A.R., 2004. p38 MAP kinase: a convergence in cancer therapy. Trends in Molecular Medicine. 10, 125:129.

146. Morton, S., Davis, R.J., Cohen, P., 2004. Signalling pathways involved in multisite phosphorylation of the transcription factor ATF-2. 2004. FEBS Lett. 572, 177-83.

147. Spandidos. D.A., Sourvinos, G., Tsatsanis, C., Zarifopoulos, A., 2002. Normal ras genes: Their ono-suppressor and pro-apoptotic function (Review). Inter. J. Onco. 21, 237:241.

148. Lavoie, J.N., L'Allemain ,G., Brunet, A., Muller, R., Pouyssegur, J,. 1996. Cyclin D1 expression is regulated positively by the p42/p44MAPK and negatively by the p38/HOGMAPK pathway. J. Biol.Chem 271, 20608-2016.

149. Bulavin, D.V., Amundson, S.A., Fornace A.J,. 2202. p38 and Chk1 kinases: Different conductors for the G2/M check point symphony. Curr. Opin. Genet. Dev. 12, 92-97.

150. Bulavin, D.V., Saito, S., Hollander, M.C., Sakaguchi, K., Anderson, C.W., Apella E, Fornace, Jr. A.J., 1999. Phosphorylation of human p53 by p38 MAP kinase coordinates N-terminal phosphorylation and apoptosis in response to UV radiation. EMBO J. 18, 6845:6854.

151. Davies, S.P., Reddy ,H., Caivano,, M., Cohen, P., 2000. Specificity and mechanism of action of some commonly used protein kinase inhibitors. Biochem

J. 351, 95-105.

152. Harlow, E., Lane, D. P., 1988. Antibodies, A Laboratory Manual, Cold Spring Harbor Laboratory, Cold Spring Harbor NY.

153. Han, J., et al. 1994. A MAP kinase targeted by endotoxin and hyperosmolarity in mammalian cells. Science 265, 808-811.

154. Lee, J.C., et al 1994. A protein kinase involved in the regulation of inflammatory cytokine biosynthesis. Nature. 739-746.

155. Rouse, J., et al 1994. A novel kinase cascade triggered by stress and heat shock that stimulates MAPKAP kinase 2 and phosphorylation of the small heat shock proteins. Cell. 78, 1027-1037.

156. Iwasa, H., Han, J., Ishikawa, F., 2003. Mitogen-activated protein kinase p38 defines the common senescence signaling pathway. Genes to Cells. 8, 131:144.

157. Allen, R. G., 1998. Oxidative stress and superoxide dismutase in development, aging, and gene regulation. Age. 21, 47-76.

158. Young, P.R., et al. 1997. Pyridinyl imidazole inhibitors of p38 mitogen-activated protein kinase binds in the ATP site. J. Biol. Chem. 272, 1216-1212.

159. Fuchs, S.Y., Fried, N.A., Ronai, Z., 1998. Stress activated kinases regulate protein stability. Oncogene. 17, 1483-1490.

160. Meisner, H., Czech, M.P., 1991. Phosphorylation of transcriptional factors and cell cycle proteins by casein kinase II. Curren. Opin. Cell. Bio. 3, 474-483.

161. Raingeaud, J., Gupta, S., Rogers, J.S., Dickens, M., Han, J., Ulevitch, R.J., Davis, R.J., 1995. Pro-inflammatory cytokines and environmental stress cause p38 mitogen –activated protein kinase activation by dual phosphorylation on tyrosine

and threonine. J. Biol. Chem. 270, 7420-7426.

162. Kang, S., Jung, M., Kim, C.W., Shin, D.Y. 2005. Inactivation of p38 MAP kinase delays the onset of senescence in rabbit articular chondrocytes. Mech. Age. Dev. 126, 591-597.

163. Koizumi, J., Okamoto, Y., Onogi, H., Mayeda, A., Krainer, A.R., Hagiwara, M. 1999. The subcellular localization of SF2/ASF is regulated by direct interaction with SR Protein Kinases (SRPK's). J.Biol. Chem. 274, 11125-31.

164. Misteli, T., Caceres, J.F., Clement, J.Q., Krainer, A.R., Wilkinson, M.F., Spector, D.L. 1998. Serine phosphorylation of SR-proteins is required for their recruitment to sites of transcripition in vivo. J.Cell.Bio. 143, 297-307.

165. Rooke, N., Markovtov,V., Cagavi, E., Black, D.L. 2003. Roles for SR proteins and hnRNP A1 in the regulation of c-src Exon N1. Mol. Cell.Bio. 23, 1874-1884.

166. Hutchinson, S., LeBel, C., Blanchette, M., Chabot, B., 2002. Distinct sets of adjacent heterogeneous nuclear ribonucleoprotein (hnRNP) A1/A2 binding sites control 5' splice site selection in the hnRNP A1 mRNA precursor. J. Bio.Chem. 277, 29745-29752.